Study of the Process-form Relationships in Continuum of Braided Channel Patterns

Thesis submitted in partial fulfilment of the requirements for the award of the degree of

Doctor of Philosophy

in

Civil Engineering

by

CHANDAN PRADHAN

[Roll No. 166104027]

with the supervision of

Dr. Rishikesh Bharti

Prof. Subashisa Dutta

Department of Civil Engineering

Indian Institute of Technology Guwahati

Guwahati – 781039, Assam, India

September, 2022

Study of the Process-form Relationships in Continuum of Braided Channel Patterns

CHANDAN PRADHAN

Indian Institute of Technology Guwahati

Department of Civil Engineering, Guwahati, Assam 781039

Dedicated To

My parents and my sister.

ACKNOWLEDGEMENTS

It's been a great, beautiful and remarkable period of my life time. Personally, I have been incredibly lucky and have full of gratitude for working with and meeting lots of even better people. There are many who are directly or indirectly part of this journey and helped me to transform into a better person. Thanks to one and all!!

I thank my supervisor Dr. Rishikesh Bharti for his constant support and motivation throughout the Ph.D. journey. His meticulous guidance, constructive suggestions and sustained patience helped me to overcome all challenges of research work. I will have full respect and affection towards Prof. Subashisa Dutta at every stage of my life. He not only introduced me to the topic of River Hydraulics and Fluvial Geomorphology, but also constantly cultivated the desire to solve fluvial problems with utmost sincerity and perseverance. It is my sublime duty to express deepest sense of reverence to my Doctoral Committee Prof. Bimlesh Kumar, Dr. Ravi K., and Dr. Tapan Mishra for their valuable suggestions, encouragement, and timely help at various stages of Ph.D. journey.

I would like to thank my school teachers- Pradhan sir and Jena sir for teaching me the basics of education and good life. Thanks to Vinay for being there as a mentor and introducing me to the area of field-based research and effective technical writing. I will remember all our riverine surveys to the Brahmaputra and Brahmani Rivers. Anju Bhaiya, you become my big brother in the last eight years and motivated me to tackle many challenges of Ph.D. Aparimita and Amrutha, our togetherness and friendship grew many folds and you both have become my second family. This work would have been much more mentally challenging without both of your emotional support, motivation and caring.

Thanks to my lab mates- Suman Bhaiya, Satish Bhaiya, Shreedevi Didi, Riddick, Suresh, Lasya, Deka, Avinash, Sandeep for their nice friendship and unconditional affection towards me. Special thanks to Ketan for helping me during the ending stage of my PhD. Smarak, you really helped me during the formatting of the thesis. I also thank to my good friends Dinesh,

Swayambhu, Ketan, Prateek, Pranesh, Ashutosh, Sameer, Saroj, Arnab and Subhro for your friendly love and care. I express my special thanks to Bazal Da for helping me in the field visits to Odisha and Assam.

It goes without saying that this journey and work would not have been possible without the love, care and support from my parents and sister. They have stood firmly by my side since childhood, and I can't even imagine reaching at this point of my career without their prayer, emotional support and encouragement. This journey and this success, all are yours and I am forever grateful!

Chandan Pradhan

*****

DECLARATION

I, **Chandan Pradhan**, author of the Ph. D. thesis "**Study of the Process-form Relationships in Continuum of Braided Channel Patterns**" would like to certify that

- The work presented in this thesis is original research work carried out by me.
- The research work has not been submitted for any degree or diploma or any other qualification either in this institute or in any other university.
- Whenever I have used resources [theory, concepts, texts, data, graphs, figures or any other similar nature] from other sources, a due credit by citing in the text of the thesis is clearly made.
- The work presented here is free from plagiarism to the best of my knowledge, and I take the responsibility for any issues.
- I also affirm that thesis supervisor is not responsible for any possible instance of plagiarism within this submitted work.

Date: 26th September, 2022

Place: IIT Guwahati

CHANDAN PRADHAN

[166104027]

Indian Institute of Technology Guwahati

Department of Civil Engineering, Guwahati, Assam 781039

CERTIFICATE

This is to certify that thesis entitled "**Study of the Process-form Relationships in Continuum of Braided Channel Patterns**" submitted by **Chandan Pradhan**, in partial fulfilment of the requirements for the award of degree of Doctor of Philosophy, to Indian Institute of Technology Guwahati, Assam, India, is a record of the bonafide research work carried out by him under our guidance and supervision at the Department of Civil Engineering, Indian Institute of Technology Guwahati, Assam, India. To the best of our knowledge, no part of the work reported in this thesis has been presented for the ward of any degree at any other institution.

Dr. Rishikesh Bharti
Assistant Professor
Department of Civil Engineering
IIT Guwahati
Assam, India-781039
Email: rbharti@iitg.ac.in

Prof. Subashisa Dutta
Professor
Department of Civil Engineering
IIT Guwahati
Assam, India-781039
Email: subashisa@iitg.ac.in

ABSTRACT

The braided rivers are governed by complex, unstable river networks formed due to the interaction of high flow energy and intense sediment transport. The generation of complex morphological adjustments over a braided corridor is a response to the changes in flow and sediment supply. Understanding braided river behavior and underlying concepts through field-based studies, modeling, analysis and cloud computing can be beneficial for their effective management. This thesis aims to understand the process-form relationships along the continuum of braided patterns.

Effective discharge plays a major part in sediment and nutrient transport, landscape modification, and river restoration. However, a complete understanding of effective discharge is still missing because of heterogeneity in various fluvial processes. The present study investigates the role of effective discharge for suspended sediment transport in a regulated weakly braided river system, the Brahmani River, India. The natural flow-sediment regime and channel pattern of the Brahmani River have been altered by the Rengali dam. The effective discharge is estimated with both analytical and deterministic methods using long-term hydrological data. The results show the control of regulated flow and sediment regime in the post-dam period contributes to the reduction in effective discharge (1849 m^3/s to 820 m^3/s), where frequent moderate floods are able to transport a maximum portion of sediment load. An effective discharge integrated stream power curve is formulated, which accurately predicts the channel transition (from sinuous to weakly braided) in the post-dam period. Finally, the proposed probability of braiding (POB) captures the chute formation correctly, which further highlights the hierarchy of energy dissipation and morphological continuum in the Brahmani River.

River recovery captures the past trajectories of channel adjustments and facilitates an understanding for the present state and future scenarios. The cross-sectional intensity entropy (CIE) is computed for the post-monsoon season along two large sub-basins of the Mahanadi, India. Further, normalized river recovery indicator (NRRI) is formulated to assess the temporal change in river health. Finally, NRRI is related to a process-based variable- LFE (low flow exceedance) to comprehend the dominating system dynamics and evolutionary adjustments. The results highlighted the existence of both thresholds modulated and filter dominated systems based on CIE and NRRI variabilities. In addition, the gradual decline in CIE and subsequent stabilization of vegetated landforms can develop an 'event-driven' state, where floods exceeding the low-flow channel possess a direct impact on the river recovery trajectory. In addition, this study emphasizes the presence of instream vegetation as an additional degree of freedom, which further govern the energy dissipation processes in the macrochannel weakly braided settings.

In highly braided rivers, integration of the Google earth engine (GEE) cloud computing platform and hydro-morphological dataset provide a basis to understand the complex process-form relationships. Two new process-based indicators- Normalised process gradient (NPG) and Normalised threshold exceedance (NTE) are proposed to address the dominant geomorphological adjustments in the Brahmaputra River. The results show that in a highly braided river system, the sand bar adjustments prevail over other forms of morphological changes and is closely dependent on the process gradient between the hierarchical thresholds. Further, the scale of planform evolution is computed from the location probability index (LPI), and the geomorphic stationarity concept is introduced for a large braided river. Finally, a multi-faceted resilience-based freedom space management approach is designed based on system state trajectory, LPI variability, proximity to thresholds, and in-channel landform configuration. The present thesis work provides the comprehensive understanding of the process-form relationships and associated management approaches along the continuum of braided channels.

*****

CONTENTS

List of Figures v
List of Tables ix
List of Symbols xii
List of Abbreviations xiii

1 INTRODUCTION

1.1 Morphological Continuum 01
1.2 Process-form relationships and Pertinent Concepts 02
1.3 Aims and Objectives of the Thesis 04
1.4 Organization of Thesis 04

2 SYNTHESIS OF LITERATURE AND CONCEPTUALIZATION

2.1 Braided River 07
2.2 Heterogeneity of Fluvial Controls 09
2.3 Impacts of Anthropogenic Stresses 10
2.3.1. Dams in India: A Growth Statistics 11
2.3.2. Upstream Impacts of Dams 13
2.3.3. Downstream Impacts of Dams 15
2.4 Conceptualization and Basis for Future Research in Braided Rivers 19
2.4.1. Relaxation Period and Process-form Relationships in Highly Braided Himalayan Rivers 21
2.4.2. Changes in Braided Belt Width and Implications of Resilience-based Freedom Space Management Concept in Highly Braided Rivers 26
2.4.3. Relaxation Period and Process-form Relationships in Weakly Braided peninsular rivers 29
2.4.4. Role of Vegetation in Recovery Assessment Along Braided Rivers: A Way Forward 31
2.4.5. The Future Direction in Fluvial Modeling 33
2.5 Chapter Summary 34

3 PROCESS-FORM RELATIONSHIPS IN A WEAKLY BRAIDED RIVER SYSTEM

3.1 Introduction 37
3.2 Study Area 39
3.3 Materials and Methods 41
3.3.1 Analytical Approach 42
3.3.2 Deterministic Approach 43
3.3.3 Morphological analysis 44
3.3.4 Stream power analysis 44
3.3.5 Potential unit stream power curve 45
3.3.6 Probability of braiding 46
3.4 Results 47
3.4.1 Hydrological data analysis 47
3.4.2 Effective discharge computation 52
3.4.3 Morphological analysis and stream power variability 55
3.4.4 Effective discharge integrated stream power curve 58
3.4.5 Probability of braiding in the Brahmani River 59
3.5 Discussion 61
3.5.1 Variation of effective discharge 61
3.5.2 Stream power distribution and its controls 62
3.5.3 Role of effective discharge in inset channel development 63
3.5.4 Hierarchy of energy dissipation and probability of braiding 65
3.5.5 Process-response yielding a morphological and behavioural continuum 66
3.6 Chapter Summary 67

4 FORMULATION OF PROCESS-BASED RECOVERY INDICATOR FOR WEAKLY BRAIDED RIVER SYSTEM

4.1 Introduction 69
4.2 Study Area 73
4.3 Data and Methodology 76
4.3.1 GEE cloud computing and instream vegetation area assessment 76
4.3.2 Cross-sectional intensity entropy 77
4.3.3 Normalized river recovery index 79
4.3.4 Process linkage 79
4.4 Results and Discussion 80
4.4.1 Longitudinal variation of instream vegetation cover 80
4.4.2 Hydrological data analysis and variability in CIE and NRRI 83
4.4.3 River recovery and process linkage 87
4.5 Chapter Summary 90

5 UNDERSTANDING THE PROCESS-FORM RELATIONSHIPS AND DEVELOPMENT OF RESILIENCE-BASED MANAGEMENT APPROACH FOR HIGHLY BRAIDED RIVER SYSTEM

5.1 Introduction 93
5.2 Study Area 96
5.3 Materials and Methods 97
5.3.1 Assessment of the complex morphology 97
5.3.2 Location probability index 98
5.3.3 Geomorphic stationarity 98
5.3.4 Formulation of process-based indicators 99
5.4 Results 100
5.4.1 The braided morphodynamics of the Brahmaputra River 100
5.4.2 Spatial variability in location probability index 104
5.4.3 Identification of geomorphic stationarity in the highly braided river system 107
5.4.4 Process-form relationships in the Brahmaputra River 108
5.5 Discussions 110
5.5.1 Energy dissipation processes in large braided river systems 110
5.5.2 Scale of planform evolution in large braided river 111
5.6 Freedom space for highly braided rivers: resilience-based management approach in the era of Anthropocene 114
5.7 Chapter Summary 117

6 SUMMARY AND FUTURE SCOPE

6.1 Summary 119
6.1.1 Process-form relationships in a weakly braided river system 119
6.1.2 Formulation of process-based recovery indicator for weakly braided river system 120
6.1.3 Understanding the process-form relationships and development of resilience-based management approach for a highly braided river system 121
6.2 Future Scope 121

Publications 123

APPENDIX A: ONE DIMENSIONAL MODELING 127

APPENDIX B: FIELD INVESTIGATIONS TO FLUVIAL SYSTEMS IN INDIA 129

References 131

LIST OF FIGURES

1.1	The continuum of braided channel patterns and corresponding study objectives.	03
2.1	Heterogeneity in fluvial controls along the Himalayan and peninsular rivers (a) High bank erosion in the Brahmaputra (Himalayan-highly braided-unregulated) (b) Debris load in the Brahmaputra (c) Composite banks and high sediment load in the Brahmaputra (d) Gravel bed in the Kameng (Himalayan-highly braided-unregulated) (e) Stable channel and sand bed in the Manas (Himalayan unregulated) (f) Steep slope and gravel bed in the Kopili (Himalayan regulated) (g) Mid-channel vegetated bar in the Brahmani (peninsular-weakly braided-regulated) (h) Mid-channel longitudinal bar in the Mahanadi (peninsular regulated) (i) Mid-channel diagonal bar dissection in the Ong (peninsular-weakly braided-regulated).	08
2.2	Total number of states-wise large dams in India (a) up to 1900 (b) 1901 to 1950 (c) 1951 to 1970 (d) 1971 to 1990 (e) 1991 and beyond (f) total. (g) Classification of large dams based on height and storage capacity. The large dams have been defined as per the classifications coined by the National Register of Large Dam (NRLD 2019).	12
2.3	Key works showing upstream impacts of dams in Indian rivers.	14
2.4	Key works showing downstream impacts of dams in Indian rivers.	17
2.5	Process-form-ecology interactions in an anthropogenically disturbed braided river	20
2.6	Hierarchical energy dissipation and yearly dynamics of a highly braided planform	23
2.7	(a) Conceptual diagram of process, form, and relaxation period variability to an event-driven disturbance along Himalayan River. (b) The possible alteration in the channel-forming effective discharge in the downstream of disturbance.	24
2.8	Field photographs of highly braided Brahmaputra River system (a) River freedom space developed from floodplain inundation (b) River freedom space due to fluvial erosion (c) Intensive morphological activity leading to bar formation (d) Stabilization of bar (island) through instream vegetation.	25

2.9	(a) The surface water variation (in percentage) along the Brahmaputra River. The image is obtained from cloud computing of JRC surface water layers in Google Earth Engine (GEE) platform. (b) Conceptualization of braided belt width dynamics and the disturbing factors in the last 100 years. (c) Conceptualization of resilience-based freedom space management concept.	27
2.10	(a) Conceptual diagram of process, form, and relaxation period variability to dam closure in a peninsular river. (b) The possible alteration in channel-forming effective discharge in downstream of the dam.	30
2.11	Conceptual diagram describing the geomorphic units and steps for recovery assessment in anthropogenically disturbed Himalayan and peninsular rivers.	32
3.1	The Brahmani River basin showing Rengali dam, and the upstream (Gomlai) and downstream (Talcher and Jenapur) gauging stations.	40
3.2	Field photographs of the Brahmani River in the post-dam period (a) Macrochannel bank (b) Inset channel, diagonal bar and chute channels (c) A lateral bar close to the flow boundary and (d) Vegetation on a mid-channel bar.	41
3.3	Cross-Plot between suspended sediment load ($\times 10^6$ t/day) and discharge (m^3/s) (a) Upstream (Pre-dam) (b) Downstream (Pre-dam) (c) Upstream (Post-dam) and (d) Downstream (Post-dam). The power function regression equations are significant at p~0.000, which consider the total sample size between the low flows and extreme events.	49
3.4	Variation of discharge class frequency in the Brahmani River (a) Upstream (Pre-dam) (b) Downstream (Pre-dam) (c) Upstream (Post-dam) and (d) Downstream (Post-dam). The flow duration is also shown, between solitary discharge values and percentage of time exceeding (PTE).	50
3.5	Sediment load histogram for (a) Upstream (Pre-dam) (b) Downstream (Pre-dam) (c) Upstream (Post-dam) and (d) Downstream (Post-dam) using the deterministic approach for class intervals of 0.25 S. The percentage of the total sediment load carried by low flow (LF), moderate flow (MF) and high flow (HF) flow classes are also shown.	51
3.6	Transport effectiveness plots for the Brahmani River (a) Upstream (Pre-dam) (b) Downstream (Pre-dam) (c) Upstream (Post-dam) and (d) Downstream (Post-dam). The maximum value of transport effectiveness is E_{peak}.	53
3.7	Seasonal transport effectiveness curve for (a) Upstream (Pre-dam) (b) Downstream (Pre-dam) (c) Upstream (Post-dam) and (d) Downstream (Post-dam) using the analytical approach.	54
3.8	(a)-(d) The study area for morphological analysis (near Jenapur) and the geomorphic units observed at Talcher and Jenapur in pre-dam and post-dam periods. (e) The	56

temporal variation of inset and chute channels lengths in the study reach. (f) A conceptual plot showing the link between observed geomorphic units, morphological analysis and process-based stream power estimation.

3.9 Meandering and braiding (SI and BR) variability with (a) Seasonal Stream Power (b) Peak Stream Power (c) Rising Limb Stream Power (d) Falling Limb Stream Power in pre-dam and post-dam periods. The threshold lines of side bar-mid bar (1000 W/m) and meandering-braided transition (4000 W/m) are also shown. 57

3.10 Potential unit stream power curve for the Brahmani River (near Jenapur) during (a) pre-dam period (b) normal year in post-dam period (c) drought year 2010 and (d) wet year 2011. 58

3.11 Relationship between probability of braiding (POB) and morphological variables (BR) for the Brahmani River. 60

3.12 (a) Stage converted bankfull (inset and macrochannel) and effective discharge (pre-dam and post-dam) in Brahmani River (b) Conceptual diagram showing geomorphic impacts of high-magnitude flood and hierarchy of energy dissipation in the Brahmani macrochannel. The energy-zone for the morphological continuum is also shown. (Q_b: macrochannel bankfull, Q_I: Inset channel bankfull) 64

4.1 Study area showing the Ong and Tel sub-basins of the Mahanadi River (India). 73

4.2 Field photographs showing the presence of instream and floodplain geomorphic units in the Ong-Tel paired catchment. (a) and (c) Macrochannel banks and instream vegetated geomorphic units in Ong River (b) and (d) Prevalence of diagonal bars and defined low-flow channel in Tel River. The dominant instream and riparian cover vegetation details are also shown along the two reaches. 75

4.3 The methodological flowchart for evaluation of process-based recovery indicator 77

4.4 The Survey of India (SOI) toposheets for (a) Ong (b) Tel Rivers (Courtesy of the University of Texas Libraries, The University of Texas at Austin). The instream geomorphic units present in the Ong (c and e) and the Tel (d and f) Rivers. The longitudinal variation of instream vegetated landforms for last the 35 years in (g) the Ong and (h) the Tel Rivers. The conceptual plots showing cross-sectional variability of plant biomass, fluvial disturbance and moisture availability in (i) the Ong and (j) the Tel Rivers. 82

4.5 Variation of flow (in m^3/s) and stage (in m- from MSL) along the (a) the Ong (1991-2011) and (b) Tel Rivers (1989-2011). 84

4.6 The temporal variation of yearly vegetation percentage, cross-sectional intensity entropy (CIE) and normalised river recovery index (NRRI) in (a) Ong (b) Tel Rivers. The linear trends of NRRI and temporal average-CIE are also shown. 84

4.7	Relation between normalised low-flow exceedance (LFE=N(Q≥QL)) and normalized river recovery index (NRRI) along (a) the Ong and (c) the Tel Rivers. The conceptual diagrams for the hierarchy of energy dissipation in macrochannel systems and dominant variables for the hotspot-zone of ecosystem engineering are also presented along (b) the Ong and (d) the Tel Rivers.	87
5.1	(a)-(b) The Brahmaputra River with the major southern and northern tributaries, and geological nodes. (c)-(e) Field photographs of the Brahmaputra River showing mid-channel bars, erodible banks with river training structures, and stable bank with riparian vegetation.	96
5.2	Temporal variation of alluvial deposits along the Brahmaputra River (1980-2020) (obtained from GEE cloud-based computing of Landsat imagery as suggested by Boothroyd et al., 2020). The outer boundaries of previous decades' alluvial deposits are also shown.	102
5.3	Spatio-temporal variability of bank migration rate in the Brahmaputra River.	103
5.4	Spatial variability of the location probability index for the Brahmaputra River using the time-driven and event-driven weighting processes.	105
5.5	Identification of geomorphic stationarity in the Brahmaputra River.	107
5.6	Relationship between normalised process gradient (NPG), normalised threshold exceedance (NTE) and morphological variable-SDBA for the Brahmaputra River	109
5.7	(a) Conceptual diagram showing two dominant thresholds (channel-forming discharges) and periodic oscillation of braided planform state in the morphological continuum. (b) Conceptual diagram showing a highly braided channel geometry with zone of morphological activities, high locational probability strip and interactions of process (fluvial energy)-form variables.	113
5.8	Conceptual diagram showing three dominant at-a-station hydraulic geometries and bank properties in the Brahmaputra River. (b) Relation between disturbance, resistance threshold and recovery, and temporal variation of system states. The variabilities of LPI, threshold, bank erosion potential and balance between nature-to-engineered solutions are also shown. (c) River freedom space concept and resilience-based management approach for a highly braided river system.	116

LIST OF TABLES

3.1	The size of class intervals (CI) and numbers of discharge classes (N) used in the evaluation of effective discharge.	43
3.2	Variation of discharge and suspended sediment concentrations in the Brahmani River	48
3.3	Analytical approach's result with effective discharge and log-normal distribution fitting parameters	52
3.4	Effective discharge estimation using the deterministic approach	53

LIST OF SYMBOLS

Symbol	Description
C	Suspended sediment concentration (g/L)
D_{50}	Bed particle size (m)
E	Transport effectiveness
E_{peak}	Peak Transport effectiveness
N	Flow discharge class
Q	Discharge (m^3/s)
Q_b	Bankfull discharge (m^3/s)
Q_e	Effective discharge (m^3/s)
Q_s	Sediment load in Tonnes/day (t/day)
S	Standard deviation of flow discharge class
S_E	Energy Slope
S_v	Valley slope
ω	Unit stream power (W/m^2)
Ω	Total stream power (W/m)
ω_{bm}	Threshold for moderately braided to highly braided
ω_{ia}	Threshold for immobile rivers to meandering with scrolls
ω_{pv}	Potential unit stream power (W/m^2)
ω_{sc}	Threshold for meandering with scrolls to weakly (moderately) braided

LIST OF ABBREVIATIONS

Terms	Description
BR	Braid-channel Ratio
CIE	Cross-sectional intensity entropy
GEE	Google earth engine
LFE	Low flow exceedance
LPI	Location probability index
MNDWI	Modified normalized difference water index
NDVI	Normalized difference vegetation index
NPG	Normalized process gradient
NRRI	Normalized river recovery index
NTE	Normalized threshold exceedance
POB	Probability of braiding
SDBA	Standard deviation of braided bar area
SI	Sinuosity Index
VI	Vegetation intensity

1

INTRODUCTION

Rivers are the pathways of water and sediment connecting landmasses and outfall points. The braided rivers consist of multi-channel flows having erratic morphological activities in a sediment-charged environment. In recent decades, the anthropogenic stresses in terms of flow-sediment regulation, sand mining, instream (or riparian) vegetation loss, and channelization have developed complex process-form relationships along the continuum of braided channel patterns (weakly to highly braided rivers). Understanding the braided river behavior and mechanism through hydrological data analysis, field investigations, numerical modeling, and cloud computing techniques can benefit their effective management. This thesis aims to work on comprehending the process-form relationships along the continuum of braided channel patterns.

1.1 MORPHOLOGICAL CONTINUUM

Rivers are believed to form a morphological continuum. This continuum is two-dimensional, defined by plan features (straight, meandering, braided) and structural levels of fluvial relief (floodplain, flood channel, low-water channel). The combinations of these categories define the diversity of patterns (Alabyan and Chalov, 1998). In particular, the braided rivers consist of a series of broad, shallow channels, bars and dry islands with elevated areas active only during floods (Miall, 1977). The channel hierarchies, flow stage,

scale of planform evolution, confluence-bifurcation zones, and grain size distribution form a continuum along the braided pattern. For example, weakly braided macrochannel systems are defined by dominant channel-in-channel physiography, where a smaller low flow channel is inset within a larger channel (Croke et al., 2014; Heitmuller et al., 2015; Thompson et al., 2016). Such channel form provides morphological adjustments space for features like benches, chutes and bars (Pradhan et al., 2021a). Similarly, the highly braided rivers sit at the extreme end of the continuum and are governed by large braided belt width variability, sand bar disorderness, erodible banks and erratic flow-sediment transport (Goswami, 1985; Chembolu et al., 2018). Therefore, a detailed understanding of river behavior and hydrodynamic characteristics is essential to plan, design, and maintain the braided rivers and associated short and long term fluvial issues,

1.2 PROCESS-FORM RELATIONSHIPS AND PERTINENT CONCEPTS

Processes are responsible for creating and reworking the *geomorphic units*- the building block of landforms (Fryirs and Brierley, 2022). The range of processes interacts and controls landscapes' patterns (form) at a particular locality (Brierley et al., 2013). Gregory (1978) proposes the way processes (P) operate on materials (M) over time (t) to produce form (F) as:

$$F = f(P, M)dt \tag{1.1}$$

In recent decades, the geomorphic units are also largely influenced by anthropogenic stresses. Significant progress has been made in quantifying this degree of disturbances, and slowly many pertinent concepts like metamorphosis, response, threshold (Schumm, 1979), timescales (Graf, 1977), style of change, order of impact (Petts, 1984), sensitivity, network, memory (Newson, 2002), recovery potential (Fryirs and Brierley, 2000), freedom space (Buffin-Belanger et al., 2015), resilience have been postulated. Still, challenges remain in comprehending the mutual and complex interactions between slope, flow-sediment transport, vegetation cover, ecosystem engineers, anthropogenic and memory imprints for different geomorphic units. This information is vital to model and interprets process–form relationships and behavioral traits that define the expected range of variability of different river types (Fryirs and Brierley, 2022).

The previous literature on braided rivers suggests an excellent quantitative understanding of changes along flow-sediment, morphological, and ecological variables. However, the

present knowledge is still limited in studying the process-based cause and effect of natural and anthropogenic stresses in the continuum of braided channels and their impact on hydro-morphological-ecological processes occurring during the relaxation period. For example, very few studies have addressed the effects of dam closure on alteration of channel-forming effective discharge along the weakly braided rivers. Furthermore, the identification of recovery potential in multi-channel rivers is still in the preliminary stages, and there is a need to develop a new inter-disciplinary multifaceted approach to understand the complex process-form relationships in these anthropogenically disturbed river systems. In addition, very few studies have analyzed the long-term morphological evolution and resilience-based management concept for the highly braided river systems.

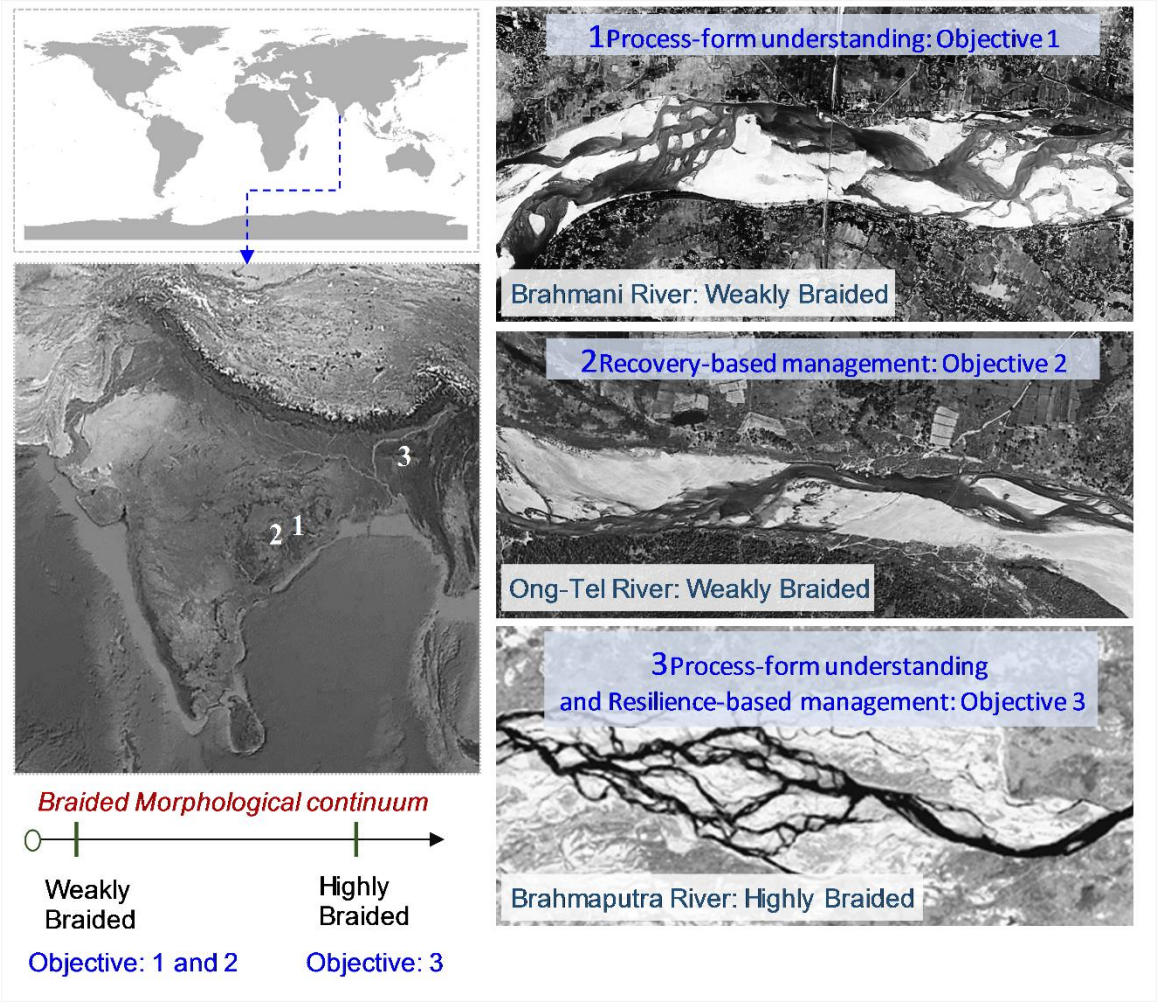

Figure 1.1 The continuum of braided channel patterns and corresponding study objectives.

1.3 AIM AND OBJECTIVES OF THE THESIS

Considering the research needs with an emphasis on understanding the behavioral regime of multi-channel flows, the aim of the thesis is outlined as-study of the process-form relationships in the continuum of braided channel patterns, with the following objectives:

- To understand the process-form relationships in a weakly braided macrochannel river system
- Formulation of river recovery index for a paired weakly braided river system using entropy and cloud computing techniques
- To investigate the process-form relationships in a highly braided river system and the development of a freedom space-based resilience approach.

1.4 ORGANISATION OF THESIS

The research work in this thesis is presented in six chapters. The thesis focuses on understanding the process-form relationships along the continuum of braided channel patterns through hydrological data analysis, field investigations, hydrodynamic modeling, and cloud computing techniques. The thesis is divided into chapters based on the objectives of the present study. The chapter-wise description of the thesis is

- *Chapter 1* discussed the overview of process-form relationships, morphological continuum, and pertinent concepts followed by the aim and objectives of the thesis.
- *Chapter 2* reports a literature review and conceptualizes the continuum of braided river, anthropogenic stresses, and management approaches necessary for the present research.
- *Chapter 3* deals with the process-form understanding of a regulated, weakly braided river system and the channel-forming forming discharge theory and morphological analysis.
- *Chapter 4* deals with the recovery-based management approach of anthropogenically disturbed weakly braided river system with entropy theory and cloud computing techniques.
- *Chapter 5* studies the process-form relationships, morphological variables and resilience-based management approach of a highly braided river system with a multi-faceted approach.

- *Chapter 6* summarizes the present research and suggests the future scope of the current work.

2

SYNTHESIS OF LITERATURE AND CONCEPTUALIZATION

The formation and dynamics of multi-thread flows or braided channels are complex in nature. This planform state signifies diversities in flow-sediment-morphodynamics-vegetation interactions at various spatio-temporal scales. The flow-sediment transport associated with periodic flood events can cause complex morphological alterations in different shapes, sizes, and spatial distributions. In addition, the abundant amount of the sediment loads may generate hierarchical bar patterns and variations in bed elevation and braided belt width (Bristow, 1987; Bridge, 1993; Skelly et al., 2003; Kelly, 2006). The channel processes are also governed by riparian (or instream) vegetation, bank erosion, river training measures, and anthropogenic stresses. Therefore, a complex process-form relationship is developed due to channel migration, the inundation of floodplains and riparian wetlands along the braided rivers. A synoptic understanding of braided rivers, process-form heterogeneity, and pertinent concepts in river science are discussed here.

2.1 BRAIDED RIVER

The synthesis of literature pertaining to braided rivers suggests that most of the studies are focused on understanding the process-form interactions through physical modeling (Rosatti, 2002; Hundey and Ashmore, 2009; Sun et al., 2015; Leduc et al., 2019; Chembolu et al., 2019), numerical approaches (Karmaker and Dutta, 2016; Williams et al., 2016; Bankhead et al., 2017; Javernick et al., 2018; Pradhan et al., 2021a; Dubey et al., 2021), and advanced geo-spatial techniques (Lane et al., 2003; Boruah et al., 2008; Bertoldi et al., 2013; Pradhan et al., 2017; Chembolu and Dutta, 2018; Pradhan et al., 2019; Dubey et al.,

2020). However, very few studies have analysed the effect of variable anthropogenic stresses on the long-term morphological evolution of braided river systems. In addition, the integration of 'pertinent concepts in river science' into river corridor management programs will facilitate a sustainable way to manage Indian rivers, where anthropogenic stress and fluvial disturbances are gradually increasing (Pradhan et al., 2021a). Therefore, the present chapter is focused on understanding the process-form heterogeneity of braided river systems, variable anthropogenic stresses and will further attempt to conceptualize management approaches in the background of Indian river systems.

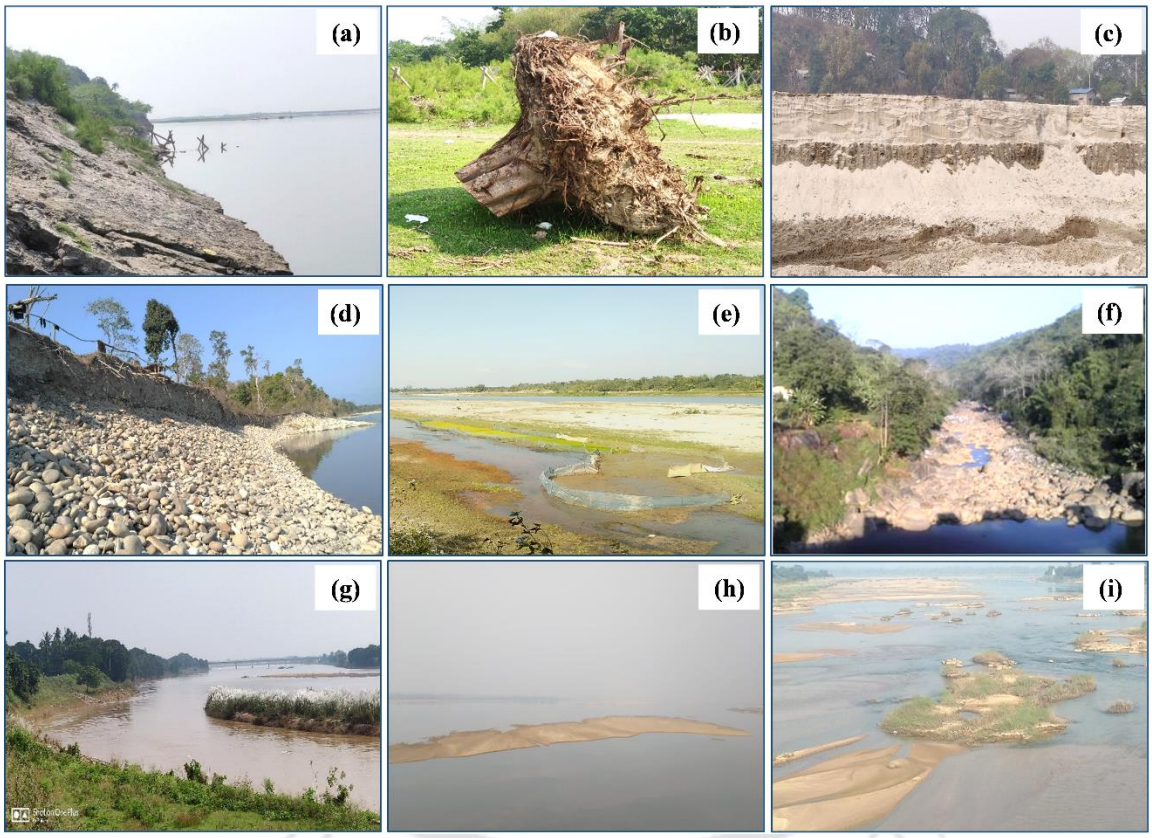

Figure 2.1 Heterogeneity in fluvial controls along the Himalayan and peninsular rivers (a) High bank erosion in the Brahmaputra (Himalayan-highly braided-unregulated) (b) Debris load in the Brahmaputra (c) Composite banks and high sediment load in the Brahmaputra (d) Gravel bed in the Kameng (Himalayan-highly braided-unregulated) (e) Stable channel and sand bed in the Manas (Himalayan unregulated) (f) Steep slope and gravel bed in the Kopili (Himalayan regulated) (g) Mid-channel vegetated bar in the Brahmani (peninsular-weakly braided-regulated) (h) Mid-channel longitudinal bar in the Mahanadi (peninsular regulated) (i) Mid-channel diagonal bar dissection in the Ong (peninsular-weakly braided-regulated).

2.2 HETEROGENEITY OF FLUVIAL CONTROLS

Indian rivers can be generally classified into four categories- Himalayan rivers, peninsular rivers, coastal rivers, and inland drainage rivers (Sinha et al., 2019). The major Himalayan rivers are Indus, Ganga, and Brahmaputra. The peninsular rivers can be east-flowing rivers like Brahmani, Mahanadi, Godavari, Krishna, and Cauvery and west-flowing rivers like Narmada and Tapti. The coastal rivers are relatively small and typically flow on the west coast of India. Inland drainage rivers like the Luni and the Macchu drain for some distance and get lost with no outlet to the sea.

Indian rivers are subjected to large variability in fluvial controls and display complex process-form interactions (Figure 2.1). Based on temperature and precipitation, six climatic zones (highland, humid subtropical, tropical wet and dry, arid, semi-arid, and tropical wet) are defined on the Indian subcontinent. The spatial distribution of rainfall pattern suggests some parts of north-west India receives less than 600 mm average annual rainfall. In contrast, the western coast, Western Ghats, and sub-Himalayan region of the northeast have an average annual rainfall of more than 2000 mm. The geological regions can be broadly classified into the Himalayas, the Indo-Ganga plain, and the peninsular shield. In addition, based on the genesis, color, composition, and location, the soils of India have been classified into alluvial (Gangetic plains), black (central-west India), red-yellow, laterite, arid, and forest soils. As per the Bureau of Indian Standards, there are four seismic zones (II-V), with the entire Brahmaputra River basin lying on the earthquake-prone zone V. Such climatic and geological influences together with varying soil conservation practices, land cover, river training measures, and anthropogenic disturbances generate heterogeneity in antecedent and flux fluvial controls. For example, the sediment load-carrying capacity of the Himalayan (Ganga-Brahmaputra) and peninsular rivers are at the opposite ends of the continuum (Figure 2.1c and 2.1g). The Ganga-Brahmaputra and Indus contribute 863 Million ton of annual suspended load to the ocean. On the contrary, the peninsular rivers collectively transport about 83 Million ton of sediment (Gupta et al., 2012). Furthermore, because of the strong seasonality of floods, the peninsular rivers can have maximum discharges in thousands of cumecs, yet run dry in that same year (Syvitski et al., 2014). Such large variability of the flow-sediment regime produces different morphological settings along Indian rivers. The Ganga has spatial variability of meandering and braided channel patterns, whereas the Brahmaputra is a highly braided river characterized by frequent bank erosion, thalweg migration, and severe morphodynamics (Chembolu and

Dutta, 2018). In contrast, the peninsular rivers are relatively more stable, weakly braided (macrochannel), flow through wide and shallow valleys and respond to moderate and extreme floods (Kale, 2003). Therefore, modifying the boundary conditions through anthropogenic stresses can disturb the existing process-form-ecology linkage and associated feedback mechanisms. The scale and intensity of disturbances may bring a static or non-linear response of morphological adjustments. Such changes may have temporal and spatial (pattern and extent) distributions along the impacted reaches.

2.3 IMPACTS OF ANTHROPOGENIC STRESSES

The idea of regulating a river started with the onset of ancient civilizations in India. India is the third-largest dam-building nation globally, with more than 5000 dams operating in different rivers. A recent study suggests that India's energy demand will grow by 4.2% a year for the next three decades, faster than any major economy (Economictimes, 2019). Therefore, Indian rivers will experience an accelerated increase in dam-building activity to facilitate clean energy, improved irrigation, and flood control in the near future.

The large dams impose an artificial flow regime and disrupt the sediment transfer between the linked river segments (Petts and Gurnell, 2005). For example, the reservoirs across Asia regulate up to 14% of total river run-off (Beaumont, 1978) and the decline in sediment fluxes to both the Bay of Bengal and the Arabian sea is proportional to the number of mega dams present in their respective catchments (Gupta et al., 2012). The artificial flow-sediment regime also induces channel morphology and ecology changes, and many Indian regulated rivers are experiencing alterations in channel pattern and vegetation-fish-macroinvertebrate habitats (Banerjee, 1999; Bahuguna et al., 2004; Islam and Guchhait, 2017). In addition, shrinking of delta, coastal erosion, saltwater intrusion, and reduction in mangrove density are conceived as emerging challenges in these rivers (Malini and Rao, 2004; Gopal and Chauhan, 2006; Rajawat et al., 2015). Recent advances in fluvial research have provided the background to understand the dam-induced changes in Indian braided rivers. Most of the studies are focused on the downstream impacts of large dams and studies dealing with the backwater associated bio-geomorphological processes are limited in Indian rivers. Furthermore, this quantitative understanding needs conceptual schemes and future research priorities to comprehend the dam-altered process-form relationship in the transient states of complex relaxation paths. The present chapter updates the knowledge of the growth of large dams in India with a detailed review of the research on the upstream

and downstream effects. Then, based on the review and synthesis, the present chapter proposes conceptual frameworks to study the anthropogenic stress-altered channel-forming discharges in highly braided Himalayan and weakly braided peninsular rivers. Then, this chapter discusses the utility and role of riparian vegetation with due emphasis on recovery potential. Finally, the development of a resilience-based management approach is proposed for the braided rivers.

2.3.1 Dams in India: A Growth Statistics

India has a long history of damming rivers. The Kallanai dam (also known as the Grand Anicut) is one of the oldest dams in human history (Agoramoorthy, 2015). This structure was built around 200 AD across the Cauvery river to support farmers with irrigation water. Similarly, other notable early dams were the Veeranam lake (907-955 AD), the Mudduk Maur dam (1500 AD), and the Meer Allum dam (1804-1808 AD) (Chaturvedi, 2015). Before 1900, India had 67 large dams, out of which 22 were present in the state of Maharashtra (Figure 2.2a). The heights of these dams were less than 50 m, which shows the absence of mega dam in India. However, in the next fifty years (1901-1950), the total number of large dams increased five times. Most dams were present in drought-prone central-western states like Maharashtra, Madhya Pradesh, and Gujrat. In this period, six mega dams with a height above 50 m and two mega dams of national importance (K.R. Sagara and Mettur) were constructed in addition to 306 small height large dams (Figure 2.2b and 2.2g). The following two decades (1951-1970) witnessed an accelerated increase in dams having national importance. Mega dams such as Bhakra, Tungabhadra, Koyna, Hirakud, and Nagarjuna Sagar started improving flood control, irrigation, and hydropower generation (Figure 2.2c). These projects were the symbol of modern India and continue to be among the largest and highest dams in the world (Outlookindia, 2017). Both dam construction and operation were at their peak between 1970 and 1990. The number of small height large dams (10-15 m) increased four times, whereas mega dams of national importance tripled their number in a twenty years (Figure 2.2g). In addition to major dam-building central-western states, other south-eastern states like Odisha, Karnataka, and Tamilnadu escalated the river regulation through large to mega dams. Since 1990, the numbers of both small height large dams and mega dams have slightly reduced. Currently, India hosts about 2453 small height dams, 3321 large dams with height more than 15 m, 480 large dams with height more than 15 m or storage more than 60 million cubic meters, 191 mega dams with height more than 50 m, and 70 mega dams of national importance,

being operated or under construction in different rivers (NRLD 2019). This makes India the third largest dam-building nation globally (after China and US) and demands a thorough investigation of the regulated braided rivers.

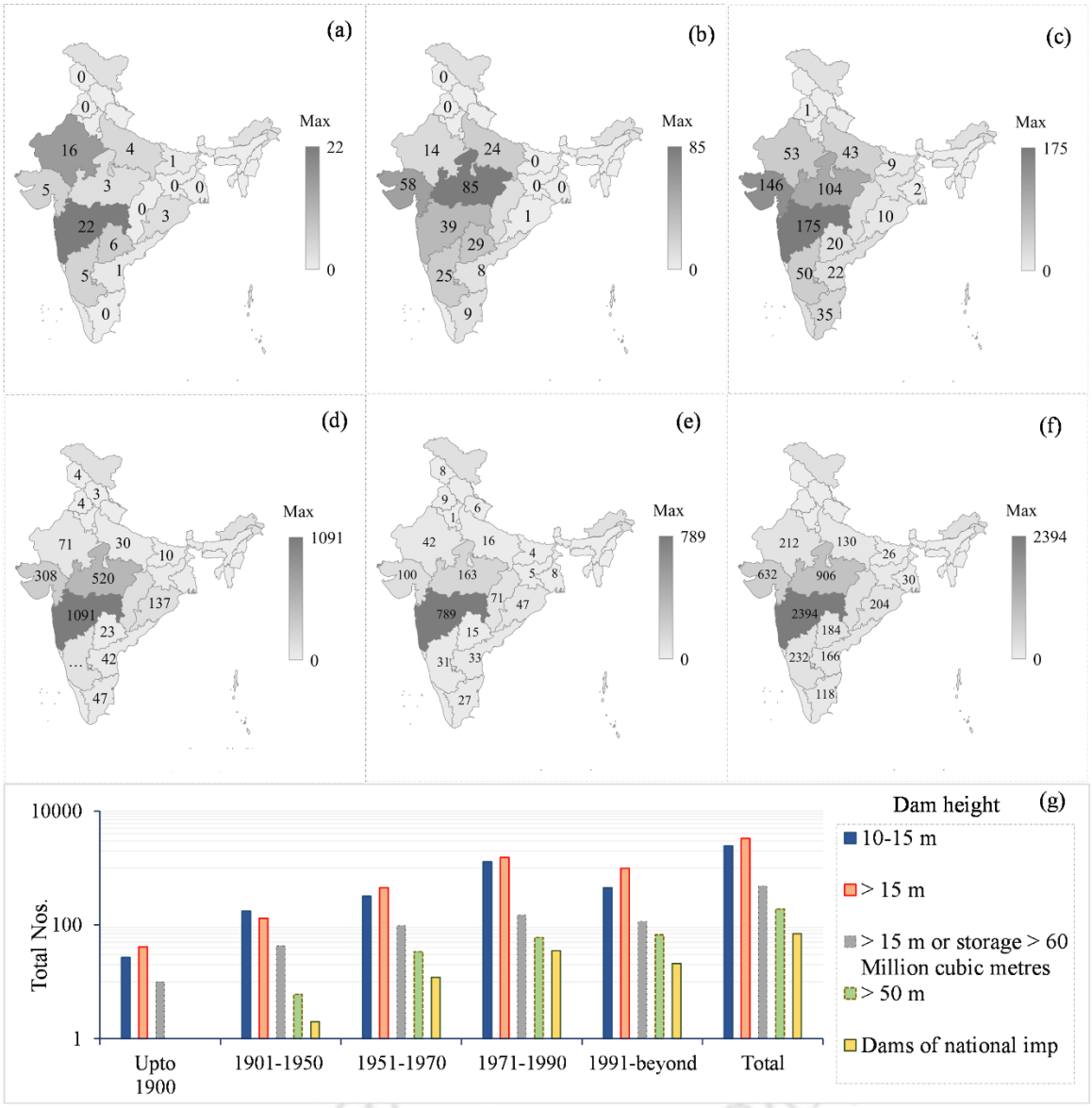

Figure 2.2 Total number of states-wise large dams in India (a) up to 1900 (b) 1901 to 1950 (c) 1951 to 1970 (d) 1971 to 1990 (e) 1991 and beyond (f) total. (g) Classification of large dams based on height and storage capacity. The large dams have been defined as per the classifications coined by the National Register of Large Dam (NRLD 2019).

2.3.2 Upstream Impacts of Dams

Reservoir sedimentation is well documented (NRLD, 2019) and many data-driven geospatial techniques have been developed to understand and monitor the trapping of sediment behind Indian large dams (Goel et al., 2002; Jain et al., 2002; Jothiprakash and Garg, 2009; Majumder et al., 2012; Narasayya 2013; Garg and Jothiprakash, 2013; Arunbabu et al., 2014; Pandey et al., 2016; Tiwari et al., 2016; Shukla et al., 2017; Tiwari and Jaiswal, 2017; Prasad et al., 2018). The deposition occurs at the head of the reservoir and sediment enters the backwater zone (Chaudhuri 2006). The sedimentology and upstream propagation of coarse and fine particles are also different, and depend upon the source areas, reservoir operation policies, and backwater effects (Liro, 2016; Pal, 2017). The upstream section of the dam, which is temporarily inundated during the reservoir stage above than normal is defined as the backwater fluctuations zone (Liro, 2019). A little is addressed about the backwater effects in Indian braided rivers and the studies dealing with backwater induced biogeomorphological processes are scarce (Figure 2.3). An earlier study by Singh (1968) has emphasized the extension of the stage-discharge relationship for backwater computations in the Ramganga dam project and the development of suitable correlations for varying friction slopes. Similarly, Amarnath and Thatikonda (2020) has assessed the backwater effect of the Polavaram dam using flood frequency analysis and HEC-RAS flow hydraulic model. Theoretical analysis and physical modeling are also helpful in estimating the backwater profile due to varying gate operations and pond levels in alluvial channels (Barman et al., 2014).

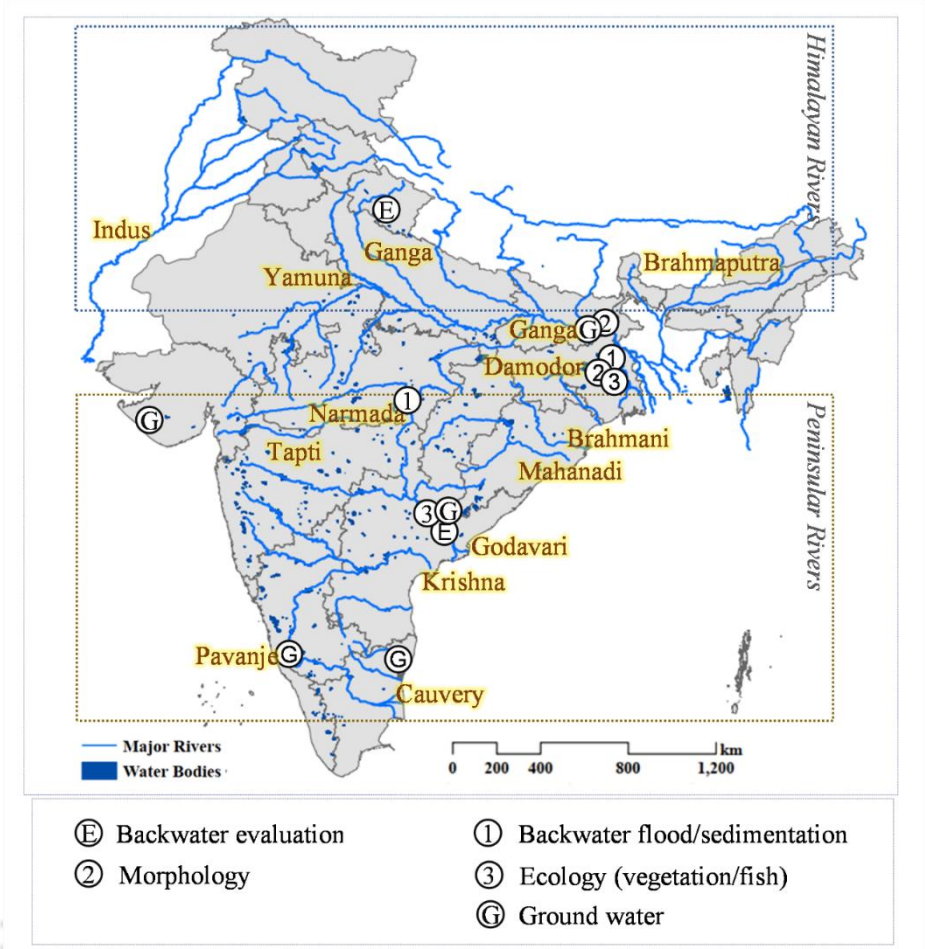

Figure 2.3 Key works showing upstream impacts of dams in Indian rivers.

The fluctuations in river flow and reservoir stage affect the backwater and its dependent fluvial processes (Liro, 2014). A few recent works reported the backwater effects of the Sanjay Sarovar dam (Kudnar, 2020) and Tilpara barrage (Pal, 2017). The study by Pal (2017) revealed that tributaries are affected by channel sedimentation, which triggers more flooding in the backwater reach. In addition, morphological adjustments like reduction in channel carrying capacity, bed slope, and flow velocity have been reported upstream of the barrage. The increase in silt and clay content has also improved the bank resistance, followed by a rise in channel sinuosity. The intensive sediment deposition may disturb the braiding character in the backwater zone. For example, bank-attached islands are established due to the attenuating river flow condition in the Kushkarni River (Pal, 2017). Similarly, the Farakka barrage in the Ganga River has profound impacts on the upstream reach (Mirza, 2004; Parua, 2010) and braiding is initiated by the gradual emergence of sand bars (Banerjee, 1999; Rudra, 2006). The interactions and feedbacks between abiotic (flow, sediment, and morphology) and biotic (vegetation, animals, and human) are crucial

components of the backwater fluvial system. The backwater induced changes in morphology and sediment transport impact the seed germination and plant growth, which further control the bio-geomorphic succession (Liro, 2019). The fine-grained sediment deposition on bedforms and astride banks has increased vegetation cover and bank resistance in the upstream reach of the Tilpara barrage (Pal, 2017). The fluvial processes and form constitute a continuum along the river and longitudinal connectivity plays a significant role in sediment and nutrient transport between the sources and sinks. Artificial barriers like dams and barrages alter this connectivity and disturb the migration of aquatic species between the linked river segments. In particular, fish communities are excellent biological and ecological integrity indicators because of their continuous exposure to changing flow conditions (Khedkar et al., 2014). A barrage in the Giri River has caused a decrease in fish diversity and habitat fragmentation (Rumana et al., 2015). The Farakka barrage has also disrupted the natural migration of valuable Hilsa fish (*Tenualosa ilisha*) from the sea (Banerjee, 2009). Although dams have disturbed the fish species distribution in the Godavari river basin, the reservoirs have positive effects by supporting a high-level fish diversity (Khedkar et al., 2014). Therefore, fisheries conservation and management are vital, as reservoirs may provide a stable environment throughout the year.

Naganna and Deka (2018) addressed the streambed hydraulic conductivity variability in the Pavanje River basin located in the mountainous, forested area of the Western Ghats. This study revealed that dam-induced sedimentation affects the hyporheic processes and high streambed hydraulic conductivity was observed near the backwater areas. Backwater fluctuations also influence groundwater level, aquifer storage and associated biogeomorphic processes. For example, the groundwater level experienced a rise in upstream of the Farakka barrage (Banerjee, 2009). In addition, small height check dams have established improved rainfall recharge and facilitated an increase in aquifer storage, groundwater quality and quantity along different Indian rivers (Muralidharan et al., 2007; Niranjan and Srinivasu, 2012; Renganayaki and Elango, 2013; Thiyagarajan et al., 2020).

2.3.2 Downstream Impacts of Dams

Dams disrupt the transfer of sediments from the headwater sources and impose an altered flow-sediment regime in downstream (Petts and Gurnell, 2005). Several studies have provided the background to underpin the downstream impacts of large dams in Indian rivers. These large dams are responsible for (i) changes in low flow (Ray and Sarma, 2011;

Abe and Joseph, 2015; Uday Kumar and Jayakumar, 2018; Pradhan et al., 2019; Sharma et al., 2021), (ii) alteration of the extreme flood (Ray and Sarma, 2011; Ghosh and Guchhait, 2016; Pal, 2016; Khan et al., 2018; Udaya Kumar and Jayakumar, 2018; Sharma et al., 2021), and (iii) modification of sediment transport (Ramesh and Subramanian, 1988; Gupta and Chakrapani, 2005; Gupta et al., 2012; Bastia and Equeenuddin, 2016; Khan et al., 2016; Pal, 2016; Khan et al., 2018; Panwar et al., 2020) (Figure 2.4).

The altered flow-sediment regime drive changes in channel form along the downstream regulated reaches (Petts and Gurnell, 2005). These changes can be cycles of erosion, deposition, armoring, incision, thalweg migration, bank erosion, tributary rejuvenation, or a complete transformation (metamorphosis). A review of the studies dealing with downstream impacts of Indian dams revealed that quantification of the morphological adjustments is well understood at different spatio-temporal scales. For example, Ghosh and Guchhait (2014) reported that bankfull discharge is decreased in the post-dam period and regulated monsoon flow has increased the channel sinuosity in the Damodar River basin. Numerous studies have also explained the channel dynamics and morphological adjustments (sand bar formation, bank erosion, channel oscillation, and meander geometry evolution) in the downstream reaches of the Farakka barrage (Basu, 1976; Banerjee, 1999; Parua, 2010; Islam and Guchhait, 2017; Islam and Guchhait, 2020; Das et al., 2020). Similarly, the Mayurakshi River has undergone morphological adjustments like narrowing of active channel, coarsening of bed material, lowering of lateral stability, and accelerated rise of braiding after the construction of Massanjore reservoir (Pal, 2016). Furthermore, peninsular river like Brahmani has reported initiation of braiding and vegetation growth on mid-channel bars in the downstream reach of the Rengali dam (Figure 2.2g) (Pradhan et al., 2017; Pradhan et al., 2019). The geomorphic effects of floods created by the southwest monsoon are impressive in Himalayan regions (Kale, 2003; Sanyal, 2017) and the studies dealing with complex morphodynamics along regulated Himalayan rivers are of crucial importance. Borgohain (2019) and Borgohain et al., (2019) addressed the channel changes (bankfull width, sinuosity, and braiding) and erratic bank erosion patterns in Dikrong River in relationship with the altered hydrological regime caused by the Ranganadi hydel project. Moreover, Sanyal (2017) made several important observations regarding possible bed changes in regulated Teesta river using Delft3D morphodynamics modeling and field observations.

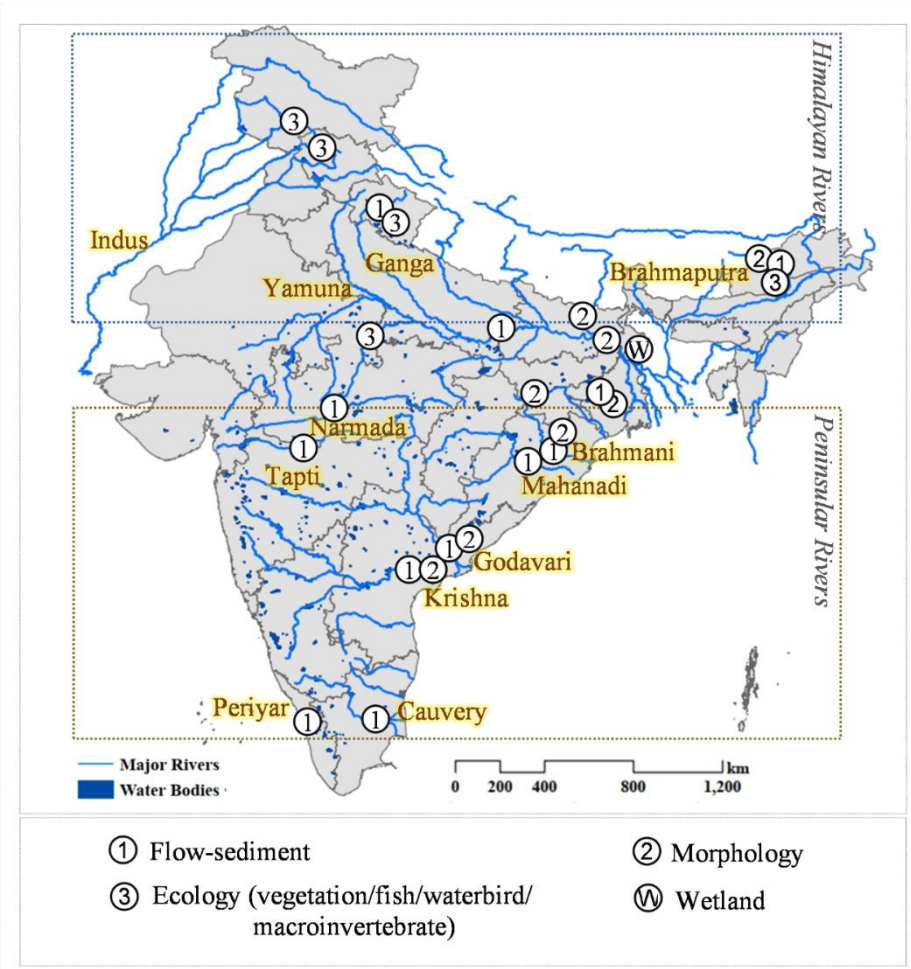

Figure 2.4 Key works showing downstream impacts of dams in Indian rivers.

The interaction of flow, sediment, and channel form determines biotic and abiotic successions, the spatial pattern of habitat functioning, and the ecological integrity of river systems. In regulated rivers, an altered flow sediment regime may bring a disconnectivity in ecological interactions (Jain et al., 2016) which triggers loss or fragmentation of freshwater habitats (Zhao et al., 2006) and disturbance in environmental flow (Bassi et al., 2014). The riverine wetlands can reduce the flood intensity and are usually considered as a natural substitute for dams (Boyd and Banzhaf, 2007). An earlier study by Foote et al., (1996) noted that inundation by dammed reservoirs is one of the controlling factors for wetland loss across India. Similarly, riparian wetland area is attenuated after damming and water diversion in the Punarbhaba river basin (Talukdar and Pal, 2017). Artificial impoundments also have both positive and negative impacts on aquatic habitats and bird species. The Pong reservoir has considerably increased the waterbird species and diversity

(Pandey, 1993). Such reservoirs may be necessary for water-bird conservation as waterfowl habitats are being reduced due to extensive drainage of wetlands in the northern India.

Comprehensive literature is established on the downstream impacts of Indian dams on aquatic and terrestrial invertebrates, fish communities, and riparian plant species. Several factors like the type of channel, condition at dam closure, mobility of boundary conditions, establishment and colonization of riparian vegetation, and tributary discharges and sediment load affects these species diversity and succession (Petts and Gurnell, 2005). Ncube et al., (2018) have noted a positive hydroecological relationship between macroinvertebrate index and seasonal changes in the regulated flow regime of the Beas River. Similar quantitative studies like Bahuguna et al., (2004) in the Ganga River, Hazarika et al., (2013) in the Subansiri River, and Singh et al., (2019) in the Alaknanda River have also addressed the relationship between macroinvertebrate diversity, density, and composition with the flow regulation. The creation of reservoirs may facilitate suitable fish spawning habitats and at the same time, many endemic fish species are adversely affected in the downstream reach (Sehgal, 1999). For instance, a dam on the Beas River has considerably reduced *Mahseers and Schizothoracines* fish species in just twenty years (Sehgal 1990). The channel-floodplain connectivity also plays a significant role in fish habitat breeding and nourishing. In the Subansiri River, dam construction along with soil deposition, deforestation, mainstream diversion, gravel collection, the establishment of stone crushers, and deposition of flushing sediments have affected the fish species in the immediate downstream reaches (Bakalial et al., 2014). Lakra et al., (2010) noted that fish diversity, habitat ecology, and conservation issues in the Betwa River and highlighted a vital issue of fish habitat fragmentation resulting from various river interlinking and intervention projects.

Artificial impoundment disturbs the watershed sediment yield, riparian communities, and mangrove habitats (Nilsson and Berggren, 2000) and creates challenges like saltwater intrusion and coastal erosion. For instance, the Farakka Barrage has affected freshwater flows to Bangladesh part of the Sundarban ecosystem (Gopal and Chauhan, 2006). In recent years, coastal erosion has emerged as a severe problem for the Indian coastline (Rajawat et al., 2015) and intensive sediment flux alteration in the peninsular rivers is one of the responsible factors. Malini and Rao (2004) revealed that sediment supply reduction due to dam construction across the Godavari river basin might be the major cause of shoreline erosion. Similarly, in the Krishna and Godavari rivers, a net erosion of 76 sq.km delta coast

is observed between 1965 and 2008, further affecting the sea level rise and coastal submergence (Rao et al., 2010). Out of 30 world river basins identified as global level priorities for protecting aquatic biodiversity, nine basins are in India (Cauvery, Ganges-Brahmaputra, Godavari, Indus, Krishna, Mahanadi, Narmada, Pennar and Tapi) (Jain and Kumar, 2014). Therefore, National Water Policy (2002 and 2012) and CWC (2007) guidelines have been formulated concerning the environmental flow (EF) to ensure the sustainment and functioning of in-stream and coastal ecosystems in Indian regulated rivers. Different methods have also been proposed to assess EF in Indian rivers, such as (i) linking of flow duration curve to environmental management classes (Smakhtin, 2006) (ii) assessment of bed submergence by different flow releases (Kumar et al., 2007) (iii) determination of the most favorable flow conditions for maintenance of aquatic life (DHI 2006) and (iv) building block methodology (WWF, 2012; Barik et al., 2014). However, despite the emergence of several assessment tools, EF science is in the preliminary stage as the knowledge base for approximate EF calculation is limited in India. Hence, a sincere effort is required to integrate and develop hydrology-ecology relationships, refine existing methods, and assess hydraulic habitat requirements (Jain and Kumar, 2014).

2.4 CONCEPTUALIZATION AND A BASIS FOR FUTURE RESEARCH IN BRAIDED RIVERS

Lane's regime theory ($Q_wS \sim Q_sD_s$) addressed the process-form relationship in alluvial rivers. This concept establishes a natural equilibrium between the discharge (Q_w) and sediment load (Q_s), which further controls the hydro-morphological responses such as channel slope (S) and bed particle size (D_s). Afterward, many geomorphologists formulated several pertinent concepts in fluvial geomorphology like the magnitude-frequency approach (Wolman and Miller, 1960), space-time-causality (Schumm and Lichty, 1965), river metamorphosis (Schumm, 1969), threshold (Schumm, 1977), rate law of channel adjustment (Graf, 1977), the role of vegetation (Wolman and Gerson, 1978), order of impact (Petts, 1984), and recovery (Fryirs and Brierley, 2000).

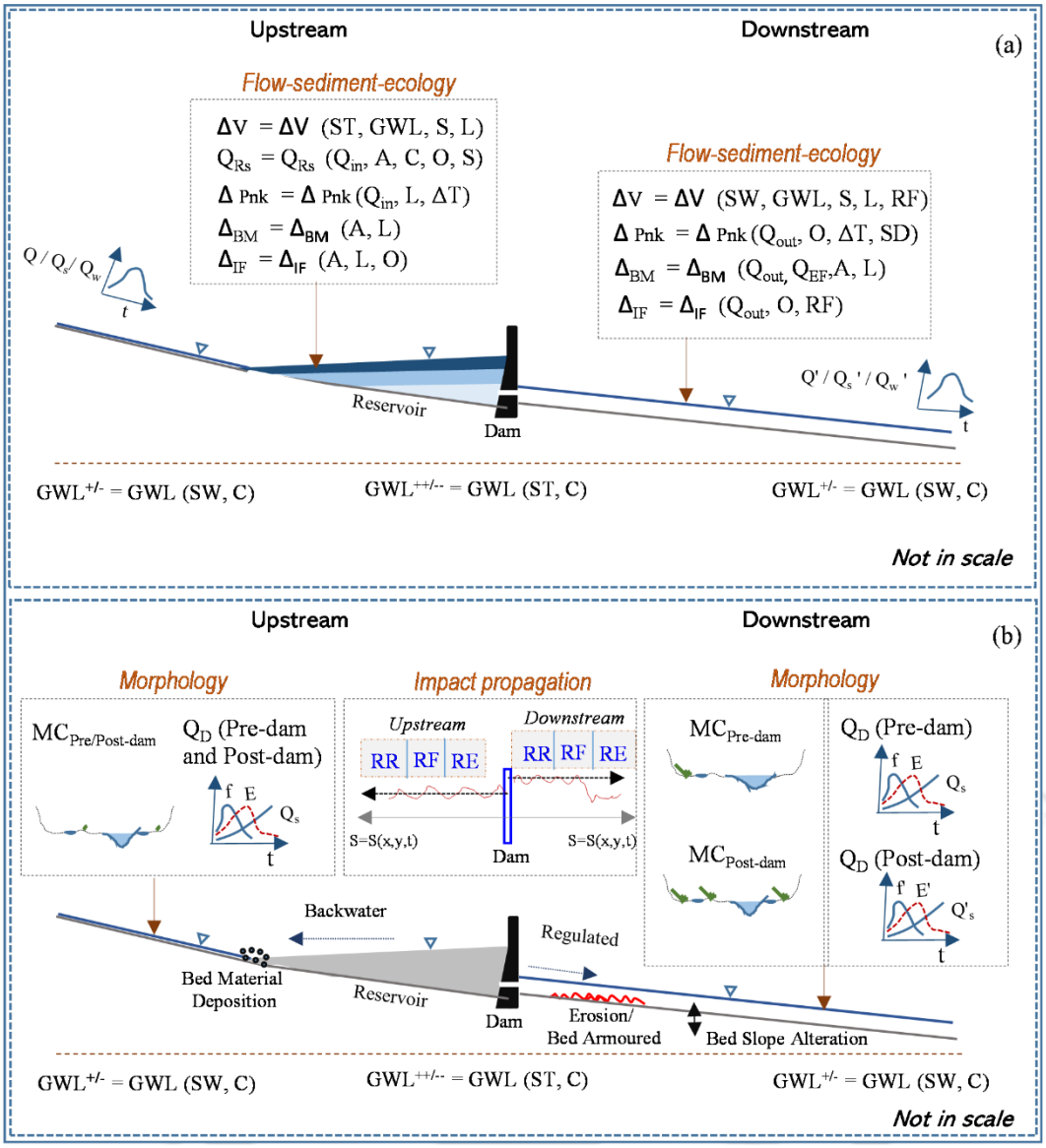

Legends

- → +
Change in thermal regime (ΔT)

+/- : Minor change
++/-- : Major change
ΔV : Change in vegetation
Q_{Rs} : Reservoir sediment storage
Δ Pnk : Change in plankton assamblages
Q : Flow
Q_s : Sediment load
Q_w : Water quality
Q_{EF} : Environmental flow
Q_D : Dominant discharge
f : Frequency of discharge
E : Geomorphic effectiveness
S (x,y,t) : Spatio-temporal variation

ST: Reservoir stage level
GWL: Ground water level
S: Gradient of drawndown zone
L: Location
Q_{in}: Inflow to reservoir
Q_{out}: Outflow from reservoir
A: Reservoir Area
C: (Upstream) catchment characteristics
O: Outflow operation
S: Storage capacity of reservoir
SW: River stage level
SD: Seasonal developement pattern
RF: River Floodplain connectivity
MC: Macochannel/ Underfit Channel
RR: River recovery
RE: River equilibrium

Figure 2.5 Process-form-ecology interactions in an anthropogenically disturbed braided river

A dam closure may generate new complex responses and modify the pertinent knowledge in the natural flow–sediment regime. The relaxation period describes the transition from natural to adjusted regime states, consisting of several transient sequences of reaction and adjustment phases (Figure 2.5) (Petts and Gurnell, 2005). This period may vary on a decadal to millennia scale (Petts and Gurnell, 2005), depending upon the geographic and geomorphic characteristics, intensity and magnitude of alteration, dam operation policies, and rate of vegetation establishment. The literature reviews on regulated rivers suggest an excellent quantitative understanding of downstream changes along flow-sediment, morphological, and ecological variables. However, our knowledge is still limited in studying the process-based cause and effect of dam closure in monsoon-dominated highly braided Himalayan and weakly braided peninsular rivers and its impacts on hydro-morphological-ecological processes occurring in the relaxation period. For example, very few studies have addressed the effects of dam closure on alteration of channel-forming effective discharge along weakly braided rivers. Furthermore, the identification of recovery potential in regulated rivers is still in the preliminary stages and there is a need to develop a new inter-disciplinary multifaceted approach to understand the complex process-form relationships in these anthropogenically disturbed braided river systems.

2.4.1 Relaxation period and process-form relationships in highly braided Himalayan rivers

The Himalayan rivers are characterized by the distinct spatio-temporal distribution of geomorphological and ecological units (Figures 2.1a to 2.1f). In particular, the Brahmaputra River and its tributaries exhibit different geomorphological elements based on their orientation, position, obstruction, flow stage, and shear zone formation. Moreover, convex bars (compound, diagonal, longitudinal, side-channel, lateral, and eddy bars), planner element (bench), and concave channels (chute, shallow thalweg, secondary and tertiary channels) are the dominant in-channel geomorphic units. The in-channel and floodplain geomorphic units show various rates of landscape adjustments (bar dissection, thalweg migration, and bank erosion) and are sensitive to event-driven (earthquake), direct (dam closure, removal of vegetation and wood), and indirect human disturbances (forest clearance, afforestation, urbanization and sand mining). Chembolu and Dutta (2018) studied the temporal variability of sand bar adjustments in the river and concluded that, during the post-monsoon season, the large bars were dissected into smaller bars, resulting in an increased entropy state. In addition, Akhtar et al., (2011) concluded that with a

temporal declination of unit stream power, the braiding process had increased in the Brahmaputra River. The wandering of thalweg or drastic changes in bed configuration is frequent in the highly sediment-charged environment of the Brahmaputra River (Coleman, 1969). The seasonal variability of primary channel shifting is relatively lower in the rising stage, which alters to a sudden, erratic pattern in the falling stage. This process is also related to the migration of sand bars during the receding stage, where deposition of excess sediment load can cause local-scale changes in the flow direction. In addition, the bedform and surface turbulence undergo significant alteration during the rising limb of flood hydrograph (Coleman, 1969). For example, the smaller bedforms (mega ripples) transform to dunes and sand waves with increasing velocity in longitudinal and lateral directions. These particular differences in velocity along the thalweg and secondary channels may develop abrupt scour, erosion, and aggradation on the channel bed. In particular, the channel experienced with extreme scour after the passage of peak flood becomes the main channel and accommodates the maximum discharge. The other channels are subjected to erosion, deposition or aggradation depending upon the local topography, mid-channel bars' location, and bankline migration status. For instance, a sediment load budget study by Goswami (1985) reported that 607 km of the Brahmaputra had experienced significant aggradation (up to 16 cm) from 1971 to 1979. Considering the mechanism of the braiding process and spatial heterogeneity in assemblages of geomorphic units, a conceptual diagram is developed for the highly sediment-charged environment of the Brahmaputra (Figure 2.6). This represents a probable hierarchical nature of energy dissipation along local scale bed slope and thalweg adjustment, reach scale erosion-deposition and planform disorderness, and finally, a larger scale braided belt migration.

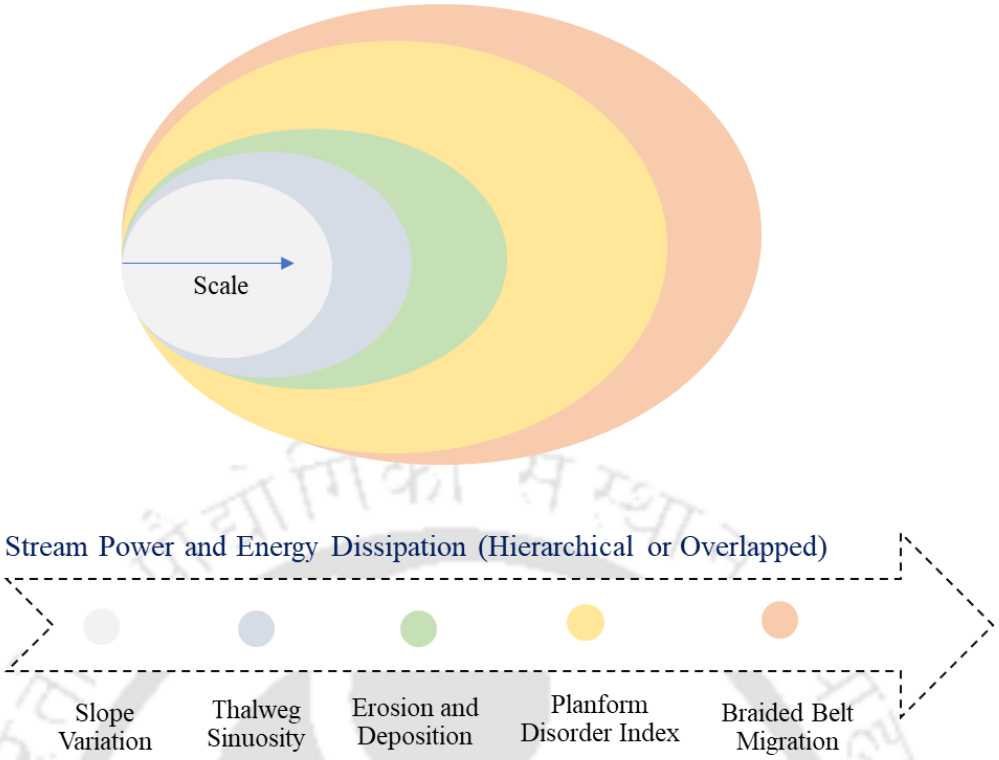

Figure 2.6 Hierarchical energy dissipation and yearly dynamics of a highly braided planform

Figure 2.7 conceptualizes a possible variability in disturbance-generated relaxation period along Himalayan rivers (the Brahmaputra and its tributaries). The process-form relationship is described over 120 years to understand the cumulative impacts of short-term and long-term anthropogenic activities. In the relaxation period, changes along process variables (flow and sediment) may be immediate, but alterations in the geomorphological and ecological systems may be lagged or occur instantaneously depending upon the type, intensity, and duration of the disturbance. The peak stream power (PSP) (unit in terms of W/m) is controlled by spatio-temporal variability of discharge and bed slope. In the Brahmaputra River, analysis of long-term hydrological data suggests a relatively high occurrence of peak floods during the 1950s (Karmaker et al., 2017), which has gradually decreased over the last four decades (Chembolu and Dutta, 2018) (Figure 2.7a). Furthermore, the bed slope of the Brahmaputra River may not show significant temporal variation due to the prevalence of an intensive braided planform along the river corridor. Hence, PSP shows an increasing trend up to the 1950s and gradually decreases in the later period. In addition, event-driven disturbances like the 1950's earthquake created natural impoundments and generated substantial sediment waves (Coleman, 1969). It is suggested that the fine fraction (clay and silt) passes quickly to downstream without significantly affecting channel morphology. However, the coarser fraction (sand) may have moved as a

wave of bed material load and took about 50 years to travel through the system, with a celerity of 10-32 km/year (Sarker and Thorne, 2006). The river responded to this alteration in sediment regime by channel bed aggradation and an increased braided belt width (Goswami, 1985). The increase in braided belt width continued up to 1973 and the morphological alteration slowly decreased in the later period (Karmaker et al., 2017). The peak morphological response may suggest a lag time of 30-40 years to the sudden change in the flow-sediment regime (Figure 2.7a). However, direct and indirect human disturbances like flow regulation, land-use change, and sand mining may gradually alter flow-sediment yield and produce cumulative and off-site channel responses (Fryirs and Brierley, 2012). For example, dam closure in any tributary of the Brahmaputra River may generate hungry water in the immediate downstream reach. At the same time, a thorough understanding of environmental setting, demographic pressure, and other historical human impacts is also required to investigate their collective influences in the regulated flow-sediment regime.

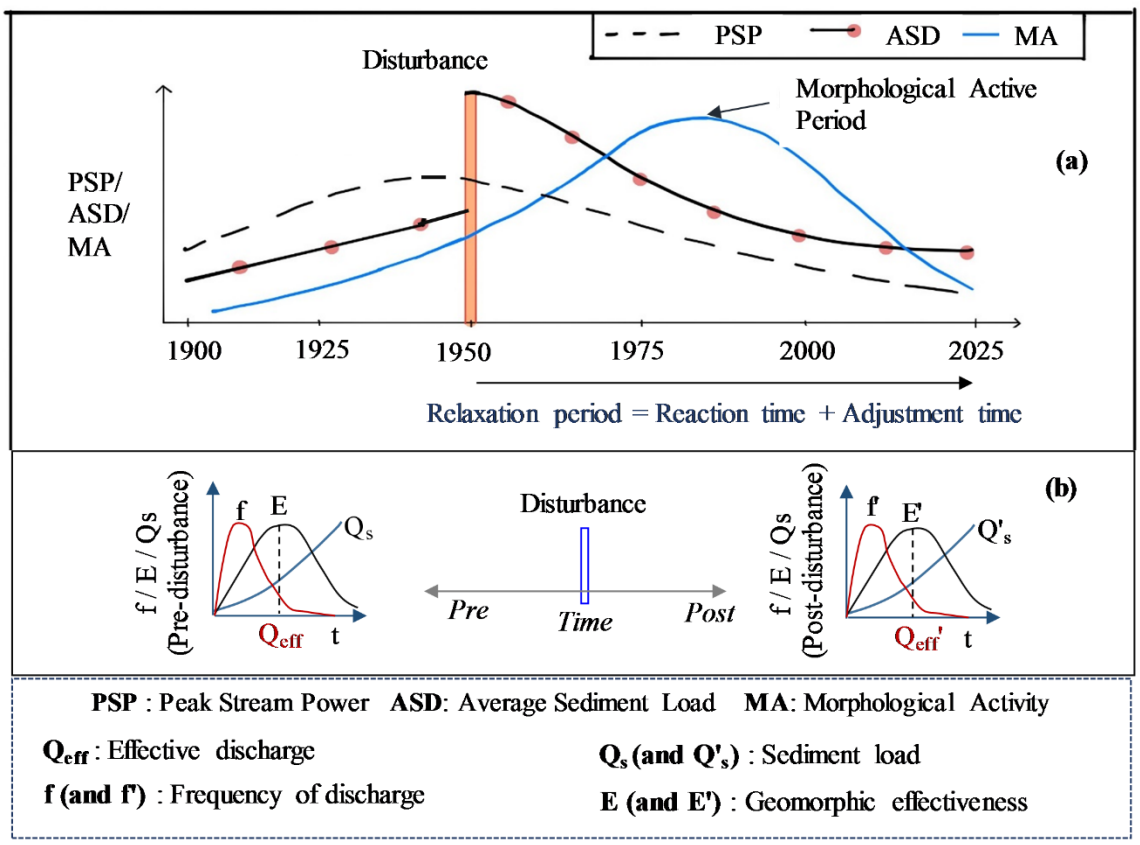

Figure 2.7 (a) Conceptual diagram of process, form, and relaxation period variability to an event-driven disturbance along Himalayan River. (b) The possible alteration in the channel-forming effective discharge in the downstream of disturbance.

Bankfull discharge, effective discharge, and flow with 1-2 year recurrence interval are considered as channel-forming discharges in fluvial systems. Wolman and Miller (1960) put forward the concept of effective discharge (Q_{eff}), which is the modal value of the geomorphic effectiveness curve (E) (Figure 2.7b). The geomorphic effectiveness curve is the product of the log-normal frequency distribution of flow (f) and sediment rating curve (Q_s) (Pradhan et al., 2021a). The Brahmaputra and its tributaries exhibit continuums in the flow pattern, bed material (alluvial to gravel), sediment transport, bed slope (steep to mild), bank erosion, channel shape (low meanders to highly braided), and energy dissipation potential (Figure 2.8). In addition, the event-driven disturbances, direct and indirect human impacts continuously modify the flow-sediment boundary conditions. Therefore, it is essential to evaluate the channel forming effective discharge, which will relate the landscape adjustments with the process boundary conditions. Q_{eff} is normally adopted as a moderate discharge having sufficient flow frequency and sediment transport capacity. Hence, the difference in the magnitudes of effective discharge and bankfull extreme events will certainly help to understand the disequilibrium caused by various forms of fluvial disturbances (f′ and Q_s′).

Figure 2.8 Field photographs of highly braided Brahmaputra River system (a) River freedom space developed from floodplain inundation (b) River freedom space due to fluvial erosion (c) Intensive morphological activity leading to bar formation (d) Stabilization of bar (island) through instream vegetation.

2.4.2 Changes in braided belt width and implication of resilience-based freedom space management concept in highly braided rivers

The high energy expenditure potential of the Brahmaputra has resulted in uneven morphological activities at different scales. In addition, the unrelenting bank erosion combined with non-uniform sediment deposition has developed a variable belt width for this highly braided channel (Figure 2.9). The braided belt width is defined as the area subjected to morphological processes (Bertoldi et al., 2010). Takagi et al., (2007) have referred to this as the area between the banklines (including channels and bars) for a braided reach of the Brahmaputra (Figure 2.9a). The spatio-temporal variability of braided belt width in the Brahmaputra can be derived from the old topographic maps, aerial photographs, and recent satellite imagery. Probably, some 200 years ago, the Brahmaputra may have followed a meander channel pattern, and old channel maps of the Bangladesh region can confirm this (Coleman, 1969). The inter-comparison of 1830 and 1963s' maps suggest the river had started the widening process and formed a braided course in this period. Further, during 1912-1928, the Brahmaputra (in Assam) had mean width close to 5949 m (Sarma and Acharjee, 2018). After the 1950s great Assam earthquake, the river significantly altered the process-form relationships. The mean width of the braided network increased up to 7455 m (Takagi et al., 2007) with intense bed aggradation (Goswami, 1985). Takagi et al., (2007) also reported that the maximum and minimum widths of the river quickly increased in the 1980-90s and finally became constant afterward (Figure 2.9b). In the 2000s, the Brahmaputra had a mean width close to 9012 m with distinct nodal points, severe braided segments, anabranching reaches, and paleo meandering channels. To summarize, the spatial differences in braided belt width were larger in the beginning (in the 1960s) and became smaller with time (till the mid-1990s).

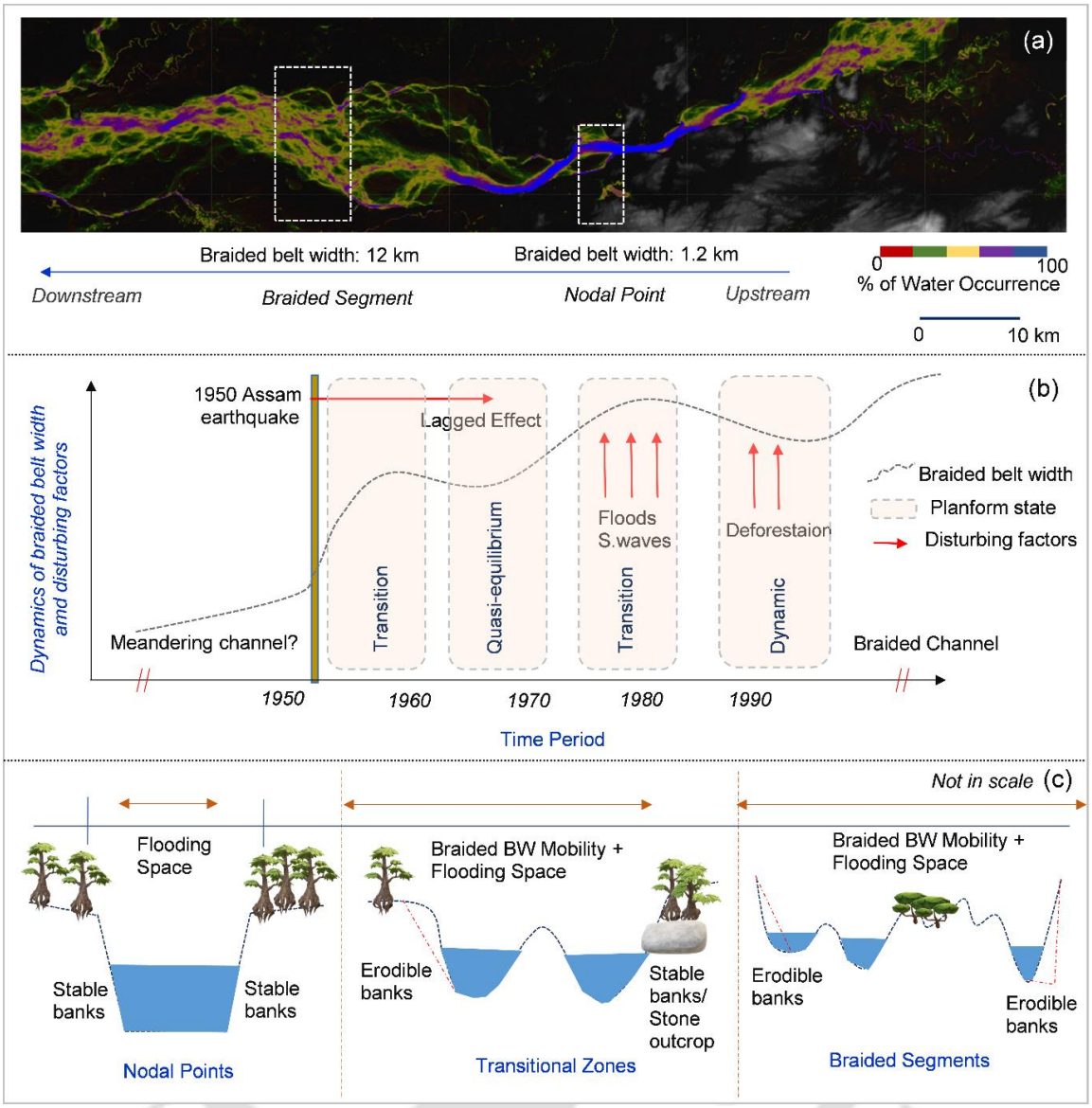

Figure 2.9 (a) The surface water variation (in percentage) along the Brahmaputra River. The image is obtained from cloud computing of JRC surface water layers in Google Earth Engine (GEE) platform. (b) Conceptualization of braided belt width dynamics and the disturbing factors in the last 100 years. (c) Conceptualization of resilience-based freedom space management concept.

The temporal dynamics in braided belt width can be attributed to numerous hydrological (flood and sediment waves), topographical (nodal points and local bed slope), and geological factors (bank erodibility, earthquakes, and landslides). Takagi et al., (2007) have reported that the Brahmaputra has undergone four geomorphological phases between 1960 and 2000, each lasting 5 to 10 years. In the 1960s, the effects of the earthquake and subsequent landslides induced sediment load had a dominating role in the morphological processes. Therefore, the river underwent an unstable transitional condition by altering the

braided belt width and activating (de)stabilizing waves. In the subsequent decade, propagation of these waves was unclear, and the river observed a quasi-dynamic equilibrium with less complex distributions of landforms. However, in the 1980s, the river was morphologically activated due to the large floods, resulting in an increased braided belt width and altered fluvial land cover. After the 1990s, the river approached a stabilized braided belt state and this morphological state may be referred to as a channel in dynamic equilibrium (Figure 2.9b).

The 'freedom space' concept has varied terminologies in fluvial geomorphology, such as 'room for the river' (Baptist et al., 2004), 'river corridor' (Kline and Cahoon, 2010), and 'fluvial territory' (Ollero, 2010). In the Brahmaputra, the altered processes have developed a complex morphological setting. In addition, this river system is continuously subjected to anthropogenic disturbances through land cover change, sand (gravel) mining, and local-scale river interventions. Therefore, an integrated ecosystem-based approach instead of a reach-scale engineering practice may be helpful for the effective management of this large river system. Biron et al., (2014) have estimated the freedom space for three contrasted river systems depending upon the meander migration and floodplain flooding. However, in the Brahmaputra, the planform shows spatial variability in terms of nodal points, transitional reaches, and braided segments (Figure 2.9c). Hence, before conceptualizing the 'river freedom space' concept, it is crucial to identify (and categorize) the homogeneous reaches based on identical geological formations and dominant morphological landforms. The lateral mobility of braided belt width can be evaluated from historical and present aerial photographs and satellite imageries in the first phase. The erosion and deposition volume and bank erodibility parameters need to be assessed through fine-scale digital elevation models and in-situ apparatus. In addition, frequent field investigations and societal feedbacks are also essential to preserve the riparian and wetland zones in the river corridor. The second stage of freedom space evaluation should prioritize the bio-morphological functionality of this river system. The identification of floodplain (terraces) extent and associated landforms are suggestive of the fluvial processes (Biron et al., 2014). Hence, the last stage of freedom space estimation may be attributed to the floodplain inundation identification by hydrodynamic modeling, forecasting and advanced geo-spatial techniques. To summarize, the identification of hierarchical or overlapped freedom spaces based on braided belt width mobility, riparian-wetland zones, and floodplain inundation may help in accelerated stabilization of the highly dynamic Brahmaputra River system.

2.4.3 Relaxation period and process-form relationships in weakly braided peninsular rivers

The peninsular rivers are mostly alluvial, weakly braided and display a compound channel form having a distinct primary channel and inset floodplains (Kale, 2003). The high banks are also stable and in-channel features like cut-offs and mid-channel bars may act as dominant geomorphic units. In the peninsular rivers, the flow regime is mostly controlled by river intervention structures (dams, barrages and weirs). However, the flow modulation of extreme events may not be significant as the reservoirs generally pass the hyper-concentrated, sediment-laden flows during the peak floods. Therefore, in the last 50 years, the temporal variability of PSP has established an unaltered peak flow regime in the peninsular rivers (Figure 2.10a). Furthermore, intensive flow regulation has caused a steady reduction of sediment load (ASD) across all the major rivers (Syvitski et al., 2005; Panda et al., 2011; Gupta et al., 2012). Such strong modification to the natural regime will generate variable relaxation periods and various forms of geomorphic adjustments may instigate at both upstream and downstream reaches. Graf (1977) has emphasized erosion just downstream of the dam and gradually decreasing adjustment rates toward a new quasi-equilibrium condition. The morphological changes will also depend upon the current physiographic setting, intensity and duration of the disturbance, inherent resistance of the channel, closeness to the threshold, and history of previous human impacts (land-use change, sand mining, and channelization). Some rivers may react quickly to the upstream impoundment, while others may delay the response. For example, the peninsular Brahmani River has transformed into a (weakly) braided channel after the operation of the Rengali dam (Pradhan et al., 2019). The cut-off and mid-channel are still forming after thirty-five years of flow-sediment regulation (Figure 2.10a). In contrast, the regulated Mahanadi River is morphologically inactive, apart from channel incision at some selected reaches. Thus, the morphologically active, regulated peninsular rivers should be thoroughly assessed to understand the direction and rate of fluvial metamorphosis in the relaxation period.

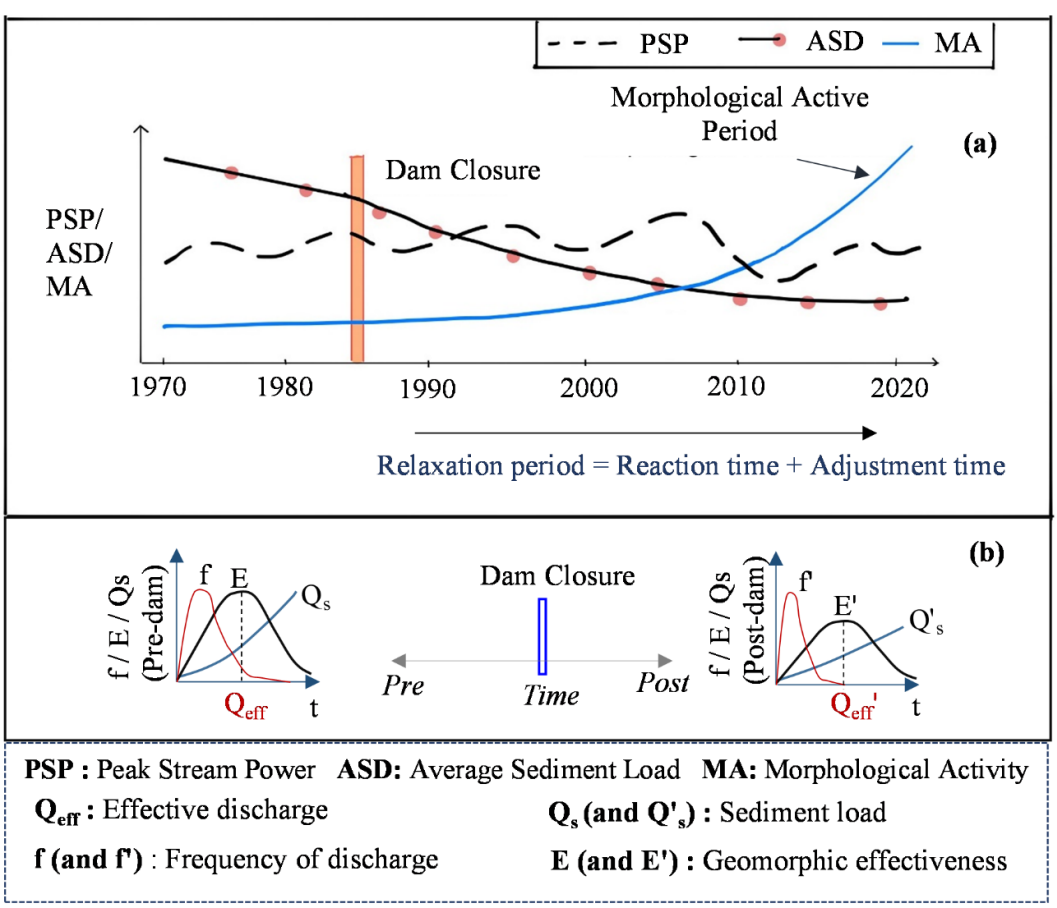

Figure 2.10 (a) Conceptual diagram of process, form, and relaxation period variability to dam closure in a peninsular river. (b) The possible alteration in channel-forming effective discharge in downstream of the dam.

The sand bed channels in semi-arid regions are more sensitive to the changes in flow and sediment supply (Petts and Gurnell, 2005). In the peninsular rivers, sediment trapping behind dams alters Q_s in the post-dam period (Figure 2.10b). f is also modified due to regulation of both low flows and extreme events. Hence, the post-dam Q_{eff}' and E′ will play significant roles in identifying the controlling factor in landscape adjustments. Unlike Himalayan rivers, peninsular rivers are strongly controlled by direct human disturbances (dam closure), dominating other forms of fluvial impacts (event-driven or indirect). Therefore, channel-forming effective discharge assessment is the correct approach to understand the trajectory and rate of metamorphosis in the relaxation period.

2.4.4 Role of vegetation in recovery assessment along braided rivers: A way forward

Geomorphic river condition is related to the physical state of the river, which measures the capacity to perform functions that are expected of the river type and environment setting (Fryirs and Brierley, 2012). A solid understanding of the direction and rate of channel evolution is also necessary to predict the likely future scenarios. River recovery is defined as the trajectory of post-disturbance changes towards the degraded or improved condition and assigning the accurate physical state (intact, degraded, turning point, created or restored) (Fryirs and Brierley, 2000; Fryirs et al., 2018; Pradhan et al., 2020). River recovery potential is also related to connectivity of the reach throughout the catchment and interpretation of the limiting factors to recovery (change in flow-sediment, vegetation and debris character, and run-off relations). In Indian regulated rivers, studies dealing with river conditions and recovery potential are scarce. In addition, riparian and in-stream vegetation are closely linked with the channel evolution processes through its impacts on flow resistance, sedimentation, and soil moisture retention. Therefore, changing vegetation and debris character may accelerate, stabilize, or diminish the recovery potential of Indian rivers and future regulated river studies should highlight the role of vegetation in transient states of the anthropogenically disturbed rivers.

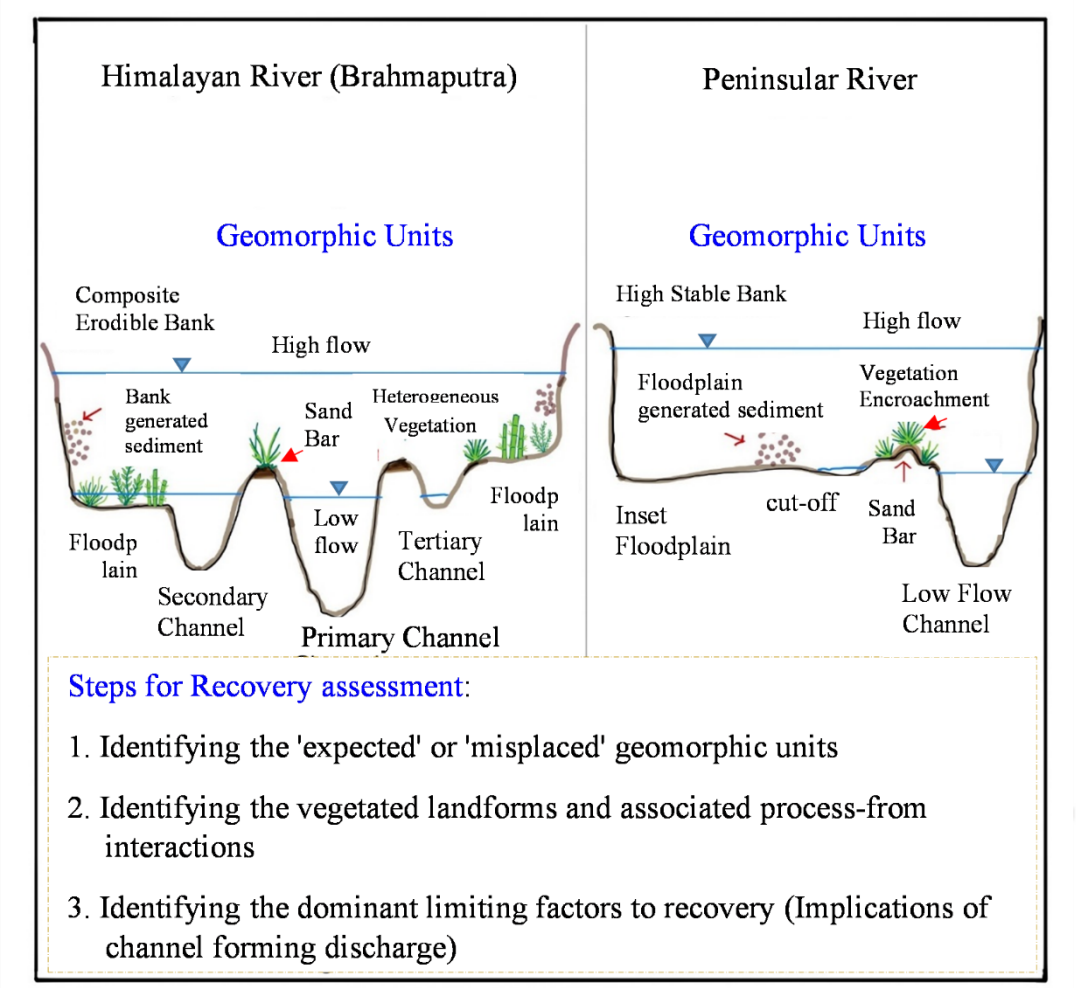

Figure 2.11 Conceptual diagram describing the geomorphic units and steps for recovery assessment in anthropogenically disturbed Himalayan and peninsular rivers.

Vegetation can play a crucial role in long-term landscape adjustments of regulated Himalayan and peninsular rivers. In particular, the Himalayan rivers are ecologically sensitive and characterized by substantial debris load and heterogeneous vegetation-dominated floodplains (Figure 2.1b). In the Brahmaputra River, the floodplain vegetation is helpful in promoting bank accretion, while in-stream vegetation influences the flow-turbulence structures and bar stabilization process (Chembolu et al., 2019). Some peninsular rivers like Brahmani and Ong have also shown gradual vegetation encroachment on mid-channel bars in the post-dam periods (Figure 2.1g and 2.1i). This vegetation growth affects the stabilization of the low flow channel and improves the geomorphic heterogeneity in the system. Kale et al., (1986) have also noted that suspended sediment concentration is usually high immediately after the monsoon and decreases thereafter due to increase in soil moisture and establishment of vegetation cover. Therefore, riparian

vegetation growth after the onset monsoon affects the geomorphic implications of sediment transport in Himalayan and peninsular rivers. Thus, framing the role of vegetation in the recovery potential of Indian regulated rivers requires identifying the vegetated landform and its associated process-form interactions (Figure 2.11). The subsequent step should be focused on detecting the 'expected', 'misplaced' or 'altered' geomorphic units with appropriate terminologies (Wheaton et al., 2015) and explanations for the human disturbances modified character and behavior of the reach. The next steps should be focused on evaluating the changes in flow-sediment boundary conditions and the implications of channel-forming discharge. In the Mahanadi River basin, Pradhan et al., (2020) have identified the change-point in suspended sediment load and its relation with at-a-station recovery potential. Similar studies are necessary in the context of anthropogenically disturbed Himalayan and peninsular rivers, with due importance on understanding the reach-scale connectivity and hotspots of bio-geomorlogical interactions. The intensity and duration of flood pulses also play a major role in the recovery assessment of Indian rivers. For instance, in peninsular rivers, three to four major flooding events are observed in any particular monsoon season. The duration of these perturbations (or disturbances) may be shorter than the relaxation period of the channel. Such channels may never recover to their pre-disturbance condition and therefore, demand a detailed assessment of river condition and recovery potential in the complex relaxation paths.

2.4.5 The future direction in fluvial modeling

In recent years, a few more concerns (like sand mining and loss of riparian cover) growing in the management of braided rivers. The modeling framework helps to establish a reach scale sequence of events generated due to the combined effect of controlled flow-sediment regime and anthropogenic activities. The local scale morphological process-response relationship due to sand mining can be studied thoroughly with laboratory experiments (Barman et al., 2018). A recent study by Sanyal (2017) addressed the future trend of braided Teesta River using morphodynamics modeling. Such studies can give insight into the future trajectory of similar regulated rivers. The proper integration of remote sensing data with extensive field-based measurements is also necessary for improving the process-based understanding of braided rivers. Advanced river surveying equipment (like ADCP, echo-sounder, and sensor-based digital sampler) can provide information on in-situ scale flow and sediment distribution at bars and other volatile reaches. Furthermore, reservoir percolation accumulates pore water pressure and may lead to earthquakes. For instance, the

Koyna region of western India has experienced several earthquakes after the impoundment of the Koyna reservoir (Shivajisagar lake) (Gupta, 1992; Chadha et al., 1997; Chander, 1997). Thus, the reservoir-triggered seismicity (Das and Mallik, 2020) must be carefully examined for similar Indian reservoirs emphasizing existing fault slip, rock mechanical properties, and fluid gradients. The backwater fluctuations induced biotic-abiotic interactions and feedback demand multidisciplinary research (Liro, 2019). In particular, the increased sedimentation may facilitate growth of diverse aquatic and riparian vegetation, influencing the alteration of channel hydraulic parameters (width, depth, velocity, and slope), delta formation, upstream sediment slug propagation and fast transition of multi-thread channels to a single channel. Hence, assessment of dominant geomorphic units (vegetated or unvegetated), channel-forming effective discharge, and recovery potential will help to understand the influence of reservoir (backwater) in different biogeographic regions.

2.5 CHAPTER SUMMARY

Literature review suggests studies in the Indian rivers are primarily focused on the quantitative understanding of the alterations, and the knowledge is still limited in studying the process-based cause and effect of dam closure in monsoon-dominated highly braided Himalayan and weakly braided peninsular rivers. The major conclusions of this chapter are as follows:

- The literature synthesis suggests that studies have generally dealt with the changes in flow-sediment, morphology, and ecological variables along the downstream reaches of Indian regulated rivers. Few of the other works also focus on studying the dam effects on sediment delivery to coastal regions, delta shrinking, and saltwater intrusion.
- Studies on the upstream dam impacts are scarce, and little is addressed about the backwater effects and associated bio-geomorphological processes in Indian regulated rivers.
- The highly braided Himalayan rivers are associated with high flow-sediment variability forming a non-uniform spatio-temporal distribution of geomorphic units. In addition, severe bank erosion combined with the dynamic processes has resulted in a varied braided belt width along the river course. Therefore, a ‘resilience-based management approach’ integrated with braided belt width mobility, riparian-

wetland zones, and floodplain inundation is necessary for effectively manage and execute riverine practices.

- Few studies have focused on the alteration of channel-forming discharges and the effective discharge assessment will help to understand the human impact generated disequilibrium in the complex relaxation paths of braided river metamorphosis.
- The identification of recovery potential in regulated rivers is still in the preliminary stages. The present chapter proposes conceptual recovery evaluation steps integrating the identification of vegetated landforms and dominant geomorphic units.

The behavior and interaction of each reservoir-catchment are unique in India. This brings an idea of a general geological framework considering a thorough understanding of the dominant geomorphic units and their gradual evolution in the complex relaxation paths. With the growing demands of water and energy, fluvial systems will play a vital role in the future. The proper geomorphological knowledge of channel changes, development of process-from-ecology-feedback models, and effective ecological restoration program are essential in these anthropogenically disturbed braided systems.

3

PROCESS-FORM RELATIONSHIPS IN A WEAKLY BRAIDED RIVER SYSTEM

A large dam strongly governs the Brahmani River system. This macrochannel river has witnessed a great reduction in sediment load along with the gradual transformation of the sinuous channel (pre-dam) into a weakly braided system (post-dam). This chapter addresses the following questions through hydrological and morphological analysis.

- It has been more than 35 years since the onset of the river regulation. How has the process-form relationship been altered in the relaxation time period?
- Can effective discharge assessment address the morphological change by a stream power curve?
- Does a morphological continuum exist in a macrochannel system and how can a process-based indicator predict the metamorphosis?

3.1 INTRODUCTION

Alluvial rivers self-adjust the channel geometry based on varying hydrologic, hydraulic, and sedimentary factors (Dury, 1973; Gomez et al., 2007; Heitmuller et al., 2015). Over the last several decades, fluvial geomorphologists have placed considerable interest in integrating channel adjustments to a single or set of flow events. One such hydrologic index is bankfull discharge, which is defined as the maximum discharge the channel can convey without overtopping onto the floodplain (Leopold and Wolman, 1957; Williams, 1978; Lenzi et al., 2006). However, uncertainty and complexity still persist in defining and understanding the bankfull discharge. The fundamental research by Williams (1978)

suggested 16 ways of evaluating bankfull discharge and discussed their applicability at different flow and hydraulic scenarios. Other researchers have further proposed methods for estimation of the bankfull discharge based on bank height (Leopold et al., 1964), the width-to-depth ratio, the break-point of bank and vegetated slope (van den Berg, 1995), the mean annual flood (Kleinhans and van den Berg, 2011) and the flow with 1.5-year return interval (Hickin, 1968; Harman et al., 1999). Few studies have also established that the bankfull discharge is comparable to the effective discharge, and this controls the channel morphology (Andrews, 1980; Leopold, 1994; Simon et al., 2004; Roy and Sinha, 2014). The effective discharge is computed from magnitude-frequency analysis, which describes the discharge that transports the largest amount of sediment over time (Wolman and Miller, 1960). Pickup and Warner (1976) and Andrews (1980) suggested the effective discharge can be referred to a high-magnitude flood by adopting a log-normal frequency distribution of discharge and establishing a power relationship between discharge and sediment load. Sichingabula (1999) reports an event-based assessment of sediment transport to avoid subjectivity in the class-based evaluation of the effective discharge. Doyle et al., (2005) established the relationship between the effective discharge and ecosystem variables to understand various hydrological processes.

Empirical and theoretical models have used the bankfull and mean annual flood to predict bar patterns (van den Berg 1995; Kleinhans and van den Berg, 2011), while overlooking the effective discharge. This represents the effective discharge as the channel-maintaining discharge instead of the channel-forming discharge (Phillips, 2002; Lenzi et al., 2006). Moreover, existing channel prediction theories may not be applicable to regulated rivers where flow hydraulics and the channel pattern are in disequilibrium. Catchment morphology, drainage pattern, and sediment transport influence the discharge. Hence, a flow event of single return interval cannot be used to represent the effective or bankfull discharges (Ashmore and Day, 1988; Nash, 1994; Phillips, 2002). Therefore, an effective discharge curve formulation may improve the understanding of river instability and morphological change thresholds (Alabyan and Chalov, 1998).

In India, peninsular rivers are relatively stable and respond to extreme magnitude floods (Kale, 2003). These large rivers also contribute to 15-20% of the global sediment flux (Gupta et al., 2012). However, in recent decades, increases in the number of large dams have altered the natural flow and sediment regime (Panda et al., 2011, Pradhan et al., 2019), morphological condition (Ghosh and Guchhait, 2014; Pal, 2016; Pradhan et al., 2017;

Borgohain et al., 2019; Islam and Guchhait, 2020), riverine habitat (Pandey, 1993) and ecosystem services (Foote et al., 1996). This makes it important to study changes in the effective discharge and its contribution to planform adjustments. The Brahmani River is one of the major peninsular rivers and is strongly controlled by a large dam. Therefore, the natural flow-sediment regime has been altered, and a gradual transition in channel pattern (from sinuous to weakly braided) is observed in the post-dam period. The objectives of the present chapter are to: (i) estimate the alteration in the effective discharge caused by the regulated flow-sediment regime; (ii) develop a stream power curve by integrating the effective discharge in an empirical stream power-based classification, and (iii) formulate the probability of braiding (POB) to understand the transitional channel pattern in the Brahmani River.

3.2 STUDY AREA

The Brahmani River is one of the major peninsular rivers with a catchment area of 39,033 km^2 and a channel length of 799 km. This inter-state flowing river connects the Chota Nagpur plateau to the Bay of Bengal, and has several major tributaries including the Sankh, Koel, Tikra and Karo. This river drains along sandy, loamy and coastal alluvium soils (Integrated Hydrological Data Year Book, 2012) and has an average annual rainfall about 1305 mm during the southwest monsoon (June to September). Two major river interventions, the Rengali dam and the Samal barrage, are present near the city of Talcher (Figure 3.1). The Rengali dam has operated since 1985, with gross and effective storage capacities of 5.15 km^3 and 3.41 km^3 (National Register of Large Dams, 2019). Two gauging stations, Gomlai and station Jenapur, are present at 50 km upstream and 160 km downstream of the Rengali dam, respectively (Figure 3.1).

The channel form of the Brahmani is described as macrochannel, in which a smaller low flow channel is inset within a larger channel. The variability of the macrochannel bankfull width between Talcher and Jenapur is 900 to 1300 m. In addition, the inset channel has a width of 100 to 200 m, which provides a large morphological adjustments space for within-macrochannel features. The macrochannel bank height is 8 to 10 m (Figure 3.2a), which can accommodate a flow regime of high hydrological variability. Tributary inflow and bank erosion are also absent and geomorphic units such as benches, chutes and various bar types are effectively confined between the macrochannel bank margins. Flow regulation has decreased the average annual suspended load from 12.3×10^6 t/yr to 5.7×10^6 t/yr between

pre-dam and post-dam periods. This significant alteration in sediment transport is accompanied by a gradual adjustment of the inset low flow channel and the surrounding instream geomorphic unit assemblage. An accelerated formation of chutes and diagonal bars has changed the channel pattern from sinuous (in pre-dam) to weakly braided (in post-dam). Such similar morphological adjustments are observed downstream of Talcher, and therefore, the 8 km long reach near Jenapur is considered as the study area (Figure 3.1). This study area is characterized by an average bed slope close to 0.00045 m/m and sand bed particle size (D_{50}) of 0.23 mm and reflects the general form-process interaction of the post-dam period Brahmani River.

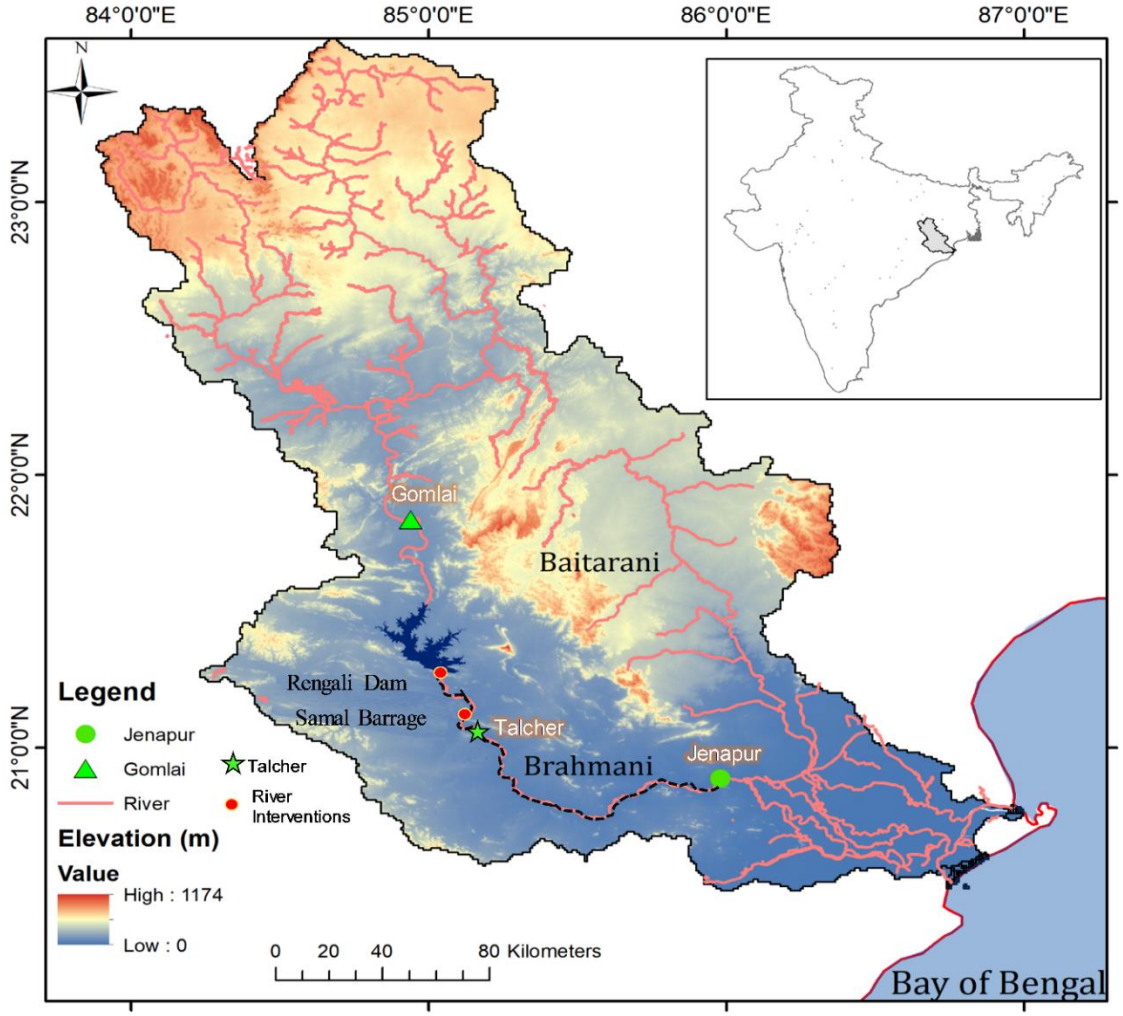

Figure3.1 The Brahmani River basin showing Rengali dam, and the upstream (Gomlai) and downstream (Talcher and Jenapur) gauging stations.

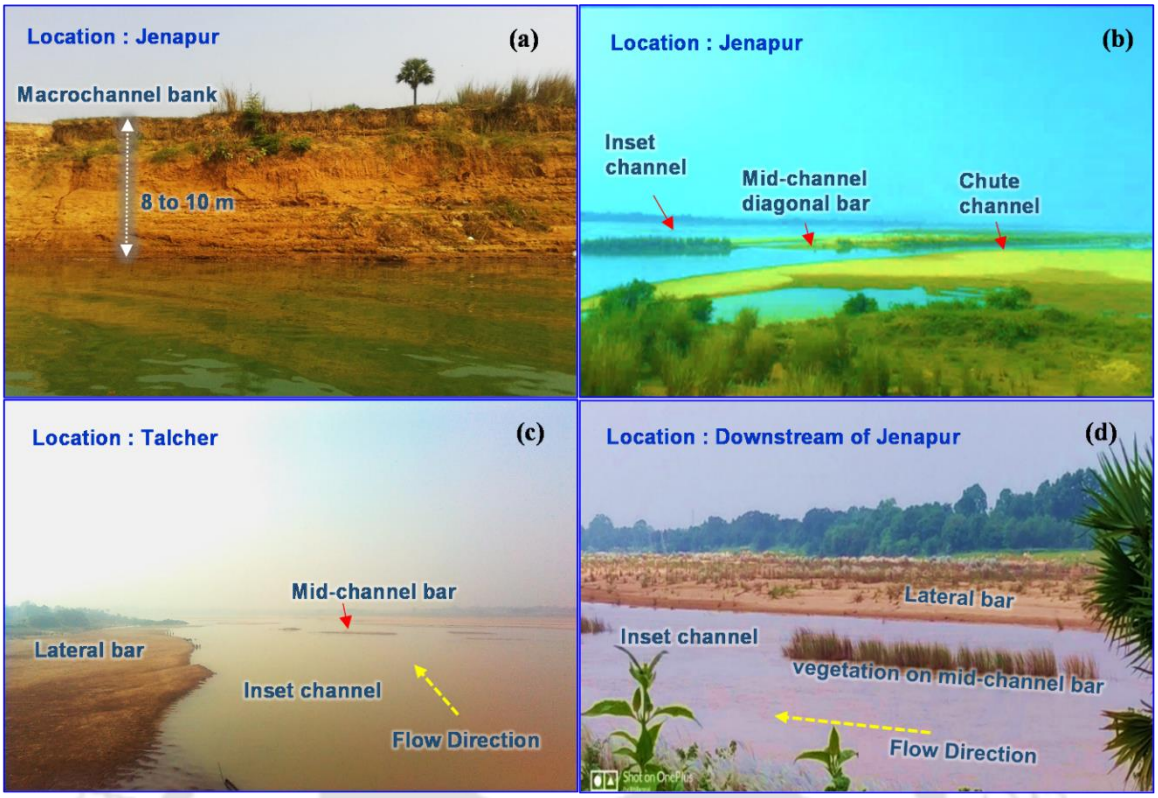

Figure3.2 Field photographs of the Brahmani River in the post-dam period (a) Macrochannel bank (b) Inset channel, diagonal bar and chute channels (c) A lateral bar close to the flow boundary and (d) Vegetation on a mid-channel bar.

3.3 MATERIALS AND METHODS

Daily hydrological data (discharge, stage level, and suspended sediment concentration), bathymetry (channel cross section) and optical satellite images (Landsat, USGS) were used to study the impacts of river regulation on the effective discharge and its transport effectiveness. The hydrological and channel cross section dataset were obtained from the Central Water Commission, India. The Brahmani River shows a large flow variability (10 m^3/s to 10,000 m^3/s) because of its high macrochannel banks. In this chapter, the bankfull discharge (Q_b) is determined to be the flow that fills the macrochannel (Roy and Sinha, 2014; Fryirs et al., 2015). The only sediment data consist of suspended sediment concentrations, which comprises the maximum portion of total load. This analysis includes both coarse to medium and fine-grained suspended sediment. The coarse to medium suspended load corresponds to medium to very fine sand on the Udden-Wentworth scale, and this is considered as temporarily suspended bed load (Roy and Sinha, 2014). The effective discharge for the Brahmani River was calculated for two time periods: pre-dam

(1981-1984) and post-dam (1985-2014) at upstream (Gomlai) and downstream (Jenapur) gauging stations. The hydrological data series of Gomlai and Jenapur were compared to study the changes in effective discharges and their transport effectiveness for this regulated river.

The effective discharges were computed based on the frequency and sediment load carried by the discharge. Effective discharge computations were performed based on two methods, the analytical approach and the deterministic approach. In the analytical approach, the log-normal distribution of the discharge series was fitted with sediment rating parameters. In the deterministic approach, the magnitude-frequency of different discharge classes was evaluated to find the discharge class carrying the maximum sediment load (Ma et al., 2010).

3.3.1 Analytical approach

The empirically-based magnitude-frequency analysis assumes a lognormal frequency distribution of natural flow (Nash, 1994; Roy and Sinha 2014; Higgins et al., 2016) and a power function between the suspended sediment load (Q_S = 86.4 CQ) and discharge (Q). If the discharge has a log-normal distribution:

$$f(Q) = \frac{1}{\sigma Q\sqrt{2\pi}} e^{-\frac{(\ln Q-\mu)^2}{2\sigma^2}} \quad (3.1)$$

the suspended sediment load can be expressed as:

$$Q_s = aQ^b \quad (3.2)$$

where μ and σ are mean and standard deviations of the logged discharge, and a and b are the coefficient and exponent of power curve, respectively. Therefore, transport effectiveness (E) (Wolman and Miller, 1960) is the product of the frequency of occurrence of an event and the magnitude of suspended sediment transported by such an event:

$$E = \frac{a*Q^b}{\sigma Q\sqrt{2\pi}} e^{-\frac{(\ln Q-\mu)^2}{2\sigma^2}} \quad (3.3)$$

$$Q_e = e^{(b-1)\sigma^2+\mu} \quad (3.4)$$

The modal value of Eq. (3.3) is known as the effective discharge (Q_e), which is obtained by computing the derivative of E with respect to Q and equating the result with zero. Several researchers have also suggested that the log-normal distribution is sufficient for

describing the frequency of discharge of most of the rivers where the recurrence interval of the effective discharge is less than a decade (Nash, 1994; Roy and Sinha, 2014).

3.3.2 Deterministic approach

The size of the class interval (CI) or the number of discharge classes (N) is generally empirically derived (Lenzi et al., 2006; Ma et al., 2010). Yevjevich (1972) specified an upper limit of the class interval of flow discharge as S/4 (where S is the standard deviation), and that the number of classes should be between 10 and 25. However, when we use a class interval of S/4, the number of classes at both stations of the Brahmani River exceeds 25 (Table 3.1). This suggests that Yevjevich's two standards are not met. Furthermore, Crowder and Knapp (2005) claimed that at least one flow event should be present in each discharge class. Following the recommendation of Crowder and Knapp (2005), the number of discharge classes in both stations of the Brahmani River would be very small, because the difference between low and extreme events is very high (10-10,000 m^3/s). To overcome the shortcomings of these methods, this study follows the procedure suggested by Ma et al. (2010) where it is assumed that each discharge class varies between 0 and S. Further, we also assumed arithmetic intervals of S, 0.75S, 0.5S and 0.25S for division of flow series into different classes. The midpoint value is taken as a reference for each corresponding discharge class. The total suspended load in each class is determined and plotted as a histogram against the representative discharge for all the river stations. The discharge corresponding to the peak value of the suspended load histogram is computed to be the effective discharge.

Table 3.1 The size of class intervals (CI) and numbers of discharge classes (N) used in the evaluation of effective discharge.

Station name	Range of discharge (m^3/s)	S CI (N)	0.75 S CI (N)	0.5 S CI (N)	0.25 S CI (N)
Upstream (Pre-Dam)	1.11- 5570.3	654 (9)	491 (12)	327 (18)	163 (35)
Upstream (Post-Dam)	1.35- 10801.19	754 (15)	565 (20)	377 (29)	188 (58)
Downstream (Pre-Dam)	5.12- 9701.79	940 (11)	705 (14)	470 (21)	235 (42)
Downstream (Post-Dam)	6.9 - 10372.06	864 (13)	648 (17)	432 (25)	216 (49)

3.3.3 Morphological analysis

To investigate pre-dam and post-dam morphological variability, optical satellite images were collected from the USGS Landsat Archive. Cloud-free satellite images of Landsat 4-5 TM, Landsat 7 ETM^{+} and Landsat 8 were selected in the dry (March) season. Moreover, the Landsat 1 (MSS) image (March 1980) was selected as a reference in the absence of pre-dam satellite images. All the satellite images were digitized with ArcGIS 10 to capture the temporal variability of the inset and chute channels in the study reach. The sinuosity index (SI) was calculated as a ratio of the inset channel length and the straight reach length. Similarly, the braid-channel ratio (BR) was defined by the sum total of all channel lengths (inset and chutes) and the inset channel length (Friend and Sinha, 1993).

3.3.4 Stream power analysis

In this study, a HEC-RAS model (Brunner, 1995) was setup for the entire 8 km reach with a 100 m cross section interval. An unsteady flow analysis was simulated to compute unit stream power (ω) (Chembolu and Dutta, 2018), total stream power (Ω) (Alabyan and Chalov, 1998) and potential unit stream power (i.e., referred to as the potential specific stream power by Kleinhans and van den Berg, 2011). Mathematically these are represented as:

$$\omega = \rho g V R S_E \quad (3.5)$$

$$\Omega = \rho g Q S_E \quad (3.6)$$

where ω is in W/m^2, Ω is in W/m, ρ is water density (1000 kg/m^3), g is acceleration due to gravity (9.81 m/s^2), V is the average velocity of the flow (m/s), R is the hydraulic radius (m) and S_E is the energy slope. In the Brahmani River, the morphological adjustments caused by moderate floods and extreme events are reflected in the late post-monsoon period (December-March). In this period, the chute channels may occupy the defined path left over or created by these flow events. Therefore, this study has evaluated the relationship between reach-averaged seasonal ω and Ω, peak (extreme event) ω and Ω, rising limb ω and Ω and falling limb ω and Ω with the next year's (March) meandering and braiding parameters (SI and BR).

3.3.5 Potential unit stream power curve

Kleinhans and van den Berg (2011) improved the understanding of river channels and bar patterns with an empirical stream power-based classification. This approach highlights that channel pattern develops a bar-pattern related continuum without hard thresholds. Moreover, the chute channels are an indicator of a gradual transition between meandering and braided states, and form a weakly braided channel pattern along the continuum. In the Brahmani River, chutes indicate the initiation of braiding. A stream power curve, instead of solitary values, helps us to understand the morphological adjustments within these defined channel states (meandering and braided). The box-shaped physiography of the Brahmani River shows an inset channel carrying the low flows for most of the time and the stable macrochannel banks act as a conduit for high-magnitude flood discharges. In such rivers, channels respond to the increase in discharge by changing the width-depth ratio (Kale, 2003). However, the Brahmani macrochannel system facilitates a greater rate of increase in flow depth relative to flow width. The flow width shows an initial step-wise increase from low flows to moderate floods and only changes slightly between the moderate floods and extreme events. Further, most of the morphological adjustments are observed at sub-macrochannel stages, which further alludes to the geomorphic importance of moderate floods in the Brahmani River. This allows integration of the effective discharge (instead of bankfull discharge) in the stream power curve, assuming flow width responds to the changes in the effective discharge. Thus, the effective discharge integrated stream power curve is proposed as:

$$\omega_{Pv} = \frac{\rho g Q s_v}{\alpha Q_e^{\beta}} = \frac{\rho g Q s_E}{SI * 4.7\sqrt{Q_e}} \tag{3.7}$$

where the valley slope (S_v) is calculated as ratio of energy slope (S_E) and sinuosity (SI). Q and Q_e are flood and effective discharges, respectively, and α and β are power coefficients and adopted as $4.7\sqrt{s/m}$ and 0.5 for a sand-bed river system (van den Berg, 1995). The discriminators (ω_{ia}, ω_{sc} and ω_{bm}) are the thresholds as suggested by van den Berg (1995) and Kleinhans and van den Berg (2011). The stream power curve (ω_{pv}) obtained from Eq. (3.7) is compared against the discriminators to predict the channel pattern of the Brahmani River in pre-dam and post-dam periods. The discriminators are evaluated empirically based on the relationship between median particle diameter and the bankfull discharge (van den

Berg, 1995). Therefore, integration of effective discharge in the stream power curve also evaluates its implication as the channel forming discharge in a macrochannel river system.

The discriminators are based on the presence and nature of bars (point, scroll, chute or braid) and active channel pattern (straight, sinuous, meandering and braided). Therefore, this classification develops four channel patterns with an increasing order of energy, which are immobile rivers (no bars), meandering with scrolls, meandering with chutes (weakly or moderately braided), and highly braided (Kleinhans and van den Berg, 2011). The threshold for transition between immobile rivers (no bars) and meandering with scrolls is:

$$\omega_{ia} = 90\ {D_{50}}^{0.42} = 2.66\ \mathrm{W/m^2} \tag{3.8}$$

Similarly, the threshold for transition between meandering with scrolls and meandering with chutes (weakly-moderately braided river) is:

$$\omega_{sc} = 285\ {D_{50}}^{0.42} = 8.4\ \mathrm{W/m^2} \tag{3.9}$$

Finally, the threshold for transition between meandering with chutes (weakly-moderately braided river) and a highly braided river is:

$$\omega_{bm} = 900\ {D_{50}}^{0.42} = 26.67\ \mathrm{W/m^2} \tag{3.10}$$

3.3.6 Probability of braiding

The probability of braiding (POB) is related to probability of the existence of chute channels in the weakly braided Brahmani River. POB is evaluated as the ratio of the number of days exceeding ω_{sc} and the total number of flood days in the effective discharge integrated stream power curve. POB in the Brahmani River is proposed as:

$$P(\omega_{pv} > \omega_{sc}) \sim P\left(\frac{\rho g Q s_v}{\alpha Q_e^{\beta}} > \frac{\rho g Q_e S_v}{\alpha Q_e^{\beta}}\right) \tag{3.11}$$

$$P(\omega_{pv} > \omega_{sc}) \sim P\left(\frac{\rho g Q s_v}{\alpha Q e^{\beta}} > \omega_{sc}\right) \tag{3.12}$$

3.4 RESULTS

3.4.1 Hydrological data analysis

The oscillation of the southwest monsoon rainfall regime has generated a unimodal wet (June-September) and dry (October-May) season in the Brahmani River. The high flows (and extreme events) are periodic, and a significant variation of discharge values is observed between dry and wet seasons. The transition between low and high flows is characterized by the moderate flows in the Brahmani River. The high value of R_{ed} (ratio of maximum daily discharge to minimum daily discharge) (>1400) suggests the Brahmani River has a large macrochannel bankfull flow capacity (Table 3.2 and Figure 3.2a). In the downstream station, C_{vd} (coefficient of variation of discharge) has decreased because of a reduction in flow variability and an increase in mean daily discharge. Moreover, trapping of peak suspended sediment, reduction in sediment variability and mean suspended sediment load has reduced the C_{vs} (coefficient of variation of suspended sediment concentration) in the post-dam period. Such changes in the sediment regime are also well reflected by sediment rating coefficients (i.e., *a* and *b*). The coefficient of determination (R^2) ranges from 0.83 to 0.93, with an average value of 0.90 (Figure 3.3). In the upstream station, coefficient *a* remains unaltered and, is close to 0.1. However, in the downstream station, coefficient *a* has decreased from 0.09 to 0.03 with smaller change in coefficient *b*. The value of b > 1 also creates effective discharge greater than the modal discharge in the Brahmani River.

In the upstream station, the low flows (exceeded 70% to 90% of the time) are between 10 m^3/s and 20 m^3/s during pre-dam and post-dam periods (Table 3.2 and Figure 3.4). These lower discharge values are associated with suspended sediment concentrations of 0.002-0.006 g/L in the dry season. However, sediment transport gradually increases with the onset of monsoon in Indian peninsular rivers. The average wet season discharge is close to 900 m^3/s with suspended sediment concentration and suspended sediment load varying between 0.42 g/L (1985-2014) to 0.66 g/L (1980-1984) and 0.057×10^6 t/day (1985-2014) to 0.081×10^6 t/day (1980-1984), respectively. On the other hand, the downstream station has observed distinct changes in the flow-sediment regime during the post-dam period. The low flows (exceeded 70% to 90% of the time) have indicated the greatest variation, i.e,. 20 m^3/s in the pre-dam period to 76.92 m^3/s in the post-dam period (Table 3.2). Similarly, the average wet season discharge is close to 1300 m^3/s, which is accompanied by suspended

sediment concentration and suspended sediment load ranging from 0.29 g/L (1985-2014) to 0.69 g/L (1980-1984) and 0.043×10^6 t/day (1985-2014) to 0.097×10^6 t/day (1980-1984), respectively (Table 2).

Table 3.2 Variation of discharge and suspended sediment concentrations in the Brahmani River

Station	Q_{max} (m^3/s)	Q_{min} (m^3/s)	Q_{dry} (m^3/s)	Q_{avgw} (m^3/s)	C_{dry} (g/L)	C_{avgw} (g/L)	$Q_{s\ avgw}$ ($\times10^6$ t/day)	R_{ed}	C_{vd}	R_{es}	C_{vs}
U/S (Pre)	5570	1.1	11	900	0.006	0.66	0.081	5018	1.96	Inf	1.77
U/S (Post)	10801	1.3	10	900	0.002	0.42	0.057	8000	2.19	Inf	1.93
D/S (Pre)	9701	5.1	20	1300	0.01	0.69	0.097	1894	1.81	Inf	1.57
D/S (Post)	10372	6.9	76.92	1300	0.03	0.29	0.043	1482	1.6	2769	1.41

Note: U/S is upstream, D/S is downstream, Pre is pre-dam, Post is post-dam, Q_{max} is maximum daily discharge, Q_{min} is minimum daily discharge, Q_{dry} is dry season discharge, Q_{avgw} is average wet season discharge, C_{dry} is dry season suspended sediment concentration, C_{avgw} is average wet season suspended sediment concentration, $Q_{s\ avgw}$ is average wet season sediment load, R_{ed} is the ratio of maximum daily discharge and minimum daily discharge, C_{vd} is coefficient of variation (ratio of standard deviation to mean of daily discharge), R_{es} is the ratio of maximum daily suspended sediment concentration and minimum daily suspended sediment concentration and C_{vs} is coefficient of variation (ratio of standard deviation to mean of daily suspended sediment concentration).

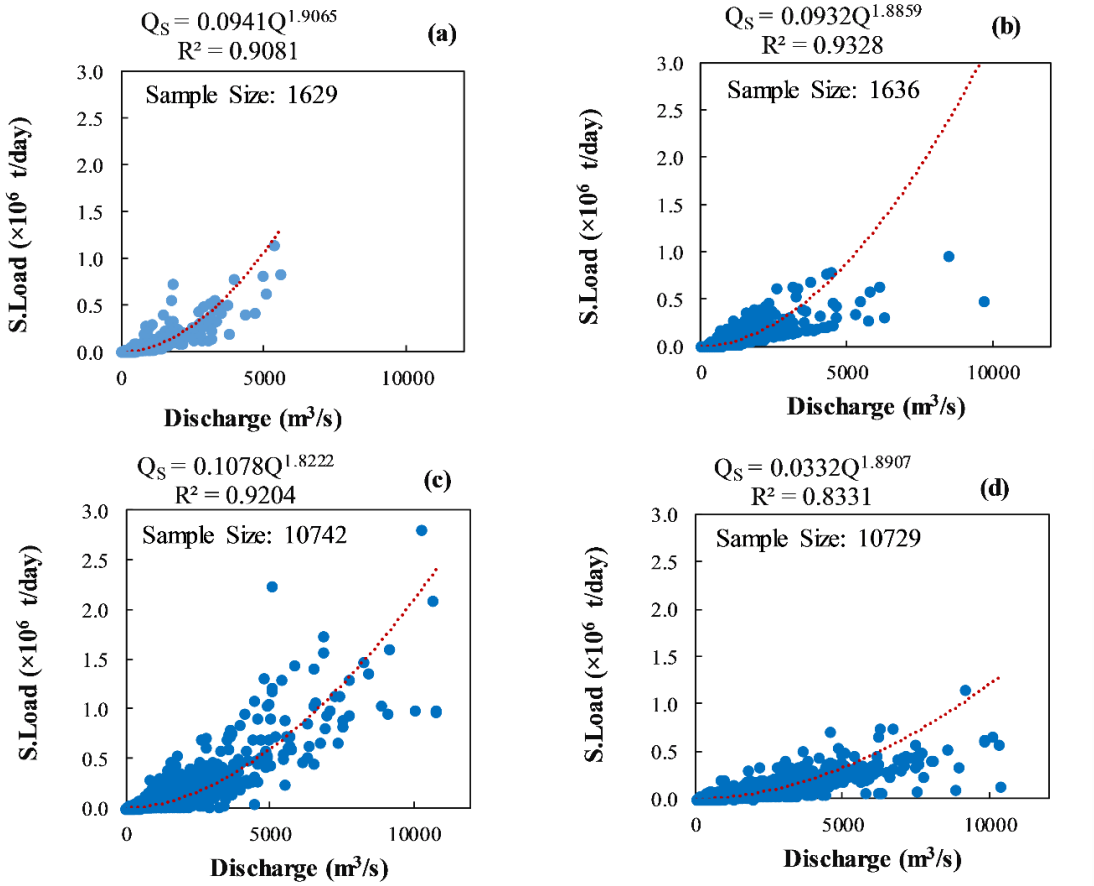

Figure 3.3 Cross-Plot between suspended sediment load (×10^6 t/day) and discharge (m^3/s) (a) Upstream (Pre-dam) (b) Downstream (Pre-dam) (c) Upstream (Post-dam) and (d) Downstream (Post-dam). The power function regression equations are significant at p~0.000, which consider the total sample size between the low flows and extreme events.

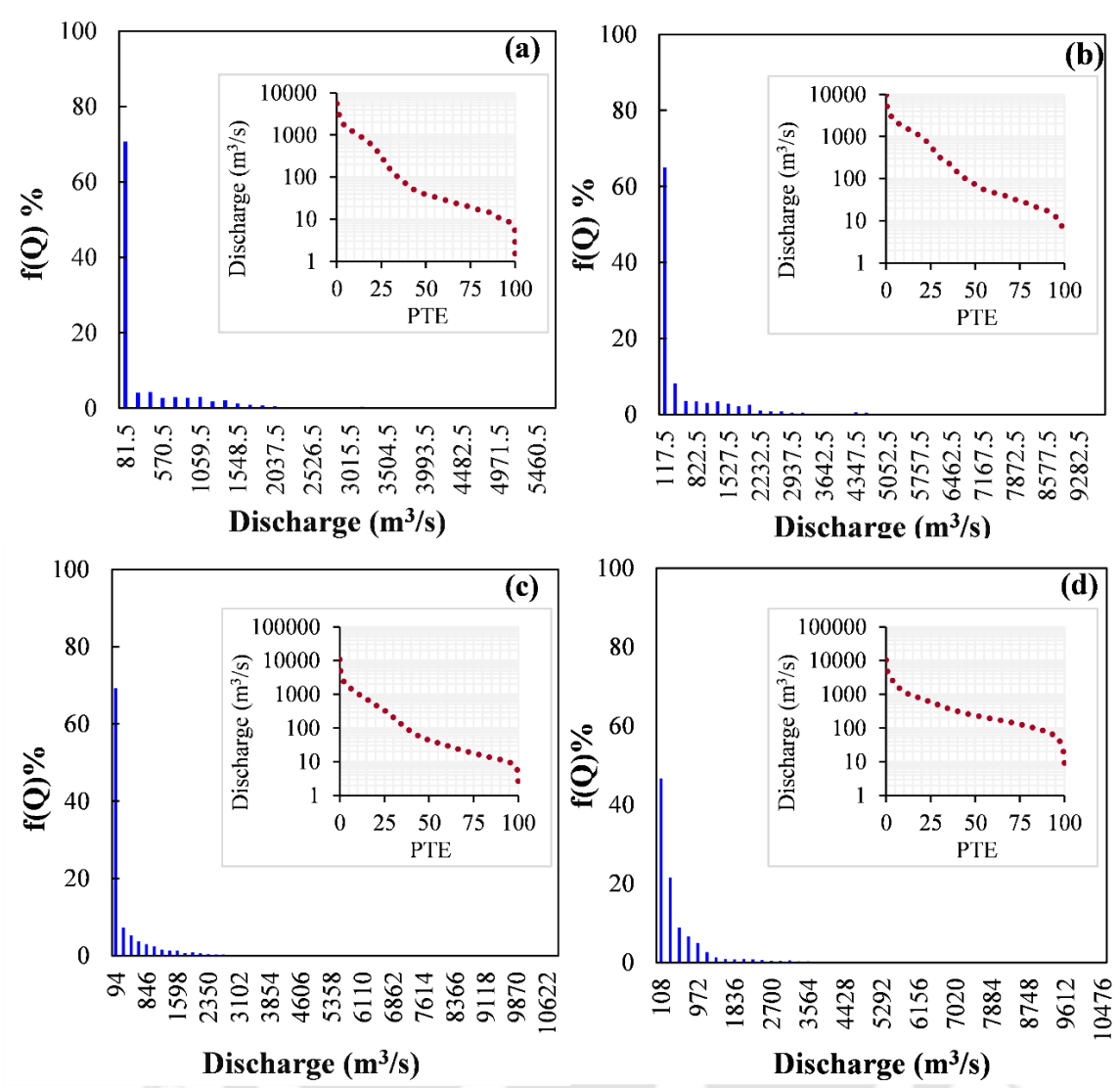

Figure 3.4 Variation of discharge class frequency in the Brahmani River (a) Upstream (Pre-dam) (b) Downstream (Pre-dam) (c) Upstream (Post-dam) and (d) Downstream (Post-dam). The flow duration is also shown, between solitary discharge values and percentage of time exceeding (PTE).

The upstream station has observed an insignificant variation in the mean daily discharge frequency, where the first discharge class (0-200 m^3/s) is close to the 70% time of occurrence in the entire study period (pre-dam and post-dam) (Figure 3.4a and 3.4c). The frequencies of moderate (300-3000 m^3/s) and high discharge classes (> 3000 m^3/s) account for ~20% and 0-1%, respectively, in pre-dam and post-dam periods (Figure 3.4a and 3.4c). The river regulation has changed the low-moderate flow regime in the downstream station (Figure 3.4d). For example, the first discharge class (0-200 m^3/s) has decreased its frequency from 64% to 46%, and the first moderate discharge class (200-500 m^3/s) has

increased its frequency from 8% in pre-dam to 20% in the post-dam period (Figure 3.4b and 3.4d). Like the upstream station, the high flows are less varied and have a frequency close to 2% for the entire study period.

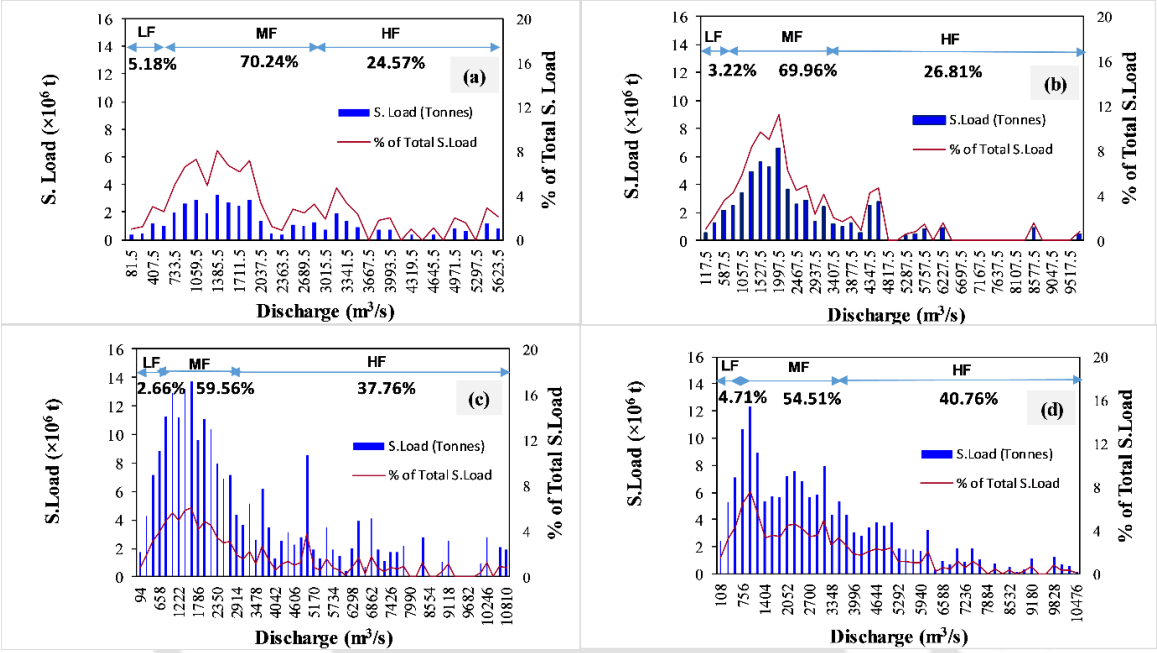

Figure 3.5 Sediment load histogram for (a) Upstream (Pre-dam) (b) Downstream (Pre-dam) (c) Upstream (Post-dam) and (d) Downstream (Post-dam) using the deterministic approach for class intervals of 0.25 S. The percentage of the total sediment load carried by low flow (LF), moderate flow (MF) and high flow (HF) flow classes are also shown.

Sediment transport occurs through a wide range of discharges in the Brahmani River (Figure 3.5). Furthermore, the mode of sediment load distribution is in the moderate flow range, which transports more than 50% of the total sediment load. An estimate of sediment transport also suggests the low flows can transport only 2 to 5% of the total sediment load in the Brahmani River. In such conditions, the flow is primarily concentrated in the inset channel. The infrequent high flow classes also have the capacity to transport quite a large proportion of the sediment load (20-40%), which facilitates coarser bed sediment transport and maintains channel capacity. In the pre-dam period, the Brahmani River shows multiple peaks in sediment transport, where the transport effectiveness of high flow classes is similar to moderate flow classes. Moreover, the regulated flow has slightly increased the sediment load-carrying capacity of peak floods (>7000 m^3/s) from 2.45 to 5.7% in the downstream station.

3.4.2 Effective discharge computation

The analytical approach's results show regulated flow, and its sediment transport has reduced the effective discharge from 1849 m^3/s (pre-dam) to 820 m^3/s (post-dam) (Figure 3.6). The upstream station has a relatively smaller variation of the effective discharge (1040 m^3/s to 859 m^3/s) between pre-dam and post-dam periods (Table 3.3). Moreover, the upstream station has an unaltered flow duration of the effective discharge, which is close to 11-12% (Figure 3.4a and 3.4c). However, the regulated flow has increased the flow duration of the effective discharge from 8.7% to 17.4% in the downstream station (Figure 3.4b and 3.4d). In contrast, the peak transport effectiveness (E_{peak}) is reduced for both stations. The downstream station has indicated a relatively larger variation, with E_{peak} reduced from 5 to 3. In the deterministic approach, effective discharges are evaluated with the class intervals of S, 0.75S, 0.5S and 0.25S. Regardless of which class interval is used, effective discharges converge on similar values of moderate floods in the Brahmani River (Table 3.4). Many studies have adopted the 0.25S class interval for accurate estimation of the effective discharge (Yevjevich, 1972; Ma et al., 2010; Roy and Sinha, 2014). For the 0.25S class interval, the upstream station has an effective discharge close to 1385.5-1598 m^3/s in both pre-dam and post-dam periods (Table 3.4). The discharge class frequency is low and varies between 1-2%. The downstream station has a reduced effective discharge from 1997.5 m^3/s to 972 m^3/s, with an increase in discharge class frequency from 2.5 to 4.93 %.

Table 3.3 Analytical approach's result with effective discharge and log-normal distribution fitting parameters

Station Name	Analytical approach's Result				
	Lognormal distribution		Sediment rating curve		Q_e
	μ	σ	*a*	*b*	m^3/s
Upstream (Pre-Dam)	4.29	1.71	0.09	1.91	1040
Upstream (Post-Dam)	4.32	1.72	0.11	1.82	859
Downstream (Pre-Dam)	4.80	1.75	0.09	1.89	1849
Downstream (Post-Dam)	5.62	1.11	0.03	1.89	820

Table 3.4 Effective discharge estimation using the deterministic approach

Station Name	S		0.75 S		0.5 S		0.25 S	
	Qe	*f(Q)%*	*Qe*	*f(Q)%*	*Qe*	*f(Q)%*	*Qe*	*f(Q)%*
Upstream (Pre-Dam)	1635	5.03	1227.5	6.93	1471.5	3.31	1385.5	2.08
Upstream (Post-Dam)	1131	8.34	1412.5	4.32	1319.5	2.97	1598	1.34
Downstream (Pre-Dam)	1410	11.4	1762.5	7.51	1645	5	1997.5	2.5
Downstream (Post-Dam)	1296	9.78	972	14.12	1080	7.56	972	4.93

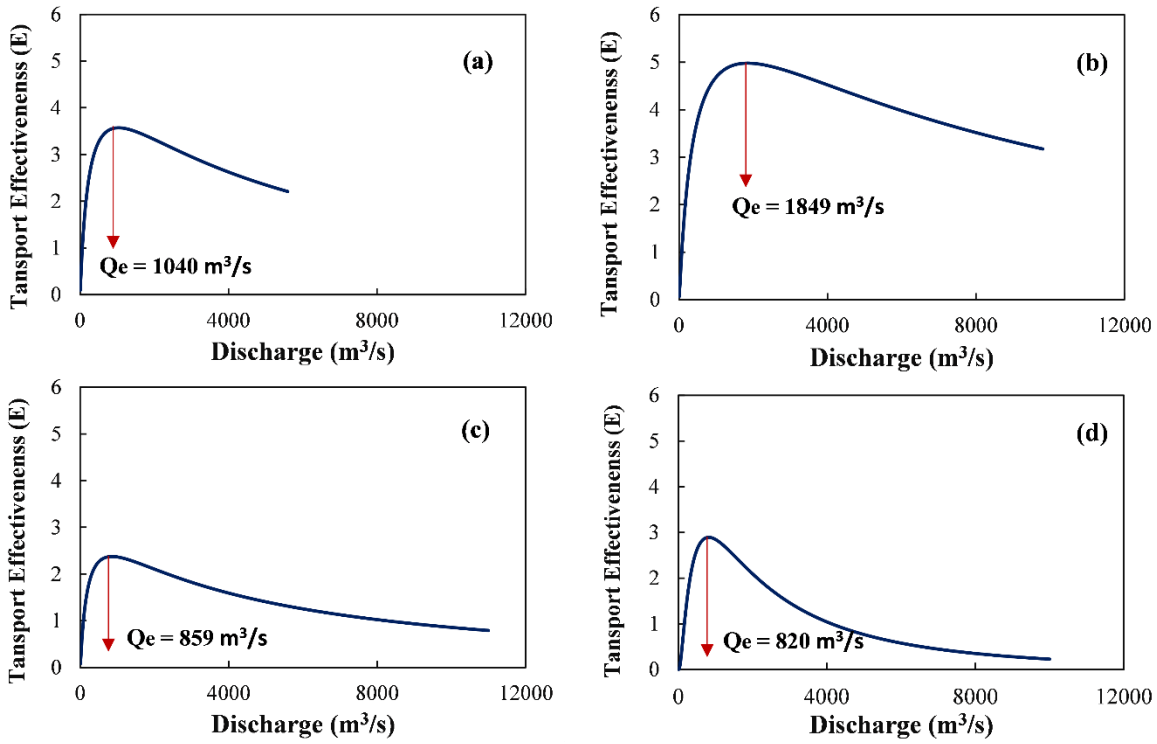

Figure 3.6 Transport effectiveness plots for the Brahmani River (a) Upstream (Pre-dam) (b) Downstream (Pre-dam) (c) Upstream (Post-dam) and (d) Downstream (Post-dam). The maximum value of transport effectiveness is E_{peak}.

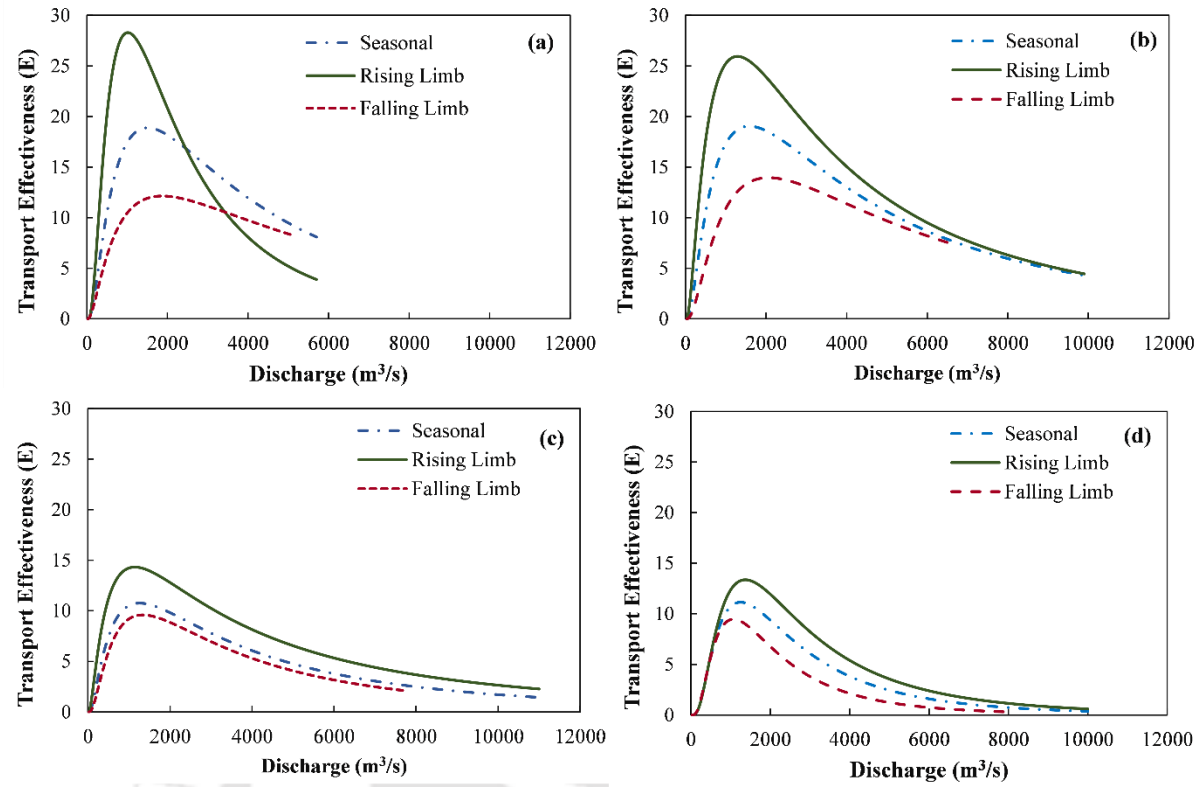

Figure 3.7 Seasonal transport effectiveness curve for (a) Upstream (Pre-dam) (b) Downstream (Pre-dam) (c) Upstream (Post-dam) and (d) Downstream (Post-dam) using the analytical approach.

The effective discharges evaluated with analytical and deterministic approaches (0.25S) match well in pre-dam and post-dam periods. Based on the 0.25S class interval, Figure 3.5a shows a bimodal transport effectiveness in the pre-dam period. However, in the downstream station, the peaks of sediment transport are seldom present in high flow classes (Figure 3.5b). In the post-dam period, an overall reduction of transport effectiveness is observed in the Brahmani River (Figure 3.5 and 3.6). The skewness of post-dam transport effectiveness is changed (Figure 3.6d), where the moderate floods produce relatively unimodal sediment transport. To evaluate the seasonal variation of transport effectiveness, the flood hydrograph is subdivided into seasonal, rising limb, and falling limb (Figure 3.7). The extreme event is incorporated in the rising limb. This analysis also establishes that seasonal, rising limb and falling limb effective discharges are in the moderate flood domain (1009-2034 m^3/s) for the Brahmani River basin. As a result of low flow modulation, overall transport effectiveness is increased. The rising limb E_{peak} is close to 25, which is reduced (up to 10) after the regulation (Figure 3.7c and 3.7d). Interestingly, the unregulated flow has produced a higher falling limb transport effectiveness when discharge is more than

4000 m^3/s in the upstream station (Figure 3.7a). This indicates the occurrence of isolated extreme events in the receding phase of the flood hydrograph.

3.4.3 Morphological analysis and stream power variability

The morphological analysis of Brahmani River is carried out to examine the configuration of the macrochannel, the inset low flow channel, and instream (chutes and diagonal bars) and bank-attached (benches and lateral bars) geomorphic units. The macrochannel position and width adjustments are insignificant over the timeframe of analysis (1980-2013) and no notable lateral migration has occurred in the study reach (Figure 3.8a to 3.8d). However, a significant alteration to the instream geomorphic unit assemblage is observed reflecting continuous erosional and depositional activities at differing flow stages. The inset channel is better defined, and the thalweg hardly shifts to a new location within the constrained macrochannel banks. The length of inset channel varies between 8.52 to 9.53 km, with an average value of 8.99 km in 2000-2013 (Figure 3.8e). Further, this time period is punctuated by three major flood events in 2001, 2005 and 2011 and a remarkable reduction of monsoon flows in 2010. Despite such extreme flow variability, the inset channel seldom realigns and abuts against the persistent benches and stable lateral bars. Benches seem to be the major sediment storing features in the macrochannel of the Brahmani River and occur in every satellite image after 1980 (Figure 3.8). These flood-built features are fixed in position and offer multiple inundation surfaces during small to moderate floods. During the period of extreme events (e.g., 2011), small benches were prone to erosion, resulting sediment re-organisation and an increase in compound bar area close to the inset channel. Time-based studies of satellite imagery illustrate that mid-channel geomorphic features are more likely to be reworked than the bank-attached units. The pre-dam satellite image establishes the occasional formation of a chute channel and a diagonal bar, which may be re-organised or disappear in the next formative flows (Figure 3.8a and 3.8c). However, in the post-dam period, a noticeable increase in chute channels and an irregular array of diagonal bars represent the fundamental change in channel pattern. The study reach has on average 6.5 km of chute channels during 2000 to 2013 (Figure 3.8e). The largest increase in chute channels and diagonal bar formation coincides with the extreme floods of 2001, 2005 and 2011. During this phase, mid-channel bars are easily short-circuited and chutes have developed in a highly sediment-charged erosional environment.

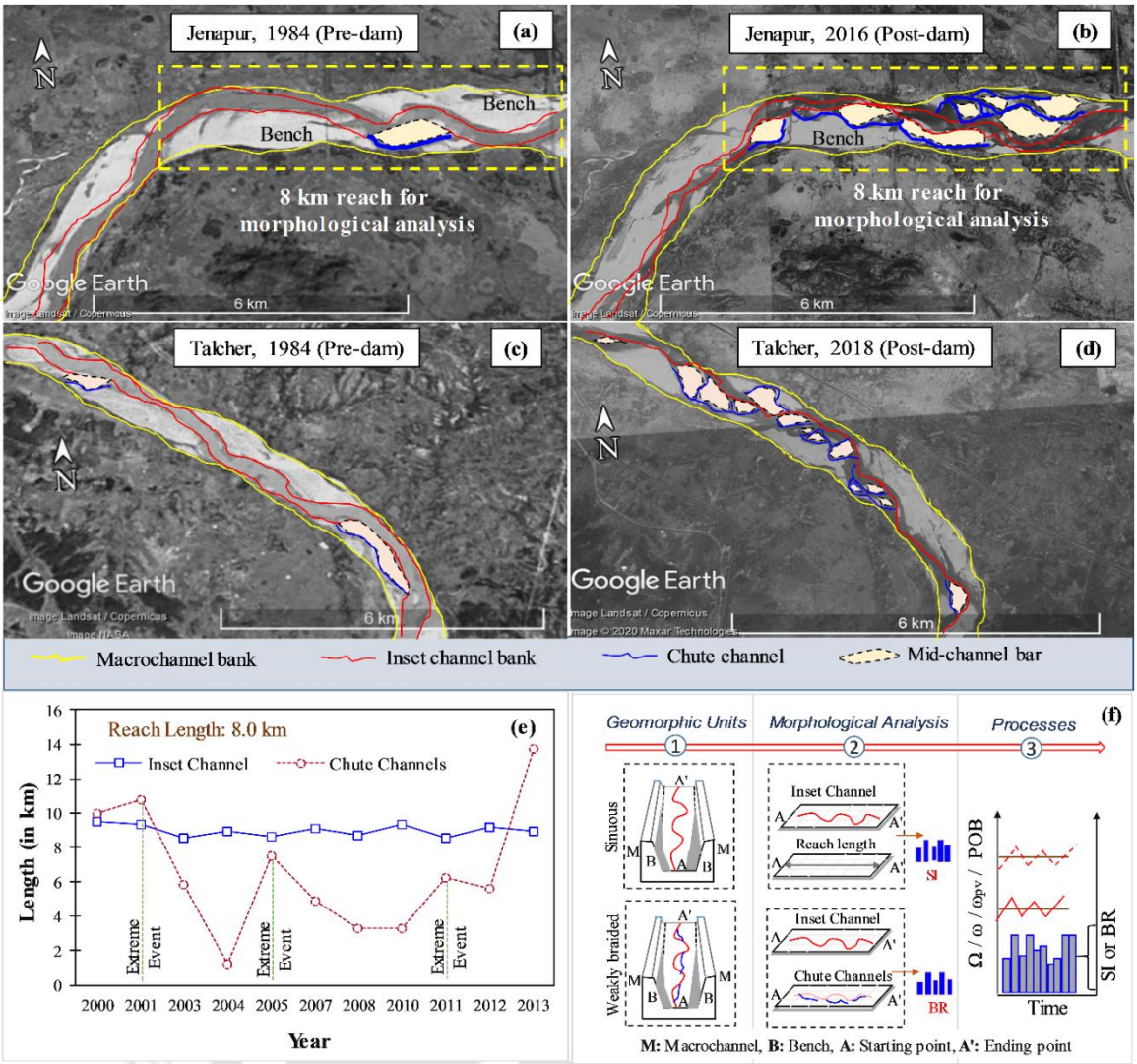

Figure 3.8 (a)-(d) The study area for morphological analysis (near Jenapur) and the geomorphic units observed at Talcher and Jenapur in pre-dam and post-dam periods. (e) The temporal variation of inset and chute channels lengths in the study reach. (f) A conceptual plot showing the link between observed geomorphic units, morphological analysis and process-based stream power estimation.

The temporal variability of inset and chute channel lengths, along with reach length is used to estimate meandering and braiding parameters (SI and BR) in the study reach. The inset channel has shown no gross adjustments and SI varies in between 1.05 to 1.18 over the entire period of analysis (Figure 3.9). Even though the low flow channel remains largely unchanged, re-organisation of features within the macrochannel (chute channels and diagonal bars) have contributed to a variable BR in the Brahmani River. In the pre-dam period, BR is close to 1, suggesting a single thread channel with occasional chutes and dissection features. However, an observable increase in chutes and diagonal bars post-1985

tends to have elevated the BR above 1.36 (except in 2004). In addition, the estimated average of BR between 2000 and 2013 is 1.73, which suggests a gradual transition of channel pattern. The peak values of BR also represent the relicts of accelerated geomorphic adjustments caused by previous major flood years. Most recently (after 2012), BR increased up to 2.53, reflecting a weakly braided planform within the macrochannel.

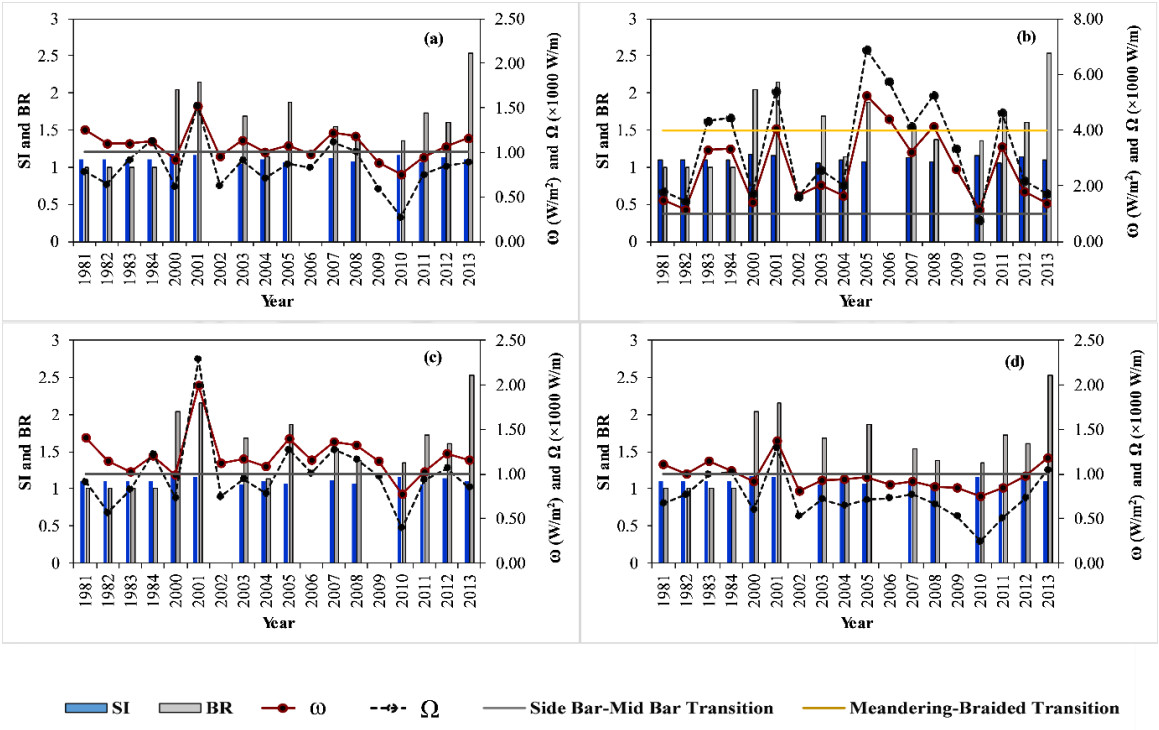

Figure 3.9 Meandering and braiding (SI and BR) variability with (a) Seasonal Stream Power (b) Peak Stream Power (c) Rising Limb Stream Power (d) Falling Limb Stream Power in pre-dam and post-dam periods. The threshold lines of side bar-mid bar (1000 W/m) and meandering-braided transition (4000 W/m) are also shown.

These within-macrochannel geomorphic adjustments are attributed to the reach averaged seasonal, peak, rising, and falling limb ω and Ω variability. In the pre-dam period, the study reach is characterized by estimated seasonal average ω and Ω of 1.14 W/m^2 and 870 W/m, respectively. Further analysis of peak ω and Ω has shown a variability up to 3.3 W/m^2 and 4400 W/m in 1983 and 1984. Both estimated averages of rising and falling ω (1.1 W/m^2) and Ω (800 W/m) are close to the seasonal magnitude. In the post-dam period, ω and Ω are also characterized by a seasonal average of 1.05 W/m^2 and 820 W/m. The wet years (2001, 2005 and 2011) have peak floods (extreme events) with ω and Ω variability up to 5.26 W/m^2 and 6900 W/m. The rising limb ω and Ω have shown marginal increases in ω and Ω,

i.e., estimated average of 1.2 W/m^2 and 1030 W/m. Finally, a gradual drop in ω and Ω is observed in the falling limb of the flood hydrograph. Figure 3.9 also shows, for most of the years, seasonal ω and Ω follow the trend of BR better than the peak ω and Ω. This analysis facilitates further understanding of differences in geomorphic adjustments associated with cumulative impacts of frequent moderate floods and infrequent peak floods in the macrochannel of the Brahmani.

3.4.4 Effective discharge integrated stream power curve

The moderate flood (post-dam effective discharge) is significantly lower than the bankfull discharge (Q_b), which suggests that frequent geomorphic adjustments may occur at sub-macrochannel bankfull stage heights. The morphological analysis also confirms accelerated development of chute channels and diagonal bars in the post-dam period. Therefore, an effective discharge integrated stream power curve allows conversion from individual discharge values to a continuous discharge spectrum and may be used to interpret these planform adjustments.

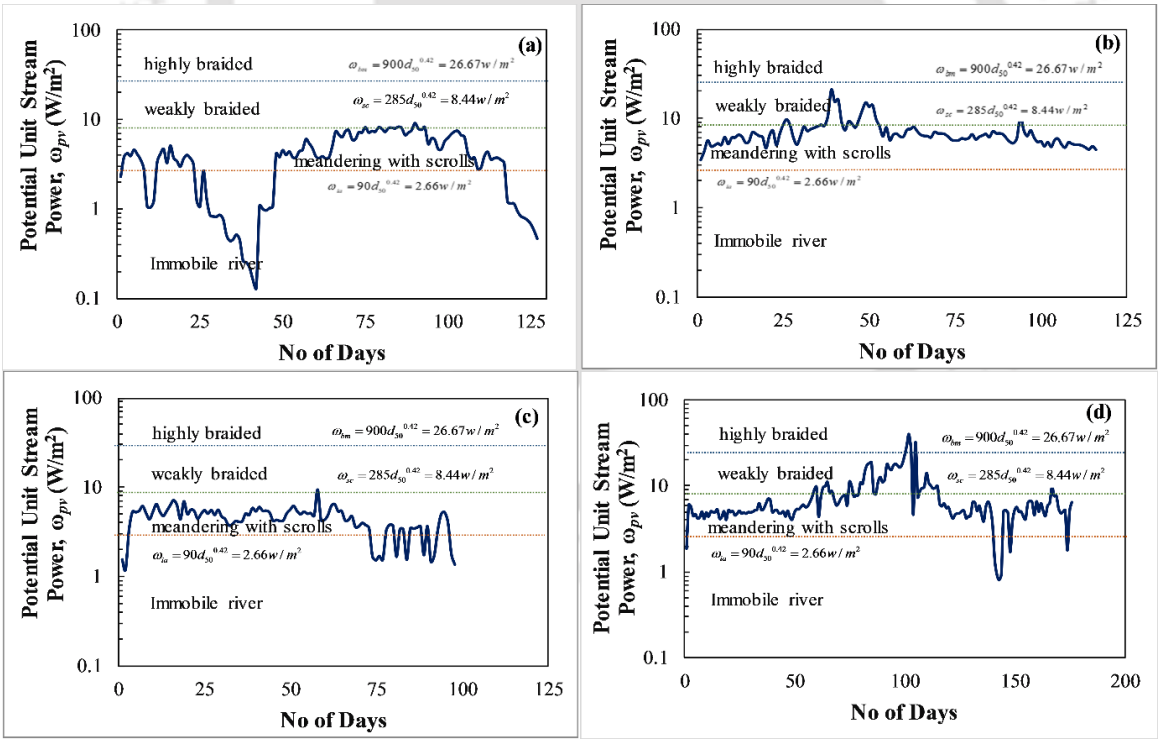

Figure 3.10 Potential unit stream power curve for the Brahmani River (near Jenapur) during (a) pre-dam period (b) normal year in post-dam period (c) drought year 2010 and (d) wet year 2011.

It is essential that the proposed stream power curve should be applicable to the macrochannel of the Brahmani, which provides the conditions of high hydrological variability. Therefore, an effective discharge integrated stream power curve is evaluated for flood discharges of pre-dam, a normal year in post-dam, and two extreme events like the 2010 drought year and the 2011 wet year (Figure 3.10). The threshold lines in increasing order of ω_{pv} are 2.66 W/m^2 (immobile river-meandering with scrolls), 8.4 W/m^2 (meandering with scrolls-weakly and moderately braided/meandering with chutes) and 26.67 W/m^2 (weakly and moderately braided-highly braided). Figure 3.10 suggests the Brahmani River has planform variability between meandering with scrolls and a weakly braided river with chutes. The scrolls or point bars are absent in the study reach. Instead, bank-attached, elongated benches are the dominant geomorphic unit when the river has low stream power ($\omega_{pv} < \omega_{sc}$). In the pre-dam period, the river had a sinuous inset channel and associated benches that carry the frequent low flows and moderate floods. Occasionally, ω_{pv} is reduced below $\omega_{ia,}$ causing no lateral migration or bank erosion. However, the river has experienced an elevated stream power to undergo geomorphic changes in the post-dam period (Figure 3.10b to 10d). During 2010 (a drought year), the flow is primarily concentrated in the inset channel, and the river has insufficient ω_{pv} for chute channel formation. In the following wet year of 2011, the Brahmani River experienced several moderate floods and extreme events with the potential for significant geomorphic adjustments. Hence, the river was subjected to a high ω_{pv}, and the uppermost threshold (ω_{bm}) was breached for a short period of time.

3.4.5 Probability of braiding in the Brahmani River

The potential unit stream power curve integrating the effective discharge as the channel forming discharge accurately predicts the channel pattern of the macrochannel of the Brahmani. It should be noted that these discriminators are not hard thresholds but indicators of transitions between different morphological states. Moreover, the chutes are related to the transition between meandering and braiding at high stream power (Kleinhans and van den Berg, 2011). The moderately braided river and meandering river with chute bars are plotted in the same energy field, as a small increase in stream power may increase the activity of chutes in meandering river, causing diagonal bar dissection, which changes the river pattern to weakly (or moderately) braided (Kleinhans and van den Berg, 2011).

Therefore, the probability of braiding (POB) is evaluated to capture the formation of chutes in the weakly braided planform state of the Brahmani River.

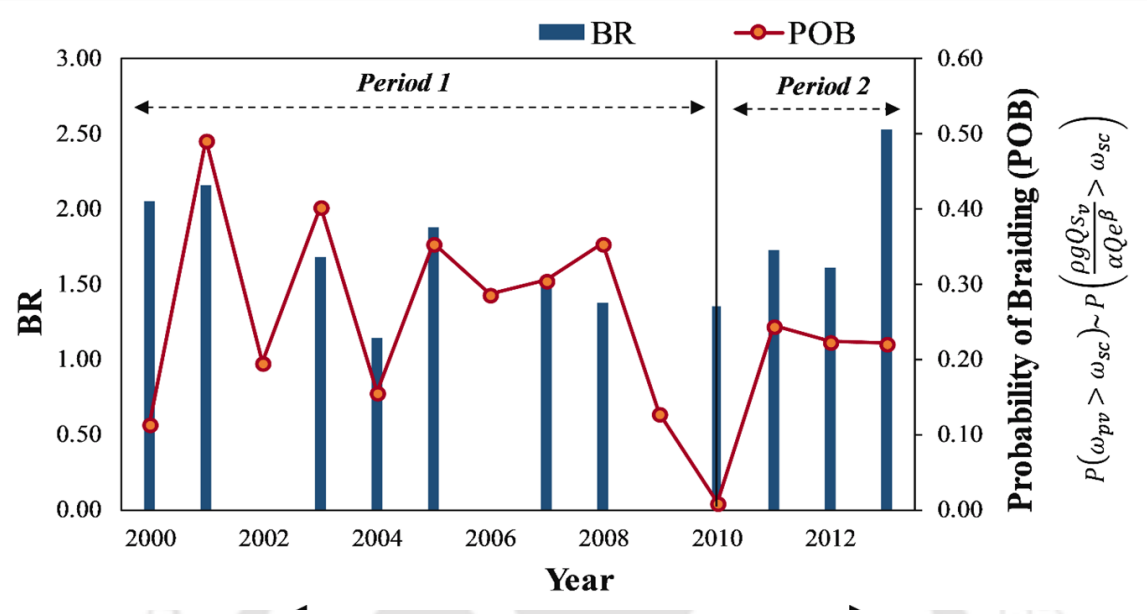

Figure 3.11 Relationship between probability of braiding (POB) and morphological variables (BR) for the Brahmani River.

The potential unit stream power for post-dam effective discharge is close to 6-7 W/m^2. The physical threshold associated with meandering with scrolls to weakly braided is 8.4 W/m^2. Therefore, this study calculates POB above ω_{sc} assuming that energy in excess of 8.4 W/m^2 is required to form chutes close to the inset channel. Figure 3.11 describes the relationship between BR and POB in the post-dam period (2000-2013). Two distinct time periods based on BR variability are observed in the Brahmani River. In period 1 (2000-2010), BR and POB are well correlated. Flood gauge data show that although the 2011 flood was the largest on record at Jenapur, major floods also occurred in 2001 and 2005. These floods of significant magnitude (POB of 0.3 to 0.45) have increased the chute channel formation (BR close to 2). In contrast, the flood of lower magnitude (like 2004) is characterized by a reduced POB of 0.2. This explains the absence of chute channels (BR=1), and that a single, sinuous inset channel has emerged at the low stage. In period 2 (2010-2013), POB is unable to capture the formation of chutes in the study reach. Period 2 witnessed drastic flow variability during consecutive drought (2010) and wet (2011) years. POB varied from a very low value of 0.01 (in 2010) to a moderate value of 0.24 (in 2011). However, the extreme events accelerated chute formation and BR was increased from 1.36 in 2010 to 2.5 in 2013.

3.5 Discussion

3.5.1 Variation of effective discharge

Few studies have estimated effective discharge on monsoon-dominated, alluvial Indian rivers (Kale, 2007; Henck et al., 2010; Roy and Sinha, 2014). Our analysis indicates a reduction in overall transport effectiveness of extreme events, and that frequent moderate floods are able to transport a major portion of the suspended load during pre-dam and post-dam periods. The present study has used three years of pre-dam flow-sediment data, which adheres to the minimum length of hydrological data suggested for effective discharge computation (Crowder and Knapp, 2005; Henck et al., 2010). Figure 3.4 and 3.5 also indicate that data gaps (in terms of discharge class) are not present in the pre-dam period and the continuous availability of low, moderate and high discharge classes can accurately evaluate the effective discharge. Further, the effective discharge computed with pre-dam data converges to a moderate flood (< 3000 m^3/s), which is integrated in the stream power curve for precise prediction of the sinuous channel pattern.

The flow and sediment transport are mostly controlled by dams in Indian rivers (Kale, 2002; Gupta et al., 2012), where major river interventions are present in the upper and middle reaches. The variation of the effective discharge is significantly influenced by drainage area (Ashmore and Day, 1988). Therefore, the upstream station has flashiness in sediment transport with a smaller effective discharge. But, for the downstream station, the suspended sediment still remains high for low discharges (Pradhan et al., 2019), which may contribute to a higher frequency of the effective discharge. Flow regulation has also changed the moderate flow regime, where small and moderate flood frequency noticeably increased in the post-dam period (Figure 3.4). During the rising limb, Indian peninsular rivers have maximum geomorphic effectiveness because of instream sediment generation from remobilization of earlier flood cycle deposits. Such local scale scouring and filling are also observed in the Ganga River basin (Roy and Sinha, 2014). Another factor responsible could be the climatic setting of Indian peninsular rivers. These tropical wet and dry climatic sand-bed rivers produce large sediment fluxes because of the low entrainment threshold (Wolman and Miller, 1960).

3.5.2 Stream power distribution and its controls

The most dramatic control on Indian rivers is exercised by the highly seasonal rainfall regime (Kale, 2002), and maximum geomorphic work occur during the summer-monsoon season (Kale, 2003). Many studies have found flood stream power controls the morphodynamics of alluvial rivers in India (Sinha et al., 2005; Kale, 2008; Akhtar et al., 2011; Bawa et al., 2014; Jain, 2018). The temporal variability of ω and Ω in the Brahmani River is controlled by hydrological variability in response to seasonal changes in rainfall. However, the spatial variability of ω is a function of changes in discharge, slope, and local variation in channel width (Kaushal et al., 2020). The spatial variability of Ω between confluence points is mostly influenced by changes in slope, while at confluence points, it is strongly governed by discharge contribution from tributaries. The downstream reach of the Rengali dam (Talcher to Jenapur) is a single channel with no major tributary contribution (Figure 3.1). Hence, the downstream discharge variability is small and strongly dependent on the lack of increase in basin area. In addition, the influence of spatial variability of rainfall on discharge is limited and assumed to be a local process (Kaushal et al., 2020). The spatial variability of ω is mostly governed by downstream changes in channel width. The downstream reach of the Rengali dam has shown macrochannel width to vary between 900 and 1300 m. This entire stretch shows similar morphological settings like high macrochannel banks with sediment storage on benches, lateral and diagonal bars (Figure 3.2). Moreover, transient geomorphological units (chutes) are observed in the entire stretch. In the Brahmani River, peak ω and Ω vary up to 5.2 W/m^2 and 6900 W/m with a seasonal average of 1.05 W/m^2 and 820 W/m. Therefore, similar geological and morphological characteristics may indicate channel slope has a dominating role in defining the limited spatial variability of ω and Ω.

Alabyan and Chalov (1998) proposed channel change thresholds corresponding to the meandering-braiding transition of 4000 W/m and side-bar to mid-bar transition of 1000 W/m (Figure 3.9). The reach-averaged pre-dam Ω (seasonal, rising limb, and falling limb) are unable to cause side-bar to mid-bar transition. On the contrary, the post-dam rising limb Ω has the energy to cause alternate to mid-bar transformation. In addition, extreme events supply excessive stream power to initiate a macro-scale shaping of the channel. It is interesting to note that falling limb ω and Ω have instigated the formation of chutes even after hydrologically extreme events of 2010 and 2011 (Figure 3.9). This is because, in the

falling limb, flow velocity starts to decrease and drapes of sediment load may be deposited over the sculpted diagonal bars.

3.5.3 Role of effective discharge in inset channel development

The form, process, and evolution of macrochannel systems are well-documented (Lecce, 1997; Heritage et al., 2004; Croke et al., 2014; Fryirs et al., 2015; Heitmuller et al., 2015; Thompson et al., 2016; Croke et al., 2017). Such channel-in-channel form provides sufficient space for erosional processes like the removal of a geomorphic unit, channel widening, bank mass failure, bend extension, occurrence of chute channels, scour, and incision. Similarly, the depositional activities include formation of new geomorphic units and accretion of sediment on multiple inundation surfaces (Fryirs et al., 2015). The classic channel evolution models (CEMs) also assume that change is possible in four degrees of freedom (cross section, planform, slope, and bed configuration) (Knighton, 1988). In the CEM, the dynamic evolution of a macrochannel system includes a cyclic pattern of within-channel adjustments like bank mass failure, bench accretion or re-vegetation of aggradational features (Thompson et al., 2016). However, the Brahmani River exhibits stable macrochannel banks because of resistant sediment, riparian vegetation, and anthropogenic margins. Thus, although the Brahmani macrochannel is predominantly alluvial, it does have reduced degrees of freedom to adjust.

As discussed earlier, the major geomorphic adjustments are in terms of chute channel formation close to the inset channel. The mid-channel diagonals bars are also present, which are the end-members of lateral bars. It should be noted that extreme events are concentrated between the macrochannel banks. In the monsoon season, the excessive energy is being stripped, which is common for a river with confined settings (Charlton, 2007). In addition, the inset channel may not increase the sinuosity indefinitely, or the slope of the channel would become too gentle to allow sediment transport. The reduction in transport effectiveness of extreme events can promote sediment deposition atop instream and bank-attached geomorphic units.

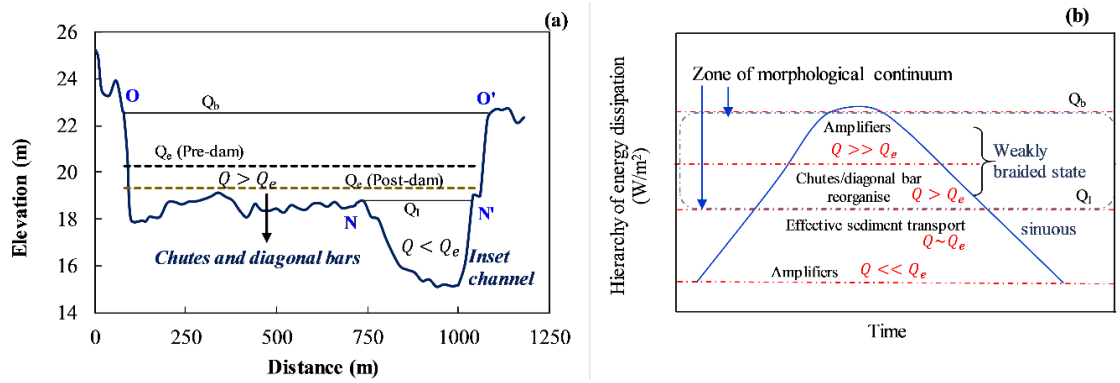

Figure 3.12 (a) Stage converted bankfull (inset and macrochannel) and effective discharge (pre-dam and post-dam) in Brahmani River (b) Conceptual diagram showing geomorphic impacts of high-magnitude flood and hierarchy of energy dissipation in the Brahmani macrochannel. The energy-zone for the morphological continuum is also shown. (Q_b: macrochannel bankfull, Q_I: Inset channel bankfull)

In the Brahmani River, a smaller low flow channel is inset within a larger channel and several platform levels (benches and bars) separate the inset channel from the macrochannel bank margin. This channel-in-channel form is disposed to high hydrological variability, introducing a dichotomy of relative frequent flows that maintain the inset channel and less frequent extreme events that maintain the macrochannel dimensions. Figure 3.12 shows the stage converted bankfull macrochannel (Q_b), inset bankfull channel (Q_I) and effective discharges (pre-dam and post-dam). The Q_b is sufficiently larger than the effective discharges when the average macrochannel bank top elevation (O-O′) is considered. The gradual departure of post-dam Q_e from pre-dam Q_e indicates an increased Q_b/Q_e after flow regulation. Interestingly, the post-dam Q_e is close to the inset bankfull stage of Q_I. The current understanding in geomorphology suggests that flow resistance reaches a minimum at bankfull flow (van den Berg, 1995). Doyle et al. (2005) has found that channels appear to adjust their geometry to allow the greatest sediment conveyance over time, although the mechanism for this remains unknown. In addition, the magnitude and frequency of the effective discharge are also potential parameters related to cross-sectional geometry (Roy and Sinha, 2014). Therefore, the effective discharge is shaping the channel in such a way that it is able to carry a maximum portion of sediment load by forming and maintaining a new set of inset channel banks (N-N′) (Figure 3.12). It also allows the minimum total rate of work and uniform energy expenditure for a river like the Brahmani (Langbein and Leopold, 1964). The Brahmani River maintains water level lower than the macrochannel bankfull level for a longer duration. In this scenario, flow lines may

get concentrated in the inset channel (thalweg) and gradually stabilise it for the effective discharge. This also agrees with previous findings where researchers have hinted that the cross section can be shaped by the effective discharge (Benson and Thomas, 1966; Andrews, 1980; Nolan et al., 1987; Ashmore and Day, 1988; Amsler et al., 2005).

3.5.4 Hierarchy of energy dissipation and probability of braiding

The effective discharge integrated stream power curve accurately interprets the planform state of the Brahmani macrochannel (Figure 3.10). The strong relationship between POB and BR suggests energy in excess of long-term sediment transport (8.4 W/m^2) is able to re-organize chutes and diagonal bars close to the inset channel (Figure 3.11 and 3.12). It should be noted that the denominator ($4.7\sqrt{Q_e}$) is constant in Eq. (7). This suggests a greater rate of increase in mean depth relative to width to compensate for the increase in discharge for both the inset and the macrochannel (Kale, 2003; Heitmuller et al., 2015). Our work also highlights the hierarchy of energy dissipation in the inset (< N-N′), the sub-macrochannel stage heights (between N-N′ and O-O′), and the macrochannel (O-O′) stage level (Figure 3.12b). The inset channel can transport a larger portion of sediment load associated with the post-dam effective discharge. The POB signifies that unit stream power in excess of 8.4 W/m^2 is sufficient to erode (or rework) the channel bar that serves as temporary sediment storage. Regulated peninsular rivers are subjected to several moderate floods (effective discharge) and few extreme events (close to macrochannel bankfull). Pitlick and Cress (2002) has reported bed material from the channel bars can be entrained by moderate floods. However, the cumulative imprint of more frequent moderate floods is obscured by the geomorphic work accomplished by the extreme events in association with resistant macrochannel banks. Similarly, in the Brahmani River, extreme events (2010 and 2011) may act as ‘amplifiers’ ($Q << Q_e$ or $Q >> Q_e$) to the geomorphic system (Phillips and Dyke, 2016). Such disruptive events can exaggerate the impacts of dam closure, with an accelerated re-organization of geomorphic units (Figure 3.11). From this study, it is inferred that the Brahmani macrochannel is probably shaped by series of formative discharges and a nested set of channel-forming discharges is necessary to understand the size, shape and sedimentary characteristics. The bankfull discharge shapes the larger macrochannel geometry and the inset channel is maintained by the effective discharge. In particular, an effective discharge integrated stream power curve highlights the morphological activities

at sub-macrochannel bankfull stages by a spectrum of flow events and questions the appropriateness of a single channel-forming discharge.

3.5.5 Process-response yielding a morphological and behavioural continuum

Thresholds and discriminators have attracted the attention of fluvial geomorphologists for many years (Alabyan and Chalov, 1998). Thresholds such as the stream power-bed erodibility ratio (Lokhtin, 1897) and gradient-discharge charts (Lane 1957; Leopold and Wolman, 1957) have emphasized discrete states (straight-meandering-braided) in the context of channel pattern. However, the morphological continuum also highlights the existence of intermediate, transitional channel patterns (Ferguson, 1987; Knighton and Nanson, 1993; Alabyan and Chalov, 1998; Heritage et al., 2001). The continuum of channel pattern is related to continuous variability of fluvial controls such as flow strength, bank erodibility and relative sediment supply or grain size trends (Bridge 1985; Knighton and Nanson, 1993). Heritage et al, (2001) investigated the continuum of channel types based on the association between different components of morphological units. In the Brahmani River, alluvial morphological units such as benches, diagonal bars, chute channels, and inset channels are the dominant components. Therefore, the degree of adjustments within the macrochannel and changing channel pattern are in response to changes in the relative influence of controlling process variables.

The first element of the continuum can be defined by the flow strength index of unit stream power and total stream power (Knighton and Nanson, 1993). The Brahmani River appears to be situated at the low end of the flow strength continuum, suggesting a limited ability to erode and transport material. However, the extreme events are concentrated between the macrochannel banks and trigger erosional processes like bench erosion and the dissection of diagonal bars. As a result, chutes and mid-channel diagonal bars develop as geomorphic units close to the inset channel. This pathway of geomorphic adjustment may represent a morphological and behavioural continuum between the single (and sinuous) inset channel and weakly braided planform. The macrochannel banks of the Brahmani River are resistant and show little tendency to migrate laterally. Such stability of high banks places this compound form similar to straight rivers with multiple channels along the continuum. Relative sediment supply is the third factor defining the continuum pattern (Knighton and Nanson, 1993). It relates to the rate sediment is supplied from bank erosion or upstream relative to downstream transport (Brotherton, 1979). The alteration of suspended sediment

transport is well observed during both low and high flows in the post-dam period. In addition, the formation of in-channel concave (chute channels) and convex (diagonal bars) features highlights a continuous erosion-deposition mechanism in the macrochannel. Therefore, fluctuation of moderate-high flows and its sediment transport, the formation of shallow thalwegs and diagonal bars, and resistant macrochannel banks may keep the channel perpetually in a state of transition rather than equilibrium.

3.6 CHAPTER SUMMARY

The present chapter has estimated the effective discharge for suspended sediment transport and its geomorphic implications as the channel-forming discharge in the regulated Brahmani River. The major conclusions of this chapter are as follows:

1. An overall reduction of transport effectiveness is observed in the Brahmani River after dam closure. The effective discharge converges to a moderate flood and is able to transport a maximum portion of suspended sediment load.
2. The seasonal stream power follows the trend of morphological adjustments better than peak stream power. Moreover, similar morphological characteristics indicate channel slope has a dominating role in defining stream power limited spatial variability.
3. The effective discharge integrated stream power curve accurately predicts the channel transition (from sinuous to weakly braided) in the Brahmani macrochannel. Most of the geomorphic adjustments occur below the macrochannel bankfull level and the river goes through a transition to accommodate the effective discharge in the inset channel.
4. The proposed probability of braiding captures the chute formation accurately, which signifies excess energy above the effective sediment transport and re-organizes chutes and diagonal bars close to the inset channel. The present study further highlights a hierarchy of energy dissipation and morphological continuum in the macrochannel of the Brahmani River.

Natural rivers are gradually subjected to altered flow-sediment conditions through various anthropogenic disturbances. Therefore, prediction of the trajectory of morphological adjustments is crucial in river management programs. Our study presented a new approach to predict the transitional channel pattern in a regulated macrochannel river. This work can be further extended to regulated rivers with different morphological settings to better understand the channel dynamics.

4

FORMULATION OF PROCESS-BASED RECOVERY INDICATOR FOR WEAKLY BRAIDED RIVER SYSTEM

The Ong-Tel paired catchment is strongly disturbed by anthropogenic activities. In recent years, the instream vegetation cover growth has influenced the process-form relationships along these weakly braided river systems. This makes it an essential initiator for river recovery and river corridor management. This chapter addresses the following questions through entropy analysis and GEE cloud computing.

- The vegetation cover may act as a stabilizing agent against the fluvial disturbances. How does it contribute to the river recovery process and morphological continuum trajectory along the weakly braided rivers?
- Previous literature has used entropy in fluvial studies. How is this theory applicable for process-based river recovery indicator formulation?
- Self-organization of vegetation and fluvial disturbance influence the trajectory of the morphological continuum. In a weakly braided macrochannel setting, how are these two processes interlinked?

4.1 INTRODUCTION

Around the globe, anthropogenic stresses in terms of flow-sediment regulation, deforestation, channelization, and clearing of (instream) riparian vegetation have created both on-site and legacy effects in the fluvial systems (Brookes et al., 1983; Shafroth et al., 2002; Syvitski et al., 2005; Coe et al., 2011; O'Donnell et al., 2016; Pradhan et al., 2017). The geomorphic impacts of such disturbances can vary from localised scour and incision to large scale transformation in channel patterns (Petts, 1984; Petts and Gurnell, 2005; Luo

et al., 2017; Fryirs et al., 2018; Zheng et al., 2018; Pradhan et al., 2019). Gregory (2019) investigated different stages of human disturbance-induced morphological adjustments and inspected the evolution of several pertinent concepts. One such key concept is recovery potential, which is defined as the capacity of the river to adjust to the prevailing boundary conditions (Fryirs and Brierley, 2000). River recovery is also related to improving geomorphic conditions over decadal frameworks, where each reach must be analysed within its catchment context (Fryirs et al., 2018). River recovery captures the past trajectories of channel adjustments and facilitates an understanding for the present state and future scenarios. The identification of evolutionary trajectories and rates of recovery is associated with historical analysis and field investigations (Montgomery, 2008). River style framework is also developed through ergodic reasoning and analysis of the assemblage of geomorphic units defining the reach (Brierley, 1996; Ferguson and Brierley, 1999; Brierley and Fryirs, 2000). The synthesis of the literature suggests that stages of recovery or deterioration have been determined by presence, absence or reconstruction of the assemblage of geomorphic units that are expected to occur for different river types (Fryirs et al., 2018; Fryirs and Brierley, 2001; Brierley and Fryirs, 2013; Fryirs and Brierley, 2016). However, it is challenging to identify the recovery stage of large fluvial systems with field-based evolutionary records of instream and floodplain geomorphic units.

The macrochannels are defined by pronounced ‘channel-in-channel’ physiography (Gupta et al., 1999; Croke et al., 2014) and formed by hierarchical low-flows and bankfull floods (Gupta, 1995; Pradhan et al., 2021a). Many rivers in Southeast Asia and Australia are macrochannels and show complex arrangements of fluvial features at varying flow depths (Heitmuller et al., 2015). The previous works on macrochannel river systems are focused on the change of flow regime (Heritage et al., 1997; Croke et al., 2014; Fryirs et al., 2015; Heitmuller et al., 2015; Heritage et al., 2015), alteration of channel hydraulics (Rountree et al., 2000; Heritage et al., 2004; Daley and Cohen, 2018; Milan et al., 2020; Wakelin-King, 2022), the influence of vegetation and ecological management (Moon et al., 1997; van Coller et al., 2000; Myburgh et al., 2005; Croke et al., 2017; Larsen et al., 2019), sensitivity and connectivity analysis (Croke et al., 2013; Khan and Fryirs, 2020), and understanding the channel evolution and metamorphosis (Pradhan et al., 2021b; Heritage et al., 2001; Rountree et al., 2011; Thompson et al., 2016). Despite the well documentation of process-form-ecological relationships, understanding the direction of morphological continuum and association-feedbacks of vegetated landforms are relatively understudied in macrochannel

systems (Thompson et al., 2016; Pradhan et al., 2021a). In addition, instream vegetation emerges as dominating factor to control the direction of fluvial form in the macrochannels with reduced degrees of freedom. The vegetation cover is also linked with river recovery process and therefore, formulating a process-based river recovery indicator for macrochannel settings provide an idea about river recovery trajectory and underlying processes, which is crucial for river corridor management in anthropogenically disturbed river systems.

The entropy theory has been used in hydro-geomorphological studies in different scales and forms. Leopold and Langbein (1962) applied the concept of entropy in landscape evolution and developed the most probable condition based on the uniform distribution of energy in fluvial systems. A similar application of entropy to river basin networks was carried out by Fiorentino et al. (1993), which further explored the relationship between mean elevation, potential energy and drainage basin morphological characteristics. The study of Singh (1997) applied entropy concept in hydrology and water resources. Gholami et al. (2019) assessed the transverse slope of bank profiles and associated hydrulic-geomotric parameters using the entropy parameter. Likewise, Chembolu and Dutta (2018) developed an entropy-based planform disorder index to understand the process-form interactions of the highly braided Brahmaputra River. Other studies have utilized the entropy concept in the evolution of river delta (Tejedor et al., 2017; Mou et al., 2020), flow monitoring (Moramarco et al., 2008), velocity measurement (Farina et al., 2014; Greco et al., 2015), discharge estimation (Ardiclioglu et al., 2010), and landscape stability (Bandyopadhyay et al., 2014). This makes entropy an important concept in geomorphic studies. In recent years, entropy theory has been used in river health assessment in terms of flow measurement (Zhang et al., 2006), flood control (Deng et al., 2015; Kong et al., 2022), water supply and quality analysis (Zuo et al., 2020), ecological biomass measurement (Silow and Mokry, 2010), development of sustainable development goals (Xue et al., 2020), and wastewater treatment rate quantification in urban areas (Yang et al., 2016). However, the macrochannel systems are subjected to considerable hydrological variability and erosion-deposition processes that affect the functional surfaces of geomorphic units and associated riverine health (Thompson et al., 2016). In addition, the seasonal switches of threshold-modulated processes (erosion to deposition and vice-versa) create divergent and convergent system states. The divergence or multiple endpoints of landscape evolution is problematic for river managers, and hence, convergence or single end system state is

often preferred (Phillips and Van Dyke, 2016). The concept of entropy emerges as an important tool to capture these cross-sectional landscape evolution processes of macrochannel systems and provide a basis for river health trajectory assessment. In the present chapter, concept of entropy and integrated Google Earth Engine (GEE) cloud computation techniques are used to contribute to this challenge.

In India, peninsular rivers are an integral part of the water-food-energy nexus, supporting millions of people through agriculture, industries, and flood control (Pradhan et al., 2021b). However, these river basins also have a large history of receiving intense anthropogenic stresses for two centuries. For example, an extensive loss of forest cover was reported for the central-east regions of India in 1880-1960 (Tian et al., 2014). The dam-building activity was also at its peak during 1970-1990, and the small height large dams and mega-dams of national importance have increased their numbers by three to four times in these twenty years (Pradhan et al., 2021b). Such large-scale anthropogenic disturbances combined with localised fluvial disturbances like sand mining, instream (riparian) vegetation loss and channelization have instigated both geomorphic and (bio)ecological adjustments along the fluvial systems (Kale, 2003; Ghosh and Guchhait, 2014; Pal, 2017; Uday Kumar and Jayakumar, 2018). The major impacts include variability in flow-sediment regime (Gupta et al., 2012), reach-scale channel pattern alteration (Pradhan et al., 2017), coastal erosion (Malini and Rao, 2004), riparian wetland area loss (Talukdar and Pal, 2017), salt-water intrusion (Gopal and Chauhan, 2006). However, the understanding of process-form relationship in these poorly gauged-anthropogenically disturbed rivers is still in the preliminary stages and therefore, demands interdisciplinary, multifaceted approaches. The study area of this chapter includes two such basins (the Ong and Tel), where both anthropogenic and natural stressors have significantly altered the bio-morphological interactions. In addition, the integration of entropy theory and GEE cloud computation techniques will be the first attempt to develop process-based recovery indicators for the macrochannel systems. Hence, the objectives of this study are to (i) develop an entropy-based indicator to incorporate the cross-sectional disorderness (ii) assess the spatio-temporal variability in instream vegetation cover using GEE cloud computations and (iii) finally, formulate process-based recovery indicators to monitor river health and system state.

4.2 STUDY AREA

The Mahanadi River basin is the fifth largest watershed in India, covering a total geographic area of nearly 4.3% (India-WRIS). The earlier studies on the Mahanadi and its tributaries include the flow-sediment-water quality variability (Syvitski et al., 2005; Bastia and Equeenuddin, 2016; Jin et al., 2018; Naha et al., 2021), understanding the morphological characteristics (Subrahmanyam et al., 2008; Gunjan et al., 2020; Satyakumar et al., 2022), and ecological entities (Ghosh et al., 2006; Das et al., 2019; Saalim et al., 2022). The Ong and Tel are the two largest tributaries of the Mahanadi (India), with a combined catchment area of 27, 946 km^2 and a channel length of 184 km (Figure 4.1). These rivers drain mix red and black soils (CWC, 2012) and has an average annual rainfall of about 1463 mm during the southwest monsoon (June to September). The Ong is governed by the Guchhepali dam (NRLD, 2019), and the Tel has a dynamic flow-sediment regime owing to the combined effects of natural and anthropogenic stresses. Two gauging stations, Salebhata and Kantamal, are present 30 km and 40 km upstream of the Ong-Mahanadi and Tel-Mahanadi confluences, respectively.

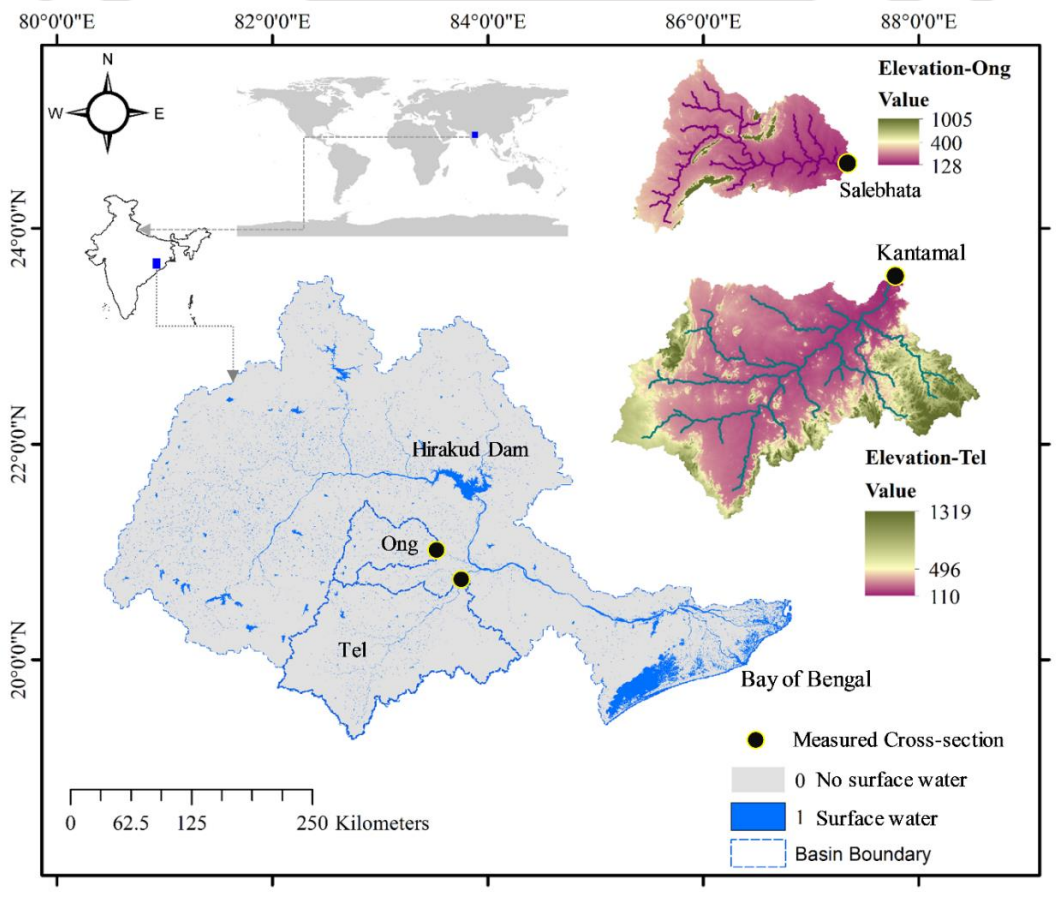

Figure 4.1 Study area showing the Ong and Tel sub-basins of the Mahanadi River (India).

The channel form of the Ong and Tel is described as macrochannel, in which a smaller low flow channel is inset within a larger channel. At the measured cross-section locations, the macrochannel and inset bankfull widths are close to 0.4 and 0.1 km, respectively. The significant difference between the inset and macrochannel dimensions offers large space for geomorphic adjustments at multiple inundation surfaces (Figure 4.2). The macrochannel bank height is 8 to 10 m, which can accommodate a flow regime of high hydrological variability. Tributary inflow and bank erosion are also absent and geomorphic units such as benches, chutes and various bar types (vegetated and unvegetated) are effectively confined between the macrochannel bank margins. The instream vegetation covers are normally shrubs, grasses, and twinners plants with soft stem, flexible bends and have deep root into the sand. The vegetations like *tamarix ericoides*, *coix lacryma-jobi*, *hedyotis corymbosa*, *cyperus rotundus*, *typha latifolia*, *polygonum aviculare* and *polygonum barbatum* spread profusely in the fluvial corridor. In particular, an accelerated conversion of the submerged shelf to bar and exposed shelf to bench with plants like *saccharum spontaneum, vetiver zizanioides and ipomoea carnea* have developed stable vegetated landforms along the study reaches (Figure 4.2).

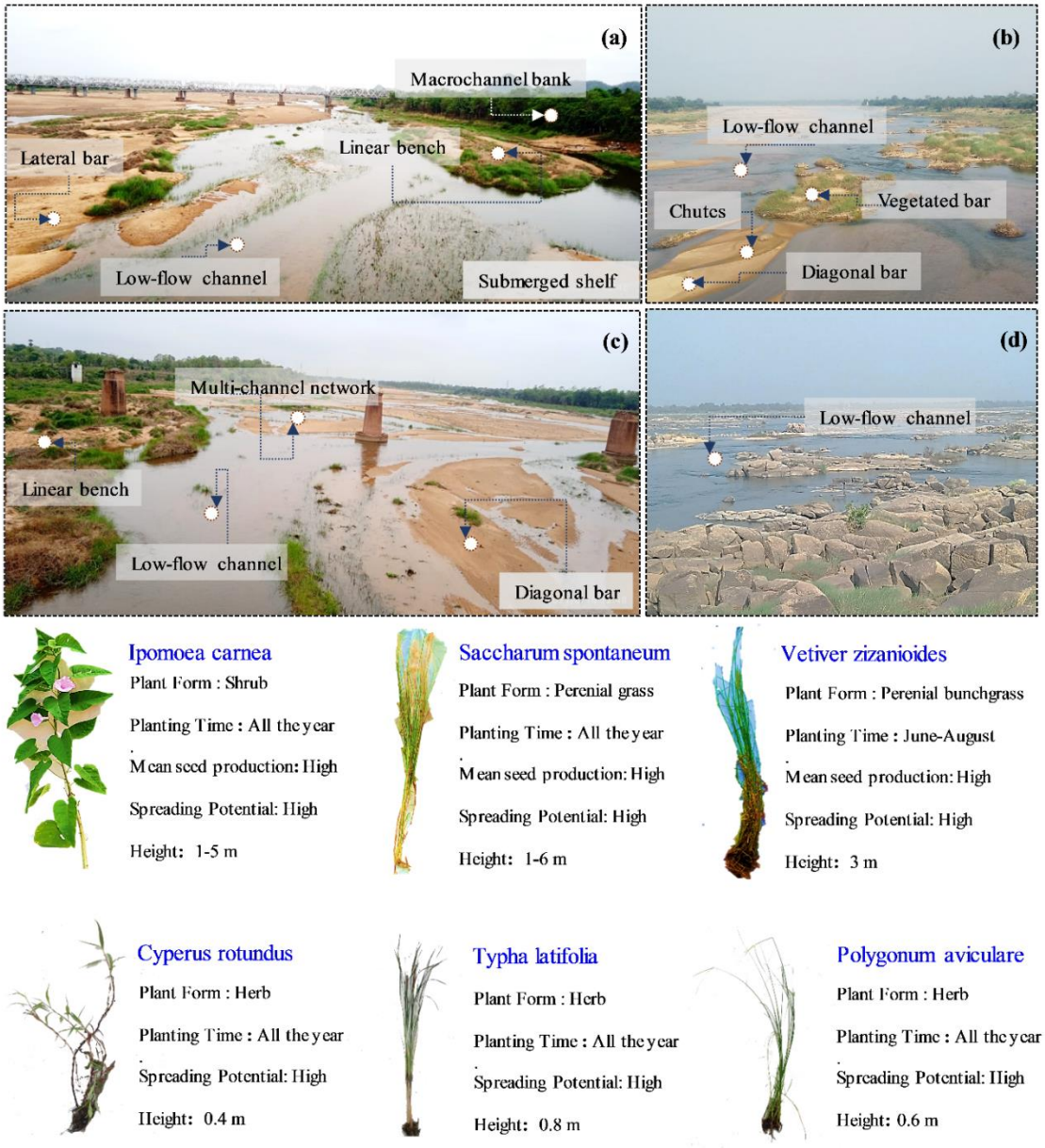

Figure 4.2 Field photographs showing the presence of instream and floodplain geomorphic units in the Ong-Tel paired catchment. (a) and (c) Macrochannel banks and instream vegetated geomorphic units in Ong River (b) and (d) Prevalence of diagonal bars and defined low-flow channel in Tel River. The dominant instream and riparian cover vegetation details are also shown along the two reaches.

4.3 DATA AND METHODOLOGY

4.3.1 GEE cloud computing and instream vegetation area assessment

The instream vegetation cover atop the bare bar and bench surfaces has been assessed with GEE for the last 35 years (1985-2020). Moreover, field investigations were carried out to identify the instream and floodplain geomorphic units along the study reaches. Then, the macrochannel bank lines were digitized based on field-observed floodplain signatures and subsequent polygon layers were generated. The space between the macrochannel bank lines was selected as the fluvial corridor for instream vegetation cover assessment. The post-monsoon time refers to the low-flow hydrological condition during October-March. In this period, the flow is majorly concentrated in the thalweg (the deepest portion of the river) and geomorphic units like bars, bench, and instream vegetation cover are effectively captured from the field investigations and satellite imagery. The atmospherically corrected and orthorectified surface reflectance from Landsat 5 ETM, and 7 ETM+ sensors are accessible by the GEE. For the given study period, these datasets were used to derive seasonal NDVI (Normalised Difference Vegetation Index) time series inside the fluvial corridor. Reflectance images in red and NIR bands of the electromagnetic spectrum from corresponding days of acquisition were used to compute NDVI. Later, the temporal median of NDVI images was evaluated to derive a single seasonal NDVI representing the most general low-flow hydrological condition in the post-monsoon season. These computations were performed in the cloud platform of GEE, and final NDVI image time-series were exported for instream vegetation cover assessment. (Figure 4.3).

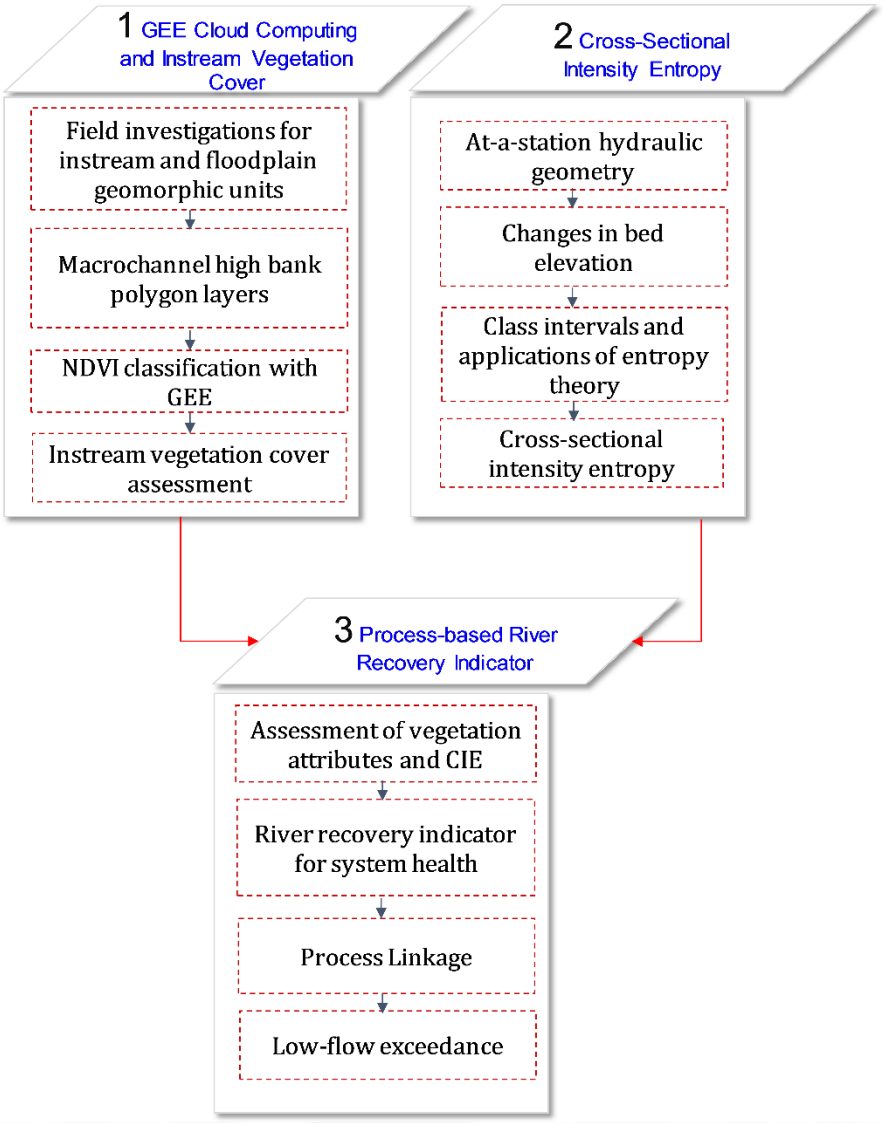

Figure 4.3 The methodological flowchart for evaluation of process-based recovery indicator

4.3.2 Cross-sectional intensity entropy

Shannon's information entropy theory is applied in this study, which is a measure of uncertainty or variability or disorder associated with the random variable $X = X\,(x_1, x_1, x_1 \cdots\cdots\cdots, x_n)$. Shannon (1948) defined uncertainty of occurrence of an event x_i from the possible events in X as entropy H(X), which is given by

$$H(x) = -\sum_{i=1}^{n} p(x_i)\log_2(p(x_i)) \qquad (4.1)$$

Here, $p(x_i)$ is the probability of x_i, which is based on the empirical frequency of X values. The present study uses the concept of intensity entropy (IE) to investigate the seasonal

(post-monsoon) variability associated with the macrochannel cross-sections. The cross-sectional intensity entropy (CIE) can be assessed as follows

1. At-a-station hydraulic geometry dataset was obtained from India-WRIS, which consisted of multi-decadal records (1989-2011). This dataset was collected with 10m bin size intervals to understand the geomorphic aggradation (or degradation) associated with the instream geomorphic units.
2. Then, the alteration in channel bed elevation was computed from the reference year (1988), and the macrochannel geometry was further segregated into different zones based on the maximum breaks in slope.
3. The class intervals are carefully selected by examining the hydraulic geometries in post-monsoon seasons and decided based on the upper and lower bounds of the alterations in bed elevation. Therefore, all possible variations in the at-a-station hydraulic geometry and gradual macrochannel adjustments like thalweg shifting, chute development and conversion of bar to bench were integrated to the analysis. The cross-sectional intensity entropy (CIE) is calculated as

$$\mathrm{CIE} = -\sum_{i=1}^{n}\left(\frac{f_i}{N}\right)\log_2\left(\frac{f_i}{N}\right) \quad (4.2)$$

Where f_i is the number of elevation change values in a particular class (n) of a season to the total number of values in that season (N). The relative frequency was calculated as $f_i/N = p(x_i)$. In this study, CIE is a measure of disorderness in the hydraulic geometry and distribution of available fluvial energy in the macrochannel system. CIE value reaches the maximum when the bed elevation changes are equally distributed between all classes and is minimum (=0) only if all values fall into a particular class. Further, CIE symbolises the aggradation and degradation of instream geomorphic units at certain intervals and provides an understanding of assemblage of landforms expected of river type and their past-to-present status and future trajectories. Fryirs et al. (2018) suggested various geomorphic adjustments like wide symmetrical channel to macrochannel, bank erosion to bench formation, actively widening to contracted channel, high width-depth ratio braid like low flow channel to well-defined low width-depth ratio thalweg as indicators between the pre-recovery and recovery states.

4.3.3 Normalized river recovery index

Recovery is related to the improvement in geomorphic conditions, normally over the decadal period. It is also associated with the adjustments of the river to the prevailing boundary conditions like flow-sediment alteration, modifications in land-use practices, changes to instream fluvial cover etc. In addition, recovery is associated with the inherent sensitivity of the river, where each reach can be placed in its catchment context. The presence, absence or reconstruction of the assemblage of geomorphic units facilitate key indicators regarding the deterioration and recovery trajectory responses. Further, it is noted that the rate at which geomorphic units emerge provides a sign about the effectiveness of the recovery process. The present study has considered two important attributes of macrochannel rivers, i.e. vegetative measures and geomorphic disorderness, to provide a snapshot of how the system is performing today. The normalized river recovery index (NRRI) as a system-state response is formulated as

$$\mathrm{NRRI} = \frac{\mathrm{NORM_{VI}} - \mathrm{NORM_{CIE}}}{\mathrm{NORM_{VI}} + \mathrm{NORM_{CIE}}} \quad (4.3)$$

Where VI is vegetation intensity, CIE is cross-sectional intensity entropy, and NORM stands for normalization with maximum and minimum values. The vegetative measures often develop some fluvial landforms that trigger and engineer the river recovery process. In the present study area, instream vegetation growth is closely linked with CIE, where, after the stability of fluvial landforms, seed germination and gradual colonization have initiated. According to Thompson et al. (2016), with-in channel benches becomes more resilient after the vegetation and may reduce the disorderness in hydraulic geometry. Moreover, instream vegetation has improved the channel boundary resistance in present macrochannel settings, and the multiple inundation surfaces (bar, bench and macrochannel bank) have approached towards recovery with increased VI and gradual reduction of CIE.

4.3.4 Process linkage

The recovery trajectory is enhanced or constrained by limiting factors and pressures. These limiting factors operate internally in the system and generally incorporate the changes to sediment supply, flow regime and instream vegetation cover. The pressures are the external agents and are integrated with environmental management policies and climate change etc. In the present study reach, it is well-established that effective discharge shapes the inset channel to carry a maximum portion of sediment load in the long term. Further, the excess

energy above the effective sediment transport level re-organises the chutes and diagonal bars close to the inset channel. Hence, a new process indicator- Low Flow Exceedance (LFE) is proposed to understand the impacts on the hierarchy of energy dissipation and river recovery processes in the morphological continuum zone of the macrochannel Ong and Tel. LFE signifies the number (N) of moderate-to-high flows exceeding the inset channel and submerging the instream vegetation zones at different platform levels. The LFE is proposed as

$$\mathrm{LFE} = \mathrm{N}(\mathrm{Q} \geq \mathrm{Q_L}) \tag{4.4}$$

Where, N is number of days, Q is flow (in m^3/s) and Q_L is carrying capacity of the inset channel (in m^3/s).

4.4 RESULTS AND DISCUSSION

4.4.1 Longitudinal variation of instream vegetation cover

No extensive changes to macrochannel position have occurred through bank erosion in the Ong and Tel Rivers. The macrochannel bank is highly stable by riparian vegetation and internal resistance of substrate lithology (Figure 4.4a and 4.4b). The major changes are in terms of within-macrochannel adjustments like chute and floodways formations, bar and bench establishment and the gradual emergence of vegetated landforms. Figure 4.4c to 4.4h show temporal changes in instream vegetation area alongside dominant geomorphic units present in the Ong and Tel Rivers. In 1985-90, both river systems had similar instream vegetation coverage, close to 7% of the total fluvial area. In this time slice, three to four selected areas were controlled by vegetated landforms close to the low-flow channels. The next time slice (1990-95) observed contrasted changes in vegetation area, where the Ong increased the vegetation coverage up to 10.4% and the Tel slightly decreased the area to 4.7%. However, steady growth in vegetation cover was observed in the next time slice (1995-2000), and the Ong and the Tel had an instream vegetated area of 18.4% and 7.39%, respectively. Between 1995 and 2000, the complete reach of the Ong river was affected by instream vegetation growth atop bar and bench surfaces, making it challenging to identify chute margins in some areas. The next decade was punctuated by major floods in 2001, 2003 and 2005 and a slight reduction in vegetation coverage was detected along the rivers. The decadal average vegetation cover was close to 14% and 4% along the Ong and Tel, respectively. It should be noted that no wholesale change to vegetated landforms occurred

in the Tel river and periodic destruction, survival, and succession continued in the 2010s. In contrast, the Ong experienced a drastic change in instream vegetation cover in the 2015-2020 time slice and increased the area from 19% to more than 30%.

The instream vegetation type, structure, density and position affect the process, form and dynamics of alluvial rivers at micro and macro scales (Baker, 1989; Naiman et al., 2005; Steiger et al., 2005; Thorp et al., 2006). In particular, the macrochannel river settings display multiple surfaces of varying inundation frequency and sediment trapping potential (Croke et al., 2017). In the Ong, major vegetated landform zones and biomass density are observed on the bench surface and close to the low-flow channel (Figure 4.4i). Furthermore, similar to the findings of Gurnell (2014), the Ong river has experienced aggradation of the submerged shelf to lateral bars and exposed shelf to a bench. These linear benches are natural repositories of seed germination and allow vegetation like *saccharum spontaneum*, *vetiver zizanioides* and *ipomoea carnea* to colonize in the post-monsoon season.

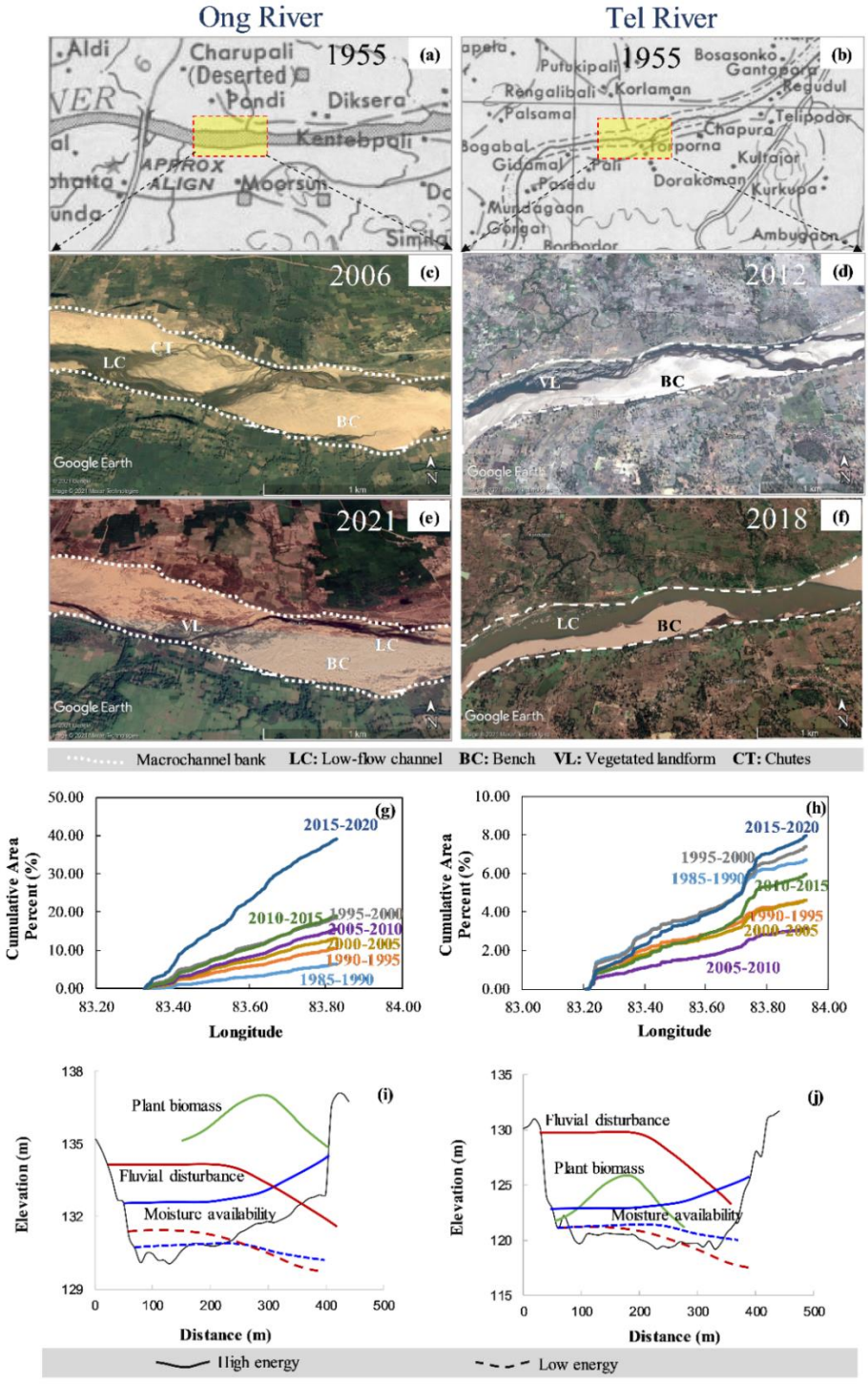

Figure 4.4 The Survey of India (SOI) toposheets for (a) Ong (b) Tel Rivers (Courtesy of the University of Texas Libraries, The University of Texas at Austin). The instream geomorphic units present in the Ong (c and e) and the Tel (d and f) Rivers. The longitudinal variation of instream vegetated landforms for the last 35 years in (g) the Ong and (h) the Tel Rivers. The conceptual plots showing cross-sectional variability of plant biomass, fluvial disturbance and moisture availability in (i) the Ong and (j) the Tel Rivers.

A schematic representation of the distribution of soil moisture and fluvial disturbance suggests that vegetation patches have the support of perennially flowing water even at the lowest discharges. Therefore, the Ong River is affected by the development of vegetated patches close to the thalweg. Further, periodic bio-geomorphological interactions have helped these vegetation patches to retain the upstream sediment, form deeper and narrower low-flow channels and eventually develop self-organized landforms. In contrast, The Tel resembles a confined channel with stable macrochannel banks, where high fluvial disturbances dominate the bio-geomorphological interactions (Figure 4.4j). In this process, small-rooting depth plants have grown until they are destroyed by excessive fluvial erosion, leaving the small patches of deeper rooted plants to colonize the bare sediment of linear benches.

4.4.2 Hydrological data analysis and variability in CIE and NRRI

The oscillation of the south-west monsoon rainfall regime generates a unimodal wet (June-September) and dry (October-May) seasons along the Ong and Tel Rivers (Figure 4.5). The wet flows (floods and extreme events) are periodic, and a significant variation in discharge and stage (with respect to mean sea level-MSL) are observed along the study reaches. The transition between wet and low flows is characterized by moderate flows that provide a significant contribution to the bio-morphological activities. The time-averaged flow and stage along the Ong River are close to 130.80 m and 60.52 m^3/s, respectively. However, the maximum water level and discharge are sufficiently larger, and close to 139.53 m and 7916 m^3/s, respectively (Figure 4.5a). The Tel River observes a notable hydrological variability with time-averaged and maximum stages are 119.02 m and 132.7 m, respectively. The maximum observed discharge is 20,000 m^3/s, which is considerably greater than a time-averaged value of 384 m^3/s. Such extreme flow and water level variability highlights the ample in-channel space of macrochannel configuration, which can capture both high floods and extreme events (Figure 4.5b).

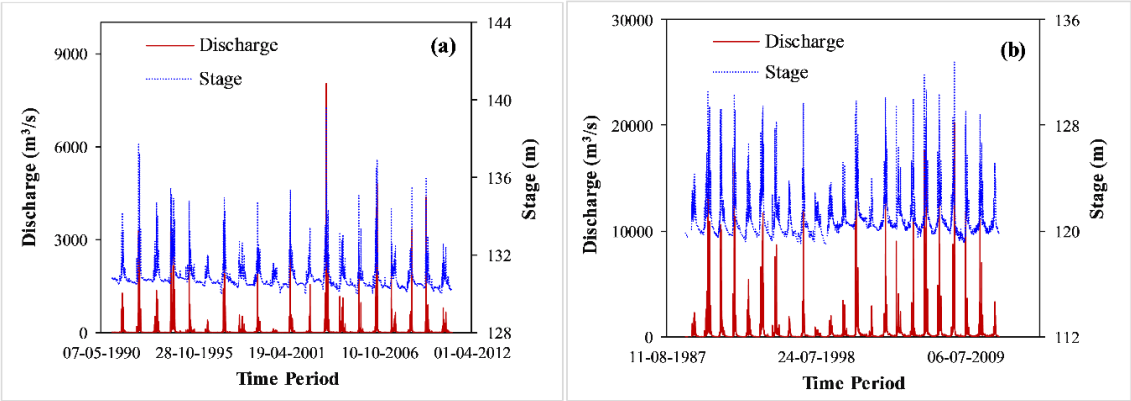

Figure 4.5 Variation of flow (in m^3/s) and stage (in m- from MSL) along **(a)** the Ong (1991-2011) and (b) the Tel Rivers (1989-2011).

Figure 4.6 shows the temporal variability of CIE along the Ong and Tel Rivers. It is observed both river systems demonstrate continued hydraulic geometry adjustments via thalweg shifting, bar formation-sculpting-erosion and bench growth-destruction. In the Ong River, the temporal average of CIE is close to 2.05, whereas the Tel river has a slightly decreased CIE of 1.88. The maximum CIE in the Ong and Tel are close to 2.34 and 2.15, respectively. The Ong has a distinct minima of CIE variability in the early 2000s. Moreover, the Ong displayed a continuous decreasing trend of CIE between 1997 and 2002 and after the extreme floods of 2003 and 2004, an increased CIE was noted in the late 2000s. In contrast, the Tel has no significant trend in CIE variability, and periodic fluctuations were noted over the entire study period.

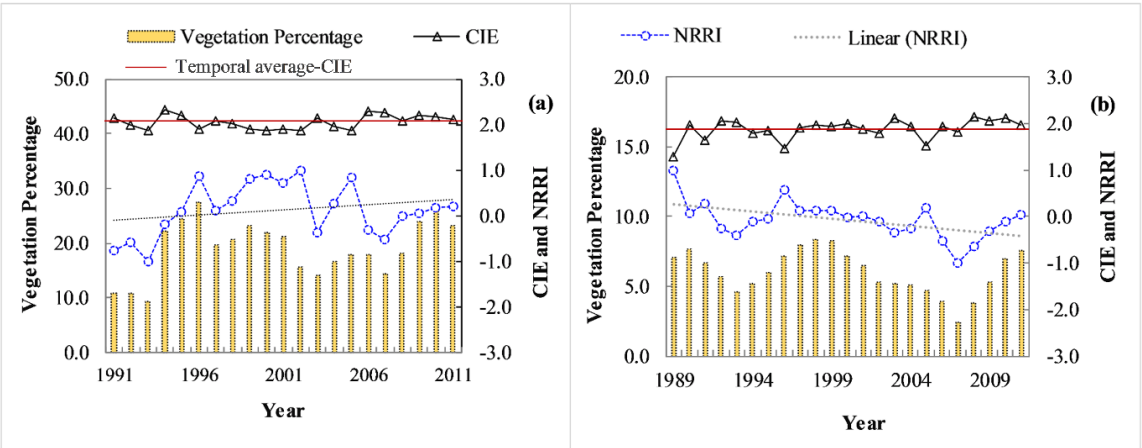

Figure 4.6 The temporal variation of yearly vegetation percentage, cross-sectional intensity entropy (CIE) and normalised river recovery index (NRRI) in (a) Ong (b) Tel Rivers. The linear trends of NRRI and temporal average-CIE are also shown.

The alteration in instream vegetation coverage and CIE have resulted in variable responses along the river recovery trajectory. In the regulated Ong, the temporal average of NRRI is close to 0.13 and it shows an inclining trend in the initial study period (1991-1992) due to the combined effect of decreased bar disorderness and slight reduction of instream vegetation cover on the bench surface (Figure 4.6a). After the passage of the 1994 catastrophic flood, the morphological responses (in terms of CIE) had continued to decrease for the next 10 years. At the same time, the instream vegetation cover had increased from 10.76% (in 1992) to 21.06% (in 2001) and therefore, NRRI had increased from -0.56 to 0.70. In contrast to the 1994-peak flood's morphological and vegetation cover responses, the Ong has reacted in a different fashion to the 2003 and 2004 peak floods. A decrease in vegetation cover from 21.06% to 14.46% along with increment in CIE from 1.91 to 2.27 altered the NRRI from 0.7 to -0.51. From this period onwards (2008-2011), the Ong river accelerated the instream vegetation growth from 14.46% to 23.14% and gradually transformed to a macrochannel dominated by well-vegetated geomorphic units. In addition, CIE followed a declining trend due to the occurrence of bench and transition to depositional form of adjustments. The temporal average of NRRI in the Tel is close to -0.06. The overall CIE trajectory establishes an initial increment of 51%, followed by a declining trend up to 1996, and finally, periodic fluctuations in the remaining years of the study period (Figure 4.6b). The instream vegetation cover shows sporadic patterns of emergence, succession and decay, and establishes an aerial coverage between 5 to 10%. Therefore, NRRI observed a noticeable reduction (1.0 to -0.1) between 1989 and 1994. After the 1994 extreme flood, diagonal bars have gradually transformed into vegetated landforms and uniform aggradation of channel bed has improved the geomorphic condition and therefore, NRRI was increased from -0.24 to 0.01. The last time slice (2003-2011) was punctuated by two major floods in 2003 and 2004 and erosional form of adjustments like chute formation, channel straightening, sculpting of diagonal bars, and degradation of bench continued for the next 3-4 years. In addition, the removal of smaller vegetated landforms and further succession in the subsequent years helped the river to improve the geomorphic health and NRRI was increased from -1.0 to 0.05. This analysis establishes that overall, the Tel river (unlike the Ong) in the Mahanadi catchment did not undergo wholesale river change but has been adjusting within its behavioural regime.

The synthesis of literature pertinent to the form, process and evolution of macrochannel systems suggest that such channel-in-channel physiography provides sufficient space for

both erosional activities (removal of a geomorphic unit, channel widening, bank mass failure, bend extension, the occurrence of chute channels, scour, and incision) and depositional processes (formation of new geomorphic units and accretion of sediment on multiple platform levels) (Lecce et al., 1997; Heritage et al., 2004; Croke et al., 2014; Fryirs et al., 2015; Heitmuller et al., 2015; Croke et al., 2017; Thompson et al., 2016; Pradhan et al., 2021a). The present study reaches along the Ong and Tel are predominantly macrochannel, where geomorphic activities are limited to re-organisation materials at different inundation surfaces. As per Phillips and Dyke (2016), a system state consists of a morphological structure held together by inter-woven form-process relationships. Therefore, in this study, CIE as a system state is concentrated on addressing the geomorphic adjustments at sub-bankfull stages. In the Ong, the linear bench gets partially eroded, washed away or accreted by floods which are discrete geomorphic disturbing events. The thalweg seldom realigns and bench evolution by sediment deposition and vegetation colonisation altered the system state of the Ong River. Furthermore, the post-disturbance states show a vegetated configuration that did not exist earlier. Thus, the gradual emergence of vegetated landforms and the declining trend of CIE can be referred to as a 'state space expansion event', coined by Phillips and Dyke (2016). However, in the Tel River, the fixed controls (macrochannel resistant banks) dominate over flux disturbances (floods) and results in a resilience system. The system state (CIE) and vegetation density oscillate about a mean structure, where the post-disturbance system state is either close to the pre-disturbance configuration or undergoes minor adjustments.

In many instances, the vegetation succession and macrochannel evolution adhere to a linear, sequential logic (Simon and Rinaldi, 2006). Binary models have also gathered recent attention, which suggests oscillation of systems between two stable states (Beisner et al., 2003; Scheffer, 2020). The present study suggests that CIE and NRRI have followed fixed sequences of developmental stages in the study reaches, unless extreme events are absent as disturbing agents. After the passage of the floods, the channel evolution is non-linear and follows complex relaxation paths. The catastrophic floods have accelerated the planform adjustments signaling a slow relaxation, less resilient and threshold modulated system where CIE and riverine health is governed by extreme events in the Ong. In contrast, the Tel River has probably fast relaxation time and a filter dominated system, where recurring impacts of catastrophic floods are quickly absorbed and finally, a dynamically stable system is developed.

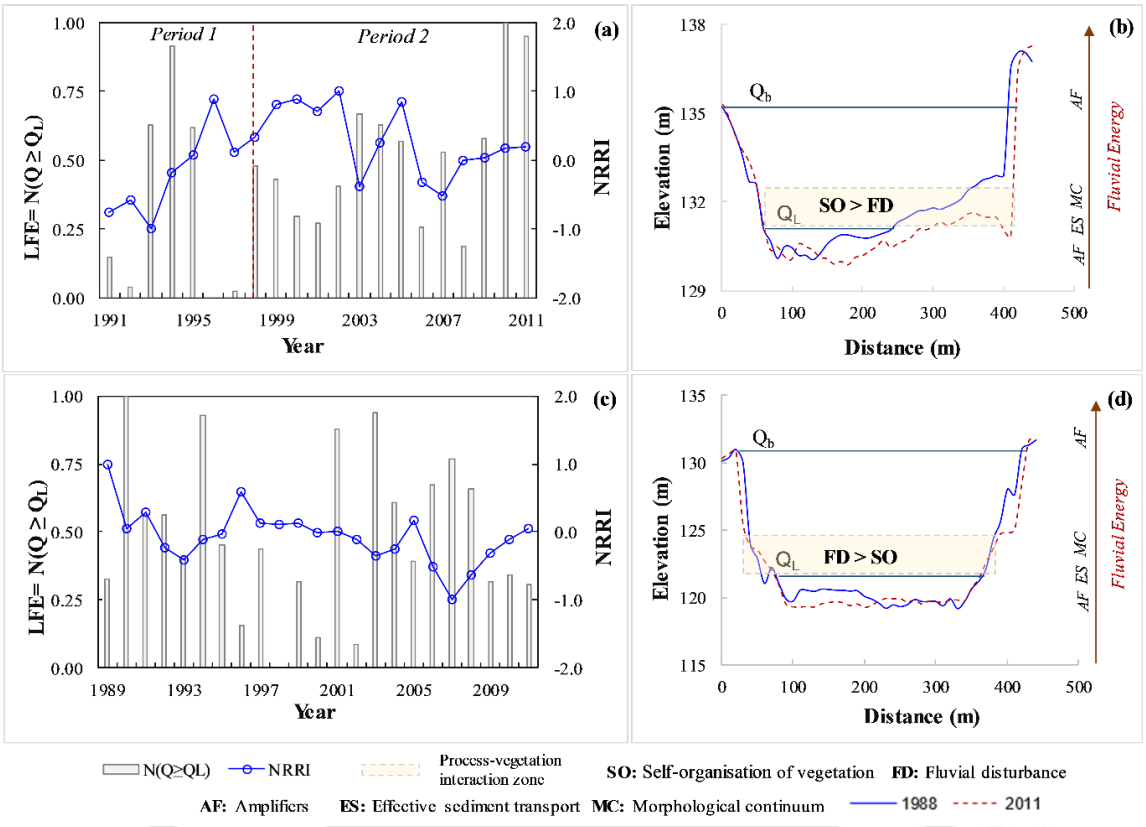

Figure 4.7 Relation between normalised low-flow exceedance (LFE=N(Q≥Q_L)) and normalized river recovery index (NRRI) along (a) the Ong and (c) the Tel Rivers. The conceptual diagrams for the hierarchy of energy dissipation in macrochannel systems and dominant variables for the hotspot-zone of ecosystem engineering are also presented along (b) the Ong and (d) the Tel Rivers.

4.4.3 River recovery and process linkage

Figure 4.7 shows the relationship between process (N(Q≥Q_L)) and recovery state (NRRI) along the study reaches. In the Ong, N(Q≥Q_L) varies between 0 (Q≥Q_L ~ 40) to 1 (Q≥Q_L ~ 130) for the daily discharge hydrographs. The temporal variability of LFE indicates the 1990s was punctuated by a distinct major flood in 1994, which increased the LFE up to 0.91. The next time slice was characterized by less number of floods in 1996-1998 and increased moderate floods in 1999-2002. The 2000s had witnessed frequent floods exceeding the low-flow channel and instigating major morphological adjustments. At the end of the study period (2007-2011), LFE had an accelerated increase from 0.53 to 0.95, suggesting alteration to both flow-regime and low-flow channel morphology in the Ong river. For the Tel River, N(Q≥Q_L) fluctuates between 0 (Q≥Q_L ~ 9) to 1 (Q≥Q_L ~ 91) for

the daily discharge hydrographs. Figure 4.7b displays three-time slices divided based on LFE variability, where the first period (1989-1994) was defined by frequent floods overtopping the low-flow channel. However, the second (1995-2000) time slice was characterised by the small number of floods exceeding the thalweg (average LFE of 0.25), and in the last period (2001-2011), the average LFE increased up to 0.54, signalling a relative change in the flow regime.

As suggested by Pradhan et al. (2021a), most of the geomorphic adjustments occur below the macrochannel bankfull level, and the river goes through a transition to accommodate the effective discharge in the inset channel. In addition, excess energy above the effective sediment transport re-organises chutes and diagonal bars close to the low-flow channel. The present research finding is pertinent to rivers with transitional channel patterns, where the river fluctuates the planform state between sinuous and weakly braided. This study highlights the hierarchy associated with the (re)organisation process in the macrochannel river system and its contribution towards the river recovery state (Figure 4.7b and 4.7d). For example, the inter-comparison of LFE and NRRI trends showed two distinct time periods are observed on the basis of low-flow exceedance number variability in the Ong River (Figure 4.7a). In period 1 (1991-1998), LFE and NRRI are less related to each other and in period 2 (1999–2011), both parameters are well-correlated. In period 1, the Ong had high fluctuations in small-moderate flood magnitudes, and CIE had initial variability due to bar disorderness, followed by an initiation of the decreasing trend. This morphological activity was combined with the erratic instream vegetation growth pattern and generated a 'lagged system', where LFE and NRRI were not correlated. However, in period 2, both parameters followed a similar trend attributed to the gradual alteration in CIE and subsequent stabilisation of vegetated landforms. Hence, the macrochannel system may have switched to an 'event-driven' state, where floods exceeding the low-flow channel possess a direct impact on the river recovery trajectory. In the Tel river, the vegetation cover is significantly low (5-10%), and this large macrochannel system has witnessed some extreme flow variability (20-20,000 m^3/s) in the 1990s. Such drastic changes to the flow regime have triggered morphological adjustments and kept the channel perpetually in transition between sinuous and weakly braided states. Therefore, for such large channel-in-channel physiography, the relationship between LFE and NRRI is challenging to establish and may entail the integration of additional process variables.

Geomorphic threshold is one of the fundamental concepts relevant to the existence of discrete planform states (straight-meandering-braided) (Lokhtin, 1897; Lane, 1957; Leopold and Wolman, 1957; Alabyan and Chalov, 1998). However, the presence of intermediate, transitional channel patterns within the behavioral regime suggests the presence of continuum in the macrochannel systems (Pradhan et al. 2021a). Fluvial controls like flow strength index, bank erodibility and sediment supply are related to the morphological continuum (Bridge, 1985; Knighton, 1993). In our river systems, amplifiers (AS) (both low-flow and extreme events) and effective sediment transport (ES) constitute the hierarchy of energy dissipation. Furthermore, the zone of morphological continuum lies just above the effective sediment transport stage level (Figure 4.7b and 4.7d), which incorporates the major form of geomorphological adjustments. As per Gurnell et al. (2016), the 'critical zone' for physical ecosystem engineering exists within the area of river corridor that is perennially inundated and adjacent areas subjected to frequent inundation and significant shear stresses and erosion-deposition of sediment. Therefore, in the present study, the zone of morphological continuum and critical areas of plant-hydrogeomorphology interactions overlap within the sub-macrochannel bankfull level (Figure 4.7). This bio-geomorphological interaction can also affect the changes in river planform type and future directions (Griffin and Smith, 2004; Collins et al., 2012). The findings suggest that the instream vegetation growth close to the inset channel affect (or control) the morphological activities in terms of cross-sectional disorderness. Hence, within the continuum zone, the vegetation patches can grow, self–organise (SO) and expand to form enlarged vegetated landforms or become smaller and widely spaced under the influence of fluvial disturbances (FD). If SO starts to dominate over FD, the vegetation growth reduces the CIE variability, stabilizes the low-flow channels and increases NRRI (Figure 4.7b). In contrast, if chutes and bar disorderness dictate SO through frequent fluvial disturbances, the rate of planform fluctuations increases between the end-points of the morphological continuum (sinuous and weakly braided states) (Figure 4.7d). The channel evolution models are also associated with channel adjustments along the four degrees of freedom (cross-section, planform, bed and slope) (Knighton, 1998). The present chapter emphasizes the presence of instream vegetation as an additional degree of freedom, which further controls the hierarchy of energy dissipation and morphological continuum in the macrochannel settings.

In the era of big data and cloud computing, assessment of system state indicator-CIE and process-based indicator-NRRI will certainly help to comprehend the fluvial trajectory and develop recovery enhancement approaches. Further, this framework will be helpful for planning and prioritizing recovery indicators which can reduce the cross sectional disorderness and promote improvements in river health. However, many fluvial systems in developing countries are poorly gauged, and assessing CIE and system disorderness with the continuous hydraulic and hydrological dataset is challenging. Therefore, the delicate balance between big data and remote sensing based tools with archival benchmark information, 'place-based understanding' and 'reading the landscape' frameworks (Brierley et al. 2013) will be key to capture and inform process-form relationships of fine-scale geomorphic units.

4.5 CHAPTER SUMMARY

The present chapter has developed a process-based river recovery indicator for anthropogenically disturbed macrochannel river systems. The major conclusions of this study are as follows:

- The disorderness in bed-elevation at sub-bankfull stages is effectively captured by a system state indicator-CIE. The temporal variation of CIE has further addressed the existence of both thresholds modulated and filter dominated systems in macrochannel settings.
- Vegetation density and CIE integrated recovery indicator (NRRI) symbolizes river health for channel-in-channel fluvial systems. The present study suggests that CIE and NRRI have followed fixed linear sequences of developmental stages, unless extreme events are absent as disturbing agents.
- A gradual decline in CIE and subsequent stabilization of vegetated landforms can develop an 'event-driven' state, where floods exceeding the low-flow channel (LFE) possess a direct impact on the river recovery trajectory.
- Finally, the dominance between self-organization of vegetated landforms and fluvial disturbances develops an additional degree of freedom and further decide the recovery state of macrochannel and planform fluctuations between the end-points of the morphological continuum (sinuous and weakly braided states).

Natural rivers are gradually subjected to altered flow-sediment conditions through various natural and anthropogenic stressors. Therefore, prediction of the trajectory of recovery

potential is crucial in river restoration programs. The present study presented a novel approach to predict the system state and recovery potential in anthropogenically disturbed macrochannels. This work can be further extended to rivers with different morphological settings and channel pattern types to better understand the fluvial dynamics.

5

UNDERSTANDING THE PROCESS-FORM RELATIONSHIPS AND DEVELOPMENT OF RESILIENCE-BASED MANAGEMENT APPROACH FOR HIGHLY BRAIDED RIVER SYSTEM

The Brahmaputra River system was strongly disturbed by a high magnitude earthquake called, the Medog earthquake in 1950. The huge source of sediment combined with large scale floods generated complex morphodynamic responses for nearly half a century. This makes it important to understand the process-form relationships and associated management approaches. This chapter addresses the following questions through hydro-morphological analysis and GEE cloud computing.

- It has been greater than 50 years since the great Assam earthquake disturbed the river planform. How are the present status of process-form relationships and braided morphodynamics?
- Previous studies argue a solitary threshold for a weakly braided river system. How is this theory applicable to the highly braided Brahmaputra River?
- There are many dominant, inter-dependent processes in the large fluvial systems. How does GEE cloud computing help to understand the underlying process and design a resilience-based management approach?

5.1 INTRODUCTION

The braided river systems are often characterised by high sediment transport, deposition and erosion rates combined with frequent channel migration and rapid bank erosion (Bristow and Best, 1993; Ashmore, 2013; Chembolu and Dutta, 2018; Pradhan et al., 2021b). The process-form interactions are complex, and the morphological setting is controlled by irregular formation of convergence-divergence zones, flow stage variability,

channel hierarchies, grain size distribution, and erratic scale evolutions (Bristow and Best, 1993; Ferguson, 1993; Ashworth, 1996; Montgomery and Buffington, 1998; Surian et al., 2015). Therefore, understanding the spatio-temporal heterogeneity in the process-response mechanism is crucial to design effective river management techniques and engineered (or nature-based) solutions (Gilvear, 1993; Piégay et al., 2006; Sambrook Smith et al., 2006; O'Donnell et al., 2016).

The synthesis of literature pertaining to braided rivers suggests that studies have been focused on comprehending the process-form interactions through physical modeling (Leddy et al., 1993; Rosatti, 2002; Hundey and Ashmore, 2009; Kasprak et al., 2015; Chembolu et al., 2019), numerical modeling (Murray and Paola, 1994; Karmaker and Dutta, 2016; Williams et al., 2016; Kang et al., 2020; Kakati et al., 2022), geo-spatial techniques (Lane et al., 2003; Picco et al., 2013; Bhuiyan et al., 2015; Pradhan et al., 2017; Langat et al., 2019), field-based studies (Williams and Rust, 1969; Reinfelds and Nanson, 1993) and advanced river surveying instruments (Szupiany et al., 2012; Williams et al., 2013; Lotsari et al., 2014; Gaurav et al., 2014). In addition, the channel-forming discharge concept has been developed to understand the complex flow-sediment dynamics and associated bio-morphological processes in the braided rivers (van den Berg, 1995; Alabyan and Chalov, 1998; Surian, 1999; Lewin and Brewer, 2001; Kleinhans and van den Berg, 2011; Pradhan et al., 2021a). The bankfull discharge, effective discharge, and flow with a certain return period have been refereed as channel-forming discharges that shape and govern the braided river geometry (Pickup and Warner, 1976; Williams, 1978; Doyle et al., 2007; Sholtes and Bledsoe, 2016). Pradhan et al., (2021a) stated that excess energy above the effective sediment transport threshold re-organises chutes and diagonal bars close to the inset channel and accurately predicted the transformation of a sinuous channel to a weakly braided (macrochannel). However, the highly braided river system sits at the extreme at the morphological continuum, where the energy dissipation process is more complex. The energy expenditure potential can be hierarchical or overlapped, where excess stream power can be responsible for the erratic morphological processes, development of macro turbulence, biological feedback and irregular sediment transport. In such river systems, identifying the channel-forming threshold remains a challenge and demands a thorough understanding of the morphological behaviour from the engineers and geomorphologists. This chapter uses the Google earth engine (GEE) cloud computing platform integrated with hydro-morphological dataset to contribute to the challenge.

GEE combines a multi-petabyte catalogue of satellite imagery and geospatial datasets with planetary-scale analysis capabilities. The cloud computing platform offers faster and more efficient handling of huge amounts of data in ways that traditional methods could not achieve (Huang et al., 2018). In fluvial geomorphology, GEE has been used for assessing the planform change (Tobón-Marín and Barriga, 2020), functional characteristics (Gao et al., 2022), wetland area (Hardy et al., 2020), discharge (Hardy et al., 2020), ecological impacts (Gautama et al., 2021), channel migration (Boothroyd et al., 2021) and surface water (Huang et al., 2018). However, evaluation of the complex morphodynamics and scale of planform evolution with GEE are relatively understudied for the highly braided rivers. In particular, these dynamic systems are enriched with event-driven disturbances generated adjustments which are further superimposed atop local scale changes. Thus, it is possible to take advantage of existing Landsat data available since 1984 and accessible with the GEE interface for exploring the underlying fluvial processes. The present study hypothesizes that combining a sufficiently long time series of Landsat images with limited hydrological data and threshold theory can offer a new approach to reveal complex channel pattern and scale of planform evolution. Such understanding and fluvial information will help to effectively design river management approaches for large braided rivers.

The Brahmaputra River is one of the best examples of the large alluvial braided river system (Throne et al., 1993; Chembolu et al., 2018; Nandi et al., 2021; Pradhan et al., 2021d). The river is well-known for high flow-sediment variability, extreme morphological alterations and frequent geological events (Goswami, 1985; Sarma and Phukan, 2004; Zhou et al., 2022). In the Brahmaputra valley, millions of people have been disturbed by intense bank erosion, seasonal planform change and floods. For example, the recent Brahmaputra flood of 2020 affected more than 7 million people with extensive damages to agricultural lands and national parks (Times of India, 2020). Hence, enhanced knowledge on the process-form interactions is of utmost importance to further design flood mitigation strategies and river intervention structures. The objectives of the present study are to: (i) understand the complex morphodynamics of the Brahmaputra River with GEE (ii) implement the location probability theory to a highly braided river system and develop the geomorphic stationarity concept (iii) formulate two process-based indicators to address the dominant morphological change and (iv) finally, design a resilience-based freedom space management approach for the large braided river.

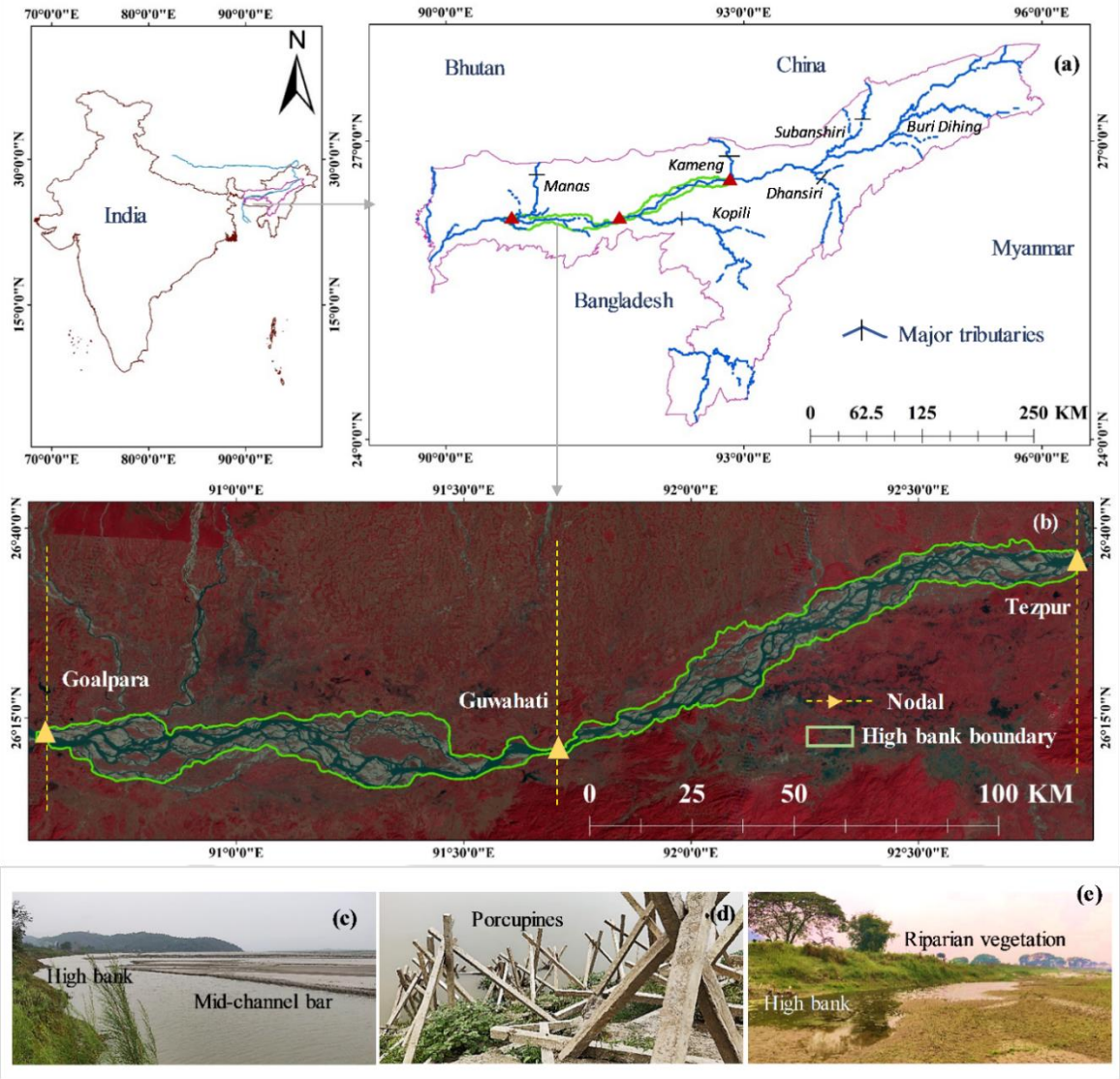

Figure5.1 (a)-(b) The Brahmaputra River with the major southern and northern tributaries, and geological nodes. (c)-(e) Field photographs of the Brahmaputra River showing mid-channel bars, erodible banks with river training structures, and stable bank with riparian vegetation.

5.2 STUDY AREA

The Brahmaputra River in Assam, between three geological nodes (Tezpur, Guwahati and Goalpara), is considered as the study area (Figure 5.1). The braided belt width of the Brahmaputra River varies between 1.2 km to 15 km, providing a large in-channel mobility space for morphological adjustments (Chembolu et al., 2018). The study reach is about 240 km long, with a discharge variability observed between 4,420 m^3/s and 51,516 m^3/s (Singh et al., 2004). The morphology is active by in-seasonal changes like thalweg migration, bar disorderness, island sculpting and instream vegetation cover alteration (Figure 5.1c) (Sarma

and Phukan, 2004; Karmaker et al., 2017). The bank of the Brahmaputra is cohesive composite, which is prone to extensive fluvial and seepage erosions (Figure 5.1d). The channel form of the Brahmaputra River is highly braided with large spatio-temporal heterogeneity in instream and floodplain geomorphic units. Such complex process-form relationships impact the biodiversity zones and further control the socio-economic life of millions of people.

5.3 MATERIALS AND METHODS

5.3.1 Assessment of the complex morphology

The Brahmaputra River shows a wide array of instream and floodplain geomorphic units. These geomorphic units operate as the building block of the fluvial landscape and control the river's character and behaviour. The present chapter has used the taxonomy suggested by Wheaton et al., (2015) to define and classify the geomorphic units. Such information on the configuration and assemblage of geomorphic units will support the process-based interpretations of the Brahmaputra River. The Temporal variation of alluvial deposits (1980-2020) along the Brahmaputra River is obtained from GEE cloud-based computing of Landsat 1-5 MSS, Landsat 5 TM, Landsat 7 ETM+ and Landsat 8 OLI/TIRS, as suggested by Boothroyd et al., (2020). The multispectral indices-NDVI (Normalised difference vegetation index) and MNDWI (Modified normalised difference water index) were computed and a rational operator was generated. The rational operator was used with MNDWI $\geq$ -0.4 and NDVI $\leq$ 0.2 logic to classify the active water pixels and alluvial deposits.

The bankline migration of the Brahmaputra River is captured with the survey of India (SOI) toposheets and Landsat imagery. In the present study, the method suggested by Karmaker et al., (2017) is implemented for braided belt width change assessment, and the river was divided at 10 km intervals. This interval is suitable for capturing the instream geomorphic units as the scale of planform evolution in the Brahmaputra is close to 30 km (Throne et al., 1993). Further, each segment was assigned with a chronological number, and bank migration was captured between Tezpur and Goalpara for the last 80 years (1943-2020). In this study, the braided belt has considered the sand bodies except sediment splayed over the floodplain. The shallow water channels were also taken as a part of the river, and finally,

erosion (as a positive value) or deposition (as a negative value) were measured at each segment.

5.3.2 Location probability index

Joint Research Centre (JRC) monthly water history dataset contains maps of the location and temporal distribution of surface water from 1984 to 2020 and provides statistics on the extent and change of those water surfaces (GEE data catalogue). The pixel of Landsat 5 TM, 7 ETM+, and 8 OLI/TIRS was individually classified into water/non-water using an expert system and the post-monsoon monthly history results were collected for the entire time period. The algebraic expression for the location probability index (LPI) of a particular feature (low flow channel) for each pixel of the final image is

$$LPI = W_1F_1 + W_2F_2 + W_3F_3 + \ldots\ldots\ldots\ldots\ldots\ldots\ldots W_nF_n \quad (5.1)$$

$$\sum W_n = 1.0 \quad (5.2)$$

Where F_n is the feature occurrence for the pixel in map n, equal to either 1 for occurrence or 0 for none, n is the number of images of the study area, and W_n is the weighting value assigned to each map n, determined by time-based and event-based methods (Graf, 2000). In the first method, the length of the time has a control on the weighting:

$$W_n = \frac{t_n}{m} \quad (5.3)$$

Where t_n is the number of years represented by the image and m is the total number of years in the record. This technique is better suited to the prediction of the expected distribution of the low-flow channel in any randomly selected year. In the event-based method, LPI predicts the arrangement of the low-flow channel after passing of the channel-forming discharges. These floods are responsible for morphological instigation, assuming each image shows the configuration of the geomorphic system in the post-monsoon season. Therefore, the weighting value assigned is:

$$W_n = \frac{1}{\text{Number of images}} \quad (5.4)$$

5.3.3 Geomorphic stationarity

The concept of stationarity is associated with the permanency of geomorphic units in a sediment-charged, highly braided environment. This also refers to the characteristics of

geomorphic unit to occupy a static location within the defined riverine space. In the Brahmaputra River, the geological nodes have temporal stability that governs the channel morphology. The instream and floodplain geomorphic units have spatio-temporal variability, making it challenging to identify the permanent landforms and associated underlying processes. Therefore, a novel geomorphic stationarity concept is developed from the LPI images to extract the permanent features (>65% of occurrence). Such understanding will also inform the prevalence of a mean channel form and oscillated geomorphic units within the lateral freedom space.

5.3.4 Formulation of process-based indicators

The highly braided rivers are characterised by meta-stable islands, mobile sand bars, nodal reaches, shifting anabranches and bank erosion (Throne et al., 1993). In particular, the Brahmaputra River has first, second and third order channels with associated bars that scale on the dimensions of the channel. The third order channels changes rapidly, while the second order channels have alteration in seasonal scale. Therefore, for highly braided rivers, ranges of flow (instead of solitary discharge) may be responsible for cross-sectional and planform configuration. Throne et al., (1993) evaluated the channel-forming effective discharge for the Brahmaputra River and observed braid bars are 'adjusted' to the dominant flow and are the contemporary morphological expression of process-form interactions. The dominant flow over-tops the braid bars (Q_{t1}), which are active, but does not inundate the islands. In weakly braided river systems, excess energy above the effective sediment transport re-organises chutes and diagonal bars close to the inset channel and further develops a transitional braided pattern (Pradhan et al., 2021a). In addition, the seasonal stream power follows the trend of morphological adjustments better than peak stream power, and a hierarchical energy dissipation process is observed at sub-bankfull levels. Hence, a new process-based indicator (Normalised threshold exceedance-NTE) is developed on excess energy theory and applied to the highly braided Brahmaputra River (Eq. 5).

$$\mathrm{NTE} = \frac{\mathrm{N}\,(Q \geq Q_{t1})}{\mathrm{S}} \tag{5.5}$$

Where N is number of days, Q is flow (m^3/s) and S is total duration of flood hydrograph. At the barfull stage, braided bars are drowned out and the planform of the river is simplified. In this range of flows, the sediment stored in the braid bars becomes accessible to the river

for sediment transport and the transport rate is large because of this free availability of loose sediment coupled with gains in hydraulic efficiency and transport capacity. Thus, discharges between barfull and bankfull (Q_{t2}) are confirmed as being the dominant range of flows responsible for much of the sediment transport and for forming the major contemporary morphological features of the channel. Therefore, the second process-based indicator integrates the gradient of energy dissipation between the hierarchical thresholds and linked to a form variable (SDBA-standard deviation of braided bar area).

$$\mathrm{NPG} = \frac{(Q_{t2} - Q_{t1})}{\Delta t} \tag{5.6}$$

Where NPG is Normalised process gradient, Q_{t2} is bankfull discharge (m^3/s) and Δt is time duration between barfull and bankfull flows.

5.4 RESULTS

5.4.1 The braided morphodynamics of the Brahmaputra River

The Brahmaputra River exhibits multi-channel networks with volatile sand bars and distinct-stable islands. This highly braided river system is also defined by significant flow and sediment variation that partly or wholly submerges the alluvial deposits. These sediment deposits also interact with the heterogeneous surface morphology, low-flow surface water slope, grain size relative roughness, shear zone, and aquatic (and riparian) vegetation and thereby, develop instream and floodplain geomorphic units at different spatio-temporal scales. The dominant in-stream geomorphic units are compound bar, confluence bar, diagonal bar, eddy bar, expansion bar, chute, shallow thalweg, and secondary channel. Similarly, examples of out-of-channel (floodplain) geomorphic units include the paleo channel, alluvial terrace, anabranch, swamp, wetland, flood channel and valley fill.

The temporal variation of alluvial deposits in the Brahmaputra and its floodplain reveals frequent morphological changes in terms of bar formation, migration, and sculpting at varying flow stages. In addition, the cohesive composite banks are prone to bank erosion, and a large-scale braided belt migration was observed for the Brahmaputra River (Figure 5.2). In the 1980s, the Brahmaputra displayed significant braided belt width variability (Figure 5.2a). The three geologic nodal sections (Tezpur, Guwahati and Goalpara) are the narrowest reaches that are partly (or completely) restricted by valley confinement. The

widest braided belt was observed just upstream and downstream of the Guwahati nodal section. The average braided belt width was close to 7455 m during the 1980s, and the maximum and minimum width of the river remained fairly constant in the next decade. However, few selected reaches have observed low-sinuous secondary channels atop floodplain instead of the bar top. These flood channels have gradually been abandoned in the 1990s, and ancestral channels have been formed (Figure 5.2b). In the 2000s, the average braided belt width was increased up to 9012 m and growth of a large island (20 km length) signaled the dynamic morphology of the Brahmaputra in a highly sediment-charged environment (Figure 5.2c). The last decadal epoch (2010-2020) witnessed gradual stabilization of islands where surface elevation was close to the bankfull level. In addition, few flood channels downstream of Guwahati have been deactivated leading to a concentrated flow towards the left bank (Figure 5.2d). Finally, the overlay analysis of bank lines reveals nodal reaches have less erosion rate. In contrast, the bar (island) dominated reaches are prone to higher fluvial erosion and a southward migration of braided belt width has been observed during the last four decades.

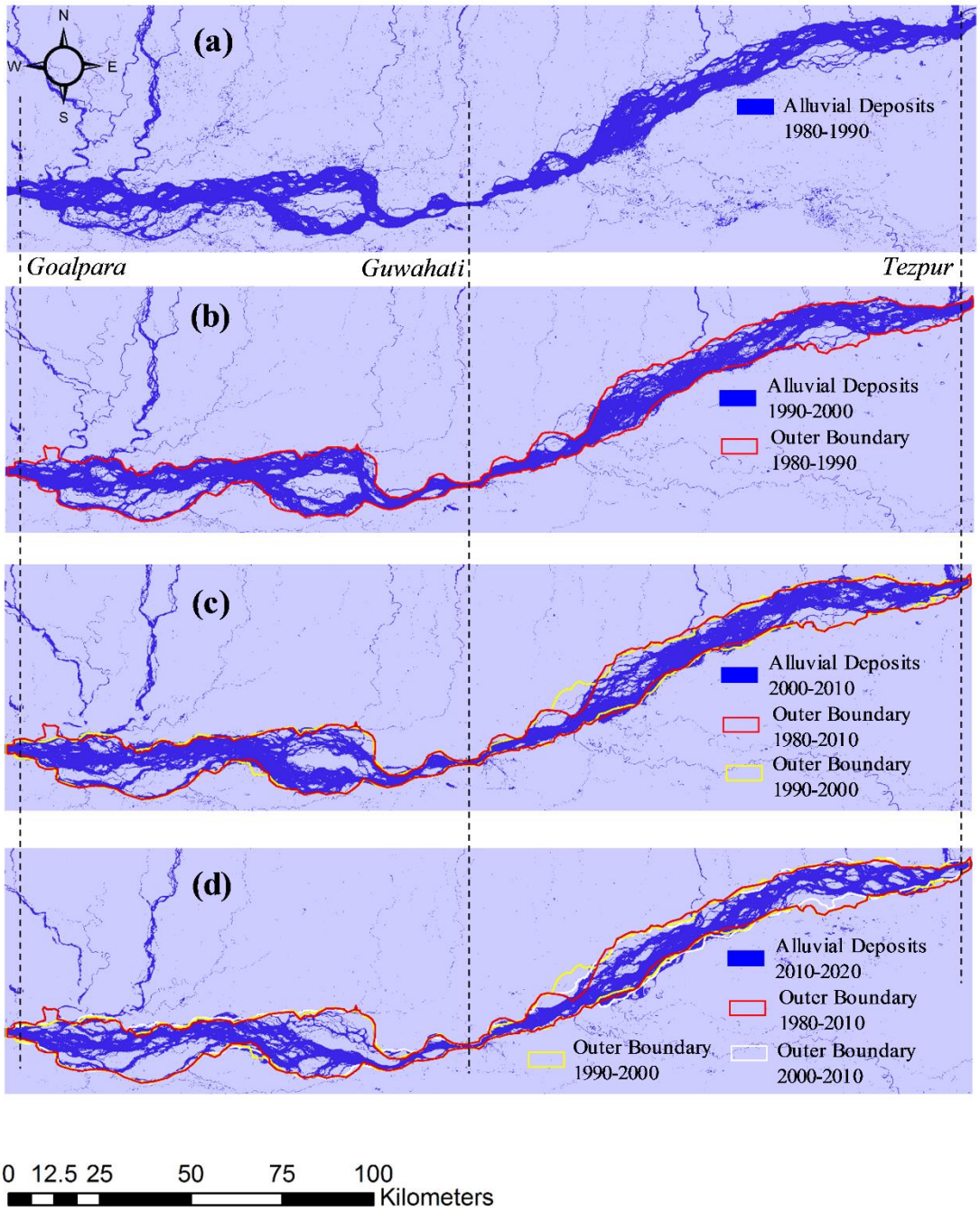

Figure 5.2 Temporal variation of alluvial deposits along the Brahmaputra River (1980-2020) (obtained from GEE cloud-based computing of Landsat imagery as suggested by Boothroyd et al., 2020). The outer boundaries of previous decades' alluvial deposits are also shown.

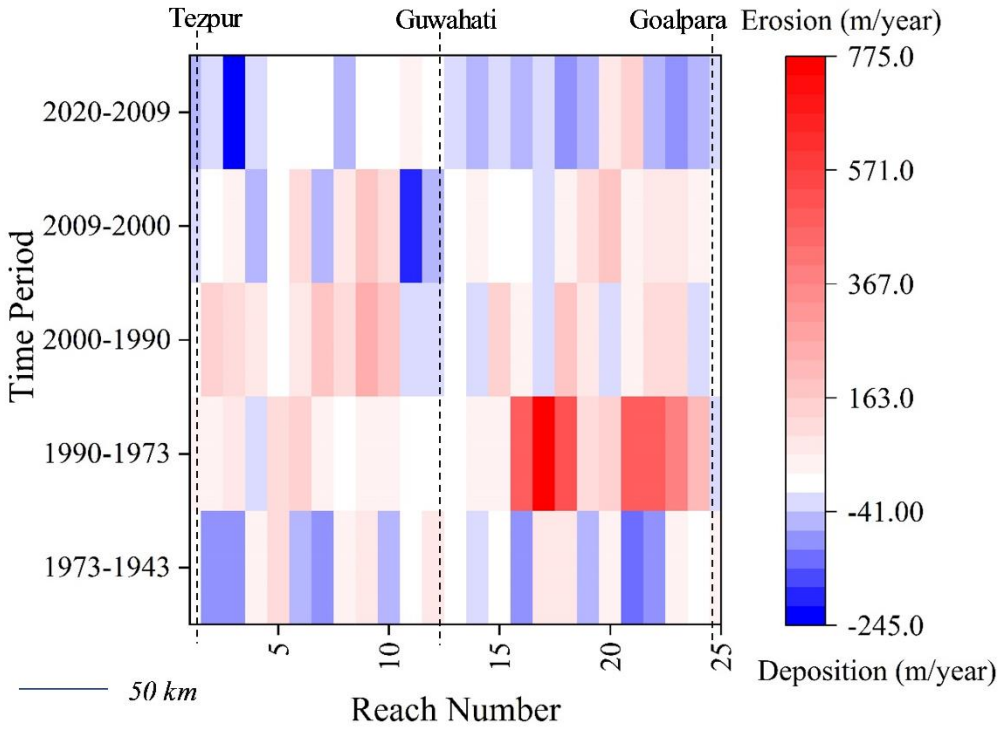

Figure 5.3 Spatio-temporal variability of bank migration rate in the Brahmaputra River.

No large-scale avulsion of the first order channel is observed for the Brahmaputra River, but old toposheets and recent satellite imagery suggest preferential bank retreat in the last eighty years (Figure 5.3). In the first decadal epoch (1943-1973), the spatial average of braided belt width and annual bank migration rate are close to 5618 m and -1 m/year (deposition). There is a marked variability in the rates of bankline movement along the length of the study reach. Interestingly, reaches with bank erosion are sandwiched between the channel segments showing bank accretion and this interchanging pattern is spaced with a reach distance of 10-20 km. In the next time period (1973-1990), the average braided belt width and bank migration rate increased up to 8475 m and 169 m/year. The complete study reaches experienced severe, sustained bank retreat, and in particular, the downstream reaches of Guwahati nodal section witnessed highest rate of bank erosion, at 400-750 m/year. However, the nodal sections are relatively stable, and a maximum bank retreat rate of 20 m/year is observed. The next epoch (1990-2000) is dominated by erosional regime along the study reach between Tezpur and Guwahati. A spatially averaged bank migration rate of 94 m/year is detected against a downstream migration rate of 51 m/year. In addition, the downstream reach of Guwahati has witnessed bank accretion at a few locations leading to a reach-averaged braided belt width of 8836 m. In between 2000 and 2009, bank

accretion is more prominent in the upstream reaches of Guwahati. In particular, a large flood channel has been abandoned just upstream of the nodal section, and a significant bank retreat rate of -190 m/year is noted. On the other hand, the reaches between Guwahati and Goalpara is subjected to bank erosion with the highest rate approaching up to 160 m/year and thereby producing a maximum braided belt width of 16742 m. In recent decade (2009-2020), the Brahmaputra river exhibits bank accretion at a rate of -24 m/year, which further underlines the fluctuating bank migration rate due to extreme process variability. Currently, this highly braided river system possesses a reach-averaged braided belt width of 9245 m with three stable valley confined nodal sections, large islands, unstable braided bars, hierarchical channels and erodible cohesive composite banks.

5.4.2 Spatial variability in location probability index

Large scale morphological instability is of common occurrence in the Brahmaputra River owing to the combined effect of periodic floods and sediment waves. These event-driven disturbances produce greater adjustments which are further superimposed atop local scale changes. Therefore, the location probability Index (LPI) indicates the spatial characteristics of the changing river channels (Figure 5.4). LPI ranges between 0 and 100 and empirically represents the observed past records and distributions of the geomorphic units. In the Brahmaputra, three major channel configurations (highly to moderately braided sections and nodal reaches) are observed. In the nodal sections, the active channel has lateral restrictions that reduce the available space for the low-flow channel. As a result, high probabilities and general locational stability are generated and averaged LPI is close to 90 (Figure 5.4a). This suggests that the low flow channel will be encountered most of the time at any randomly selected time over the four-decade study period. The highly braided reaches represent the general morphodynamics signature of the Brahmaputra River (Figure 5.4b). These reaches amalgamate instream and floodplain zones created by different geomorphic units' margins. Islands are the in-channel exposed channel bars with a surface elevation close to or greater than the bankfull. These elongated in-channel geomorphic units are defined with LPI of 7% (Figure 5.4d). This suggests high flow and extreme events are enriched with smaller probabilities to introduce a direct effect on the island functional surfaces. In addition, the in-channel stability has caused the low flow channels to go around the islands. The result is a larger area of higher LPI (50-60%) in the vicinity of braided bars.

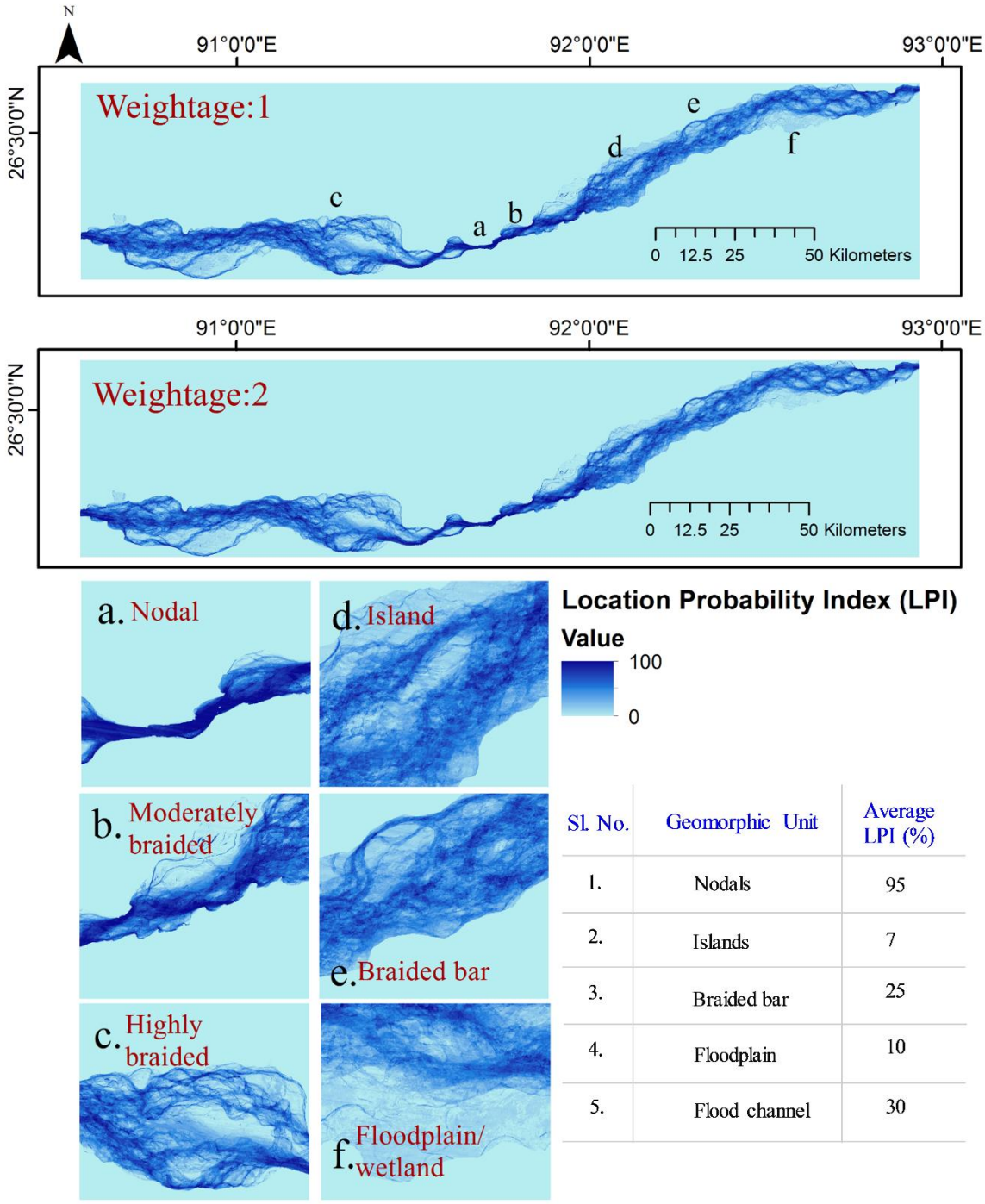

Sl. No.	Geomorphic Unit	Average LPI (%)
1.	Nodals	95
2.	Islands	7
3.	Braided bar	25
4.	Floodplain	10
5.	Flood channel	30

Figure 5.4 Spatial variability of the location probability index for the Brahmaputra River using the time-driven and event-driven weighting processes.

The braid bars are highly unstable in nature and change their shape, size and position between each seasonal high flow. This cluster of bars gives the Brahmaputra River a characteristic of multichannel cross-section, braided planform and shifting nature.

Furthermore, most are the mid-channel bars, which can be majorly classified into longitudinal, compound, confluence and diagonal bars. The transient nature of mid-channel bars is captured with LPI variability, which highlights both high water level fluctuation and energy expenditure potential of the Brahmaputra. In the proximity of braid bars, close to the stable island features, LPI is close to 25-35%. This signals higher lateral geomorphic adjustments throughout the time period resulting in braid bars of low probability. In addition, the braid bars are subjected to chute cut-off, dissection and sculpting, and the unconfined flow dominates the morphological processes. The braid bars are also subjected to significant flow variability during moderate-extreme flows and get displaced or washed away. Sometimes, the braid bars are drowned out, but the flow is still confined to the low-flow channel in the post-monsoon period. The functional surface is relatively exposed, resulting in an encounter of the water pixel below 40% of randomly selected years. The short-lived characteristics of braided bars contribute to the intermediate probabilities of the low-flow channel where high and low probability zones alternate with each other. The deepest portion of the braided cross-section (thalweg) has LPI of more than 60% and probably, lateral mobility of second-order channels along with their sinuosity affect the probability characteristics. For example, the thalweg ordinarily exhibits a moderate sinuosity (close to 1.1) in the Brahmaputra. In order to preserve this sinuosity within the defined lateral mobility space, the channel may wander right or left, but it must occupy a relatively common location (LPI of more than 60%). The moderately braided reaches connect the nodal sections and highly braided segments. These reaches are generally characterised by erodible banks on one side and stable banks on the other side (Karmaker et al., 2017) . This stability is contributed by the natural factors (stone outcrop) or river training measures (porcupine, geo bags etc.). Such lateral restrictions produce linear zones of high LPI (more than 65) irrespective of the effectiveness of bank protection works (Figure 5.4b). Furthermore, the lateral migration of the low-flow channel is up to 2-3 km, which generates a larger chance of finding water pixels in the randomly selected study year. The moderately braided reaches are also usually the transitional sections where the absence of large islands and braided bars contribute to a high flow area above the wetlands and floodplains. In the Brahmaputra, the flood channels are the secondary channels but with lower sinuosity than the main channel. These flood channels are short-circuiting on the floodplains with averaged LPI close to 10%, which suggests reworking of peak floods on the floodplain alluvial deposits. Moreover, few flood channels were active in the 1980-90s,

but the gradual shifting of the first-order channel had reduced the probability of water pixel. The floodplain pockets are at an elevation close to the bankfull stage in the Brahmaputra. Therefore, these out-of-channel geomorphic units are occasionally submerged in the post-monsoon period and generate LPI variability up to 10%.

5.4.3. Identification of geomorphic stationarity in the highly braided river system

The braided river systems are defined by spatio-temporal heterogeneity in complex processes and distinctive forms in response to fluctuating flow and sediment supply. Particularly in the Brahmaputra River, the instream and floodplain geomorphic units shift their positions seasonally (or annually) as a result of sporadic patterns in erosion and deposition processes. Therefore, geomorphic stationarity refers to the tendency of geomorphic unit to occupy a static location within the defined riverine space. The location probability analysis of geomorphic units suggests to the temporal distributions in changing fluvial environment. Hence, LPI in exceedance of 65% refers to the relative stationarity of geomorphic units inside an irregular planform configuration (Figure 5.5). In the Brahmaputra River, the energy dissipation and associated three dominant processes like braided belt dynamics, spatial sand bar distribution and instream (or riparian) vegetation dynamics occur at hierarchical or overlapped scales. The intermediate concurrent processes such as sediment trapping and bio-stabilization, erosion-transportation-deposition and vegetation growth and succession also influence the reach-scale braided form variability.

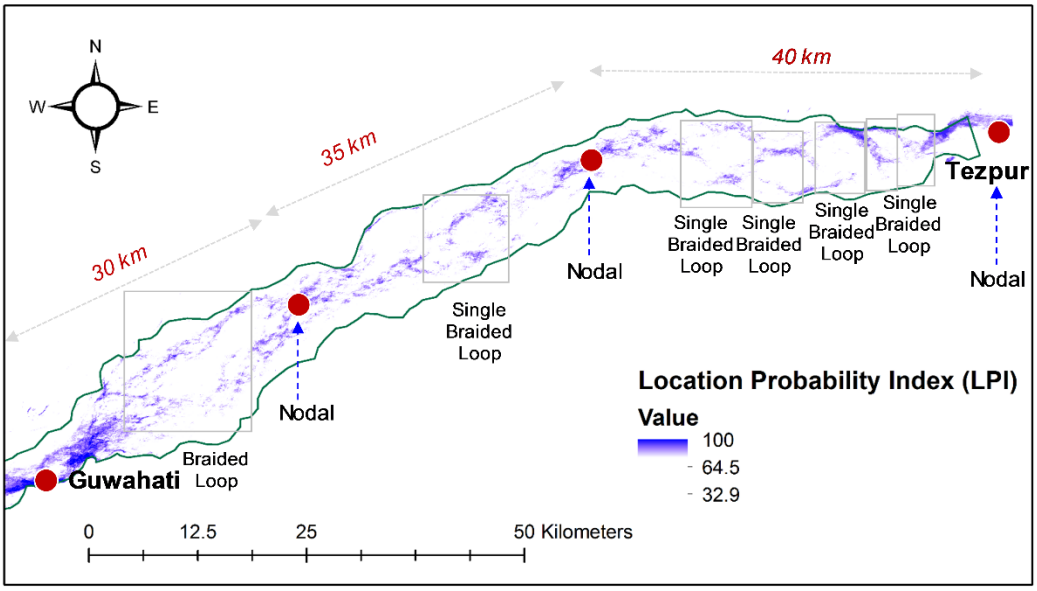

Figure 5.5 Identification of geomorphic stationarity in the Brahmaputra River.

Figure 5.5 depicts the local base level morphological variability, which has further simplified and generalised the complex processes of the Brahmaputra River. A reach-averaged bankfull width of 8.2 km is observed along with second order channels having distinct braided loops (single or double). The second order channels are of 1.9 km averaged flow width where the high probability strip is defined within the bankfull stage. This strip often occurs in the centre of the in-channel lateral mobility space. The zone of high locational probability is relatively straight, however it is not completely occupied by one single second order channel. Therefore, the thalweg changes its position after the periodic flood waves but seems to wander within the high probability strip. The islands and stable braided bars are also clearly marked that offer constriction to the low-flow channel configuration. As a result, the low-flow channels are often located in the shrunken lateral mobility space close to the islands and generate relative geomorphic stationarity. Thorne et al., (1993) reported that the location and spacing of spikes in sand bar distribution are depended on the island-node pattern. In the Brahmaputra River, two distinct nodes are present at Guwahati and Tezpur, owing to the local geological settings. However, two additional local hydrologic nodes (LPI exceeding 80%) are observed in the high probability strip. These two nodes are spaced at a distance of 35 km (Figure 5.5) and thereby producing a reach-averaged node spacing of 35-40 km. This result also agrees with the previous finding of Thorne et al., (1993), where the scales of the planform evolution of the Brahmaputra river (in Bangladesh) were spaced at an interval of 30 km.

5.4.4 Process-form relationships in the Brahmaputra River

The geometry and development of the braid bars are vital to understand the dynamic morphology of the Brahmaputra River. These braided bars possess loose sediment surafaces, sparse to dense vegetation and seasonal cropping. The braid bars are generally found as clusters around the islands, produce sub-channels and develop an anabranching channel pattern during the low-flow. However, when the flood waves arrive, braid bars are drowned out, and flow is still confined in the first-order channel. At the barfull flow stage, the river planform is simplified, still major morphological activities in terms of bar erosion, sculpting, transportation and accretion occur, and contemporary channel features are developed. After each annual hydrograph, the functional surfaces area of these features changes, even though the channel system returns to its original width in the post-monsoon period. The low-flow configuration in the post-monsoon period is relatively different from

the original arrangement and highlights the importance of dynamic process-form interactions in the Brahmaputra River.

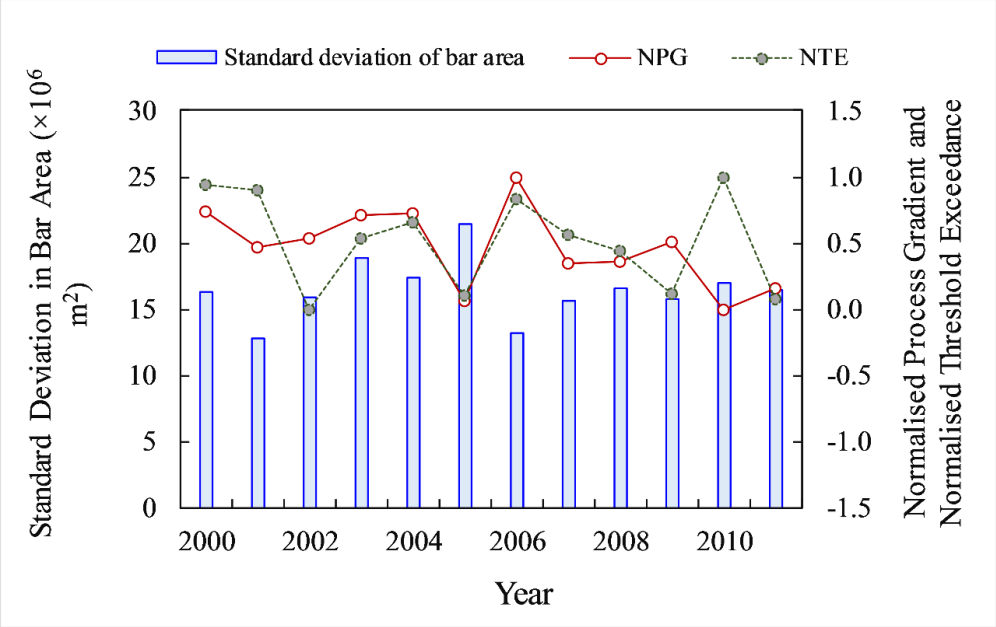

Figure 5.6 Relationship between normalised process gradient (NPG), normalised threshold exceedance (NTE) and morphological variable-SDBA for the Brahmaputra River

The Brahmaputra River experiences varying intensity of flood waves annually. The cumulative imprints of these flood waves and extreme events contribute to the deepening of shallower thalwegs, erosion of smaller unstable bars and causing extensive bank erosion. However, when the flood receeds, the transported sediments are accreted on the exposed bar surfaces. The effects of such disturbing events are reflected generally on the post-monsoon where the river occupies the channels subjected to greatest erosional activities. Therefore, the present study investigates the realtionships between process variables-normalised process gradient (NPG) and normalised threshold exceedance (NTE), and morphological parameter (standard deviation in bar area-SDBA). Three distinct time periods based on sand bar area variability are observed in the Brahmaputra River. Flood gauge data show that the last observed extreme flood events were in 1998 and the next major flood events occurred in 2004. Therefore, process and form variables are well correlated at the beginning of the study period (2000–2004). In 2000, both NPG and NTE are at higher values (> 0.5) with SDBA close to 15×10^6 m^2. This refers to the erosional activities like discetion, sculpting, and transportation produced by both moderate floods and extreme events. The next year witnessed the absence of major floods and a delay in approach time to peak flood waves (NPG < 0.5). Hence, a reduced SDBA of 12×10^6 m^2 is

detected in the study reach. In the following years, an increasing trend in NPG is witnessed, where the Brahmaputra River approached the peak flood waves with a higher gradient (~80 days). Such rapid behaviour of flood hydrograph resulted in intense dissipation of fluvial energy and was well reflected in SDBA of 18×10^6 m^2. The impact of the 2004 flood waves is preserved in the next years where the incoming seasonal monsoon floods readily occupied the defined paths leftover or created by the peak flood and increased the SDBA up to 21×10^6 m^2. After 2005, an alteration in the planform regime is witnessed along the Brahmaputra River, where the SDBA stays close to 15×10^6 m^2. The change in morphological state is well captured more by NPG than NTE. In this period (2006-2011), the NPG has shown a decreasing trend where the gradient to peak flood waves is close to a time-averaged of ~110 days. The relative steadier expenditure of fluvial energy resulted in a stable planform configuration at the end of the study period.

5.5 DISCUSSION

5.5.1 Energy dissipation processes in large braided river systems

Understanding the energy dissipation process in large braided rivers is challenging issue owing to the complex interactions between flow, sediment, sedimentary architecture, channel morphology and vegetative attributes. In general, the processes of erosion and deposition decide the braid bar initiation, confluence-bifurcation evolution, the nature of sedimentary lithology, and the impact of flow depth and aggradational regime on sedimentological architecture across a spectrum of channel scales. For example, the formation (and conversion) of central and transverse bars are primarily the result of depositional activities. Similarly, chute cut-off is triggered more by deposition during the formation of diagonal bars than by chute erosion (Wheaton et al., 2013). In contrast, lobe dissection comprises erosion of various chutes through an existing lobate bar. The other erosional mechanisms include channel incision, bank erosion, and bar sculpting. As per Thorne et al., (1993), the bank erosion process and growth-evolution of braiding are complimentary within the larger-scale framework of the bar (island) node pattern. Many braided rivers like the Sacramento (US), the Nile (Africa), the Tagliamento (Italy), and the Yangtze (China) morphodynamics are governed by the bank erosion process. The annual erosion rates in these rivers are up to 10-50 m/year in comparison to about 100 m/year in the Brahmaputra (Larsen et al., 2006; Mosselman, 2006; Surian et al., 2009; Mount et al., 2013; Deng et al., 2019). The study also suggests that at a few locations, the Brahmaputra

has maximum bank erosion rate of up to 1 km/year, signalling a tremendous energy expenditure potential. As suggested by Karmaker and Dutta (2013), the cohesive bank plays a critical role in controlling the braiding of the Brahmaputra river. The main cause of erosion in cohesive banks is the breakdown of electromechanical forces between the aggregates resulting from water level variability during the extreme floods and lean periods. In addition, it has been observed that the bank erosion process does not depend only on the flow energy produced due to extreme floods. Somehow, the gradual small flood waves can saturate the soil mass and trigger the failure of bank materials. The water levels fall rapidly during the recession of flooding, initiating a decreasing pressure at the wall that leads to lateral flowage of sand and silt, causing the subsequent failure. Furthermore, the divergent flow can impinge on the bank at a greater angle, causing bank erosion and subsequent channel widening, as well as an increase in sediment material availability on a local scale. This likely commenced the establishment of a new braid bar along the downstream. In addition, the channel conditions such as deflection angle, slope, the composition of bed/bank materials can actively influence the erosion of the bank (Mosselman, 2006; Surian et al., 2009; Karmaker and Dutta, 2013). The eroded sediment material is subjected to transfer processes into and out of alluvial storage in a reach scale. This process may include deposition on the flood plain (levees, crevasse splays, meandering scroll deposition), downstream braid bar-main channel exchange (lateral accretion, avulsion), input from tributaries and outflow to distributaries. The sedimentation process impacts the channel morphology by initiation of small deposits to island formation, decrease in sediment load through bed aggradation or slack water and levee deposition. In some cases, frequent channel migration can cause the migratory channel to intersect the bank line, which raises the water level and saturates the bank. As the sediment saturates, it liquefies and forms well-defined shear planes and triggers the bank failure mechanism. This process continues and can significantly contribute to the braided belt dynamics of the river.

5.5.2 Scale of planform evolution in large braided river

The morphology of the braided rivers depends on the dynamic sediment load and local hydraulic regime conditions. This leads to a complex planimetric configuration and variable scale of planform evolution attributing to an erratic network of channel, number and typology of nodes, confluences and bifurcations geometry. For example, the Waiapu and Waiapoa Rivers (New Zealand) have undergone a substantial increase in the braided

belt from 60 m to 400 m (DeRose et al., 1998; Piégay et al., 2006) whereas, the Arve and Fier Rivers (northern French Alps) were incised up to 12 to 14 meters and undergone significant narrowing (Peiry et al., 1994; Marston et al., 1995). In case of the Tagliamento River (Italy), the bank erosion is evidently a major factor behind the braided dynamics, and it was reported that the annual total erosion and erosion volume are about 5630 m^2 and 12,214 m^3, respectively (Picco et al., 2013). Similarly, the Mississippi River has two huge geologic uplift features, such as the Lake County Uplift and the larger Monroe Uplift (Gupta et al., 2007; Harmar and Clifford, 2007). In the upstream of the Yazoo basin, Fisk and Mordvin, 1944; Fisk, 1947) and Saucier (1994) observed that former channel belts spanned up to 25 km in the Holocene floodplains. In a large river like the Brahmaputra, Nandi et al., (2022) observed that sand-bar dynamics play an important role in the planform alteration, which can range from 600 m^2 to over 100 km^2 in surface area and this results in braided belt variability between 1.2 km and 18 km. In addition, description of network complexity through nodes is an excellent alternative to the measure the geomorphic configuration. The Brahmaputra possess distinctive geologic and hydrologic nodes that connects both upstream and downstream reaches.

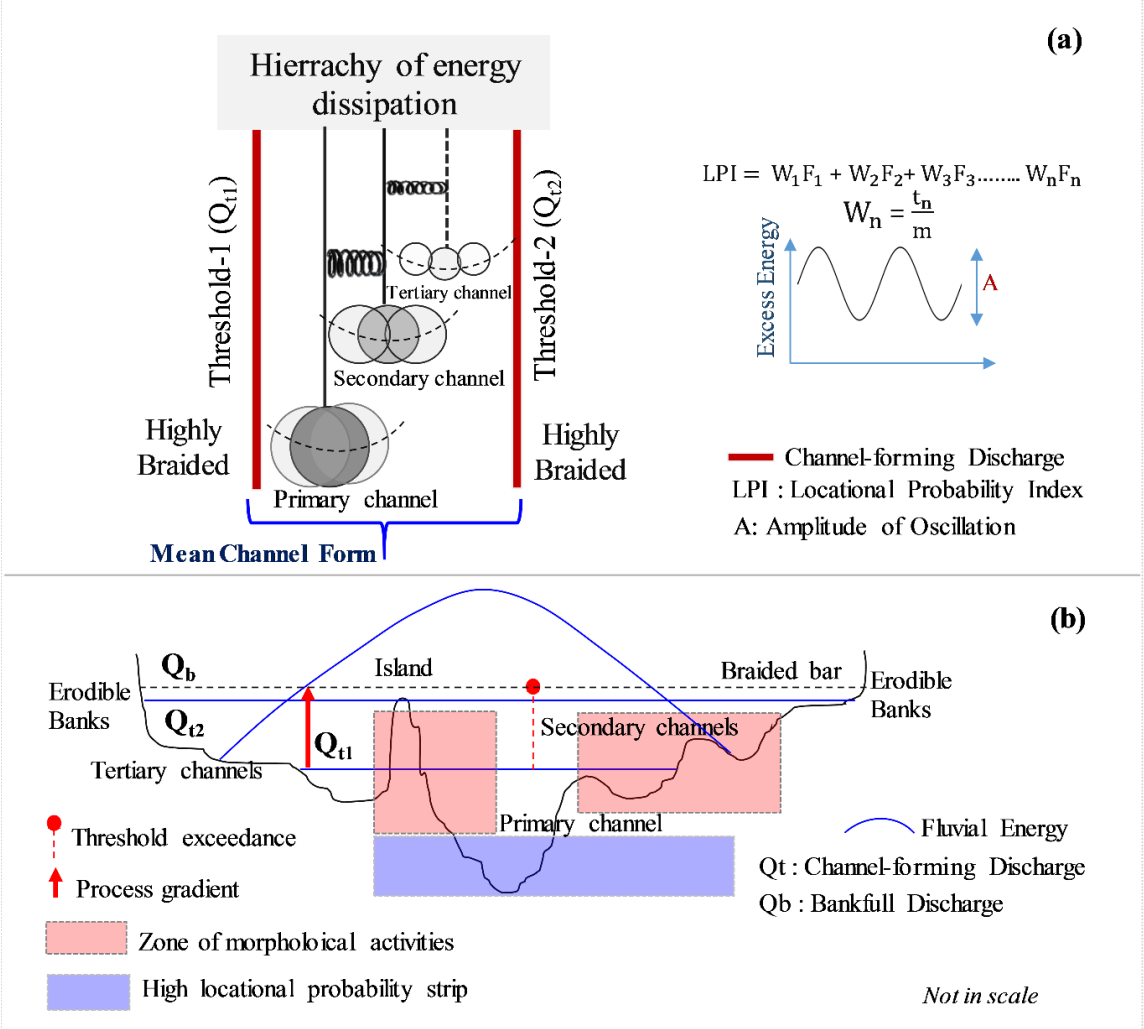

Figure 5.7 (a) Conceptual diagram showing two dominant thresholds (channel-forming discharges) and periodic oscillation of braided planform state in the morphological continuum. (b) Conceptual diagram showing a highly braided channel geometry with zone of morphological activities, high locational probability strip and interactions of process (fluvial energy)-form variables.

Previous research findings suggest that the Brahmaputra River is governed by the prevalence of geologic nodes spaced apart at a distance of 100 km (Rinaldo et al., 2006; Sarma and Akhtar, 2017; Prasujya and Nayan, 2021). However, the present research advocates that two new hydrologic nodes are present in the high locational probability strip that connects the major geologic nodes. Therefore, the new spacing between the nodes has been reduced to 35 km, which highlights the prominence of the island-node pattern and the scale of planform evolution in highly braided river system. This also agrees with the previous research finding of Thorne et al., (1993), where the length of dominant

geomorphic units is highly dependent on the width of the channel. The reach-averaged braided belt width of the Brahmaputra is near to 8 km, which provides abundant flooding and mobility spaces for geomorphological activities. The planform configuration of the river is mostly confined to a highly braided state with the emergence of two dominant channel-forming discharges (Figure 5.7a). The mean channel geometry oscillates between these hierarchical thresholds (Q_{t1} and Q_{t2}), and depending upon the gradient, and exceedance probability of energy dissipation, major geomorphic adjustments in terms of bar dissection, island sculpting, macro-turbulence and shallow thalweg erosion occur (Figure 5.7b). The present study also finds that process gradient is better related to morphological adjustments than the threshold exceedance. The normalised threshold exceedance (same as probability of braiding-POB, as coined by Pradhan et al., 2021a) suggests that chunk of energy in excess of effective sediment transport is dissipated forming chutes in weakly braided macrochannel river system. However, for a large braided river system, two hierarchical thresholds operate between the pre-monsoon averaged barfull discharge and bankfull stage (Q_b). Hence, the flow exceeding the barfull stage inundates the loose sediment atop exposed bedforms and braided bars, and eventually contributes to the morphological activities in a sediment-charged environment. This gradient of energy dissipation, instead of threshold exceedance, may decide the rate at which fluvial stream power will be distributed among the three major forms of energy dissipations (sand bar adjustments, braided belt width variability, and flow-vegetation interactions) (Nandi et al., 2022). To conclude, in a highly braided river system, the sand bar adjustments prevail over other form of morphological adjustments at the initial stage of flood hydrograph and is closely dependent on the process gradient between the hierarchical thresholds.

5.6 FREEDOM SPACE FOR HIGHLY BRAIDED RIVERS: RESILIENCE-BASED MANAGEMENT APPROACH IN THE ERA OF ANTHROPOCENE

The Indian fluvial environments are increasingly stressed due to the rapid growth in urbanization and agricultural activities near the river corridor. Therefore, sustainable nature-based river corridor management approaches are essential in preserving the pre-disturbed functionality of hydro-geomorphological processes. The hydro-geomorphic river corridor space is also described as “room for the river” (Baptist et al., 2004), “erodible corridor” (Piégay et al., 2005) and “fluvial territory” (Ollero, 2010). At first, the freedom

space approach is focused on managing the space available for migration (mobility space). Similarly, the following approach considers the room/space available for riverine floods (flooding space). The management styles also vary depending on the physio-graphic settings, such as mobility being a key parameter for meandering rivers in France (Malavoi et al., 1998; Piegay et al., 2005), Spain (Ollero, 2010), and the Canadian Province of Ontario (Parish Geomorphic, 2004). On the other hand, the focus is more on flooding space for rivers in the Netherlands and the United Kingdom (Defra, 2005).

The discharge and sediment variabilities in the Brahmaputra River are extreme, along with a complex planform configuration and dynamic river-wetland-floodplain interactions. The river goes through abrupt geological disturbances (earthquakes), absorb periodic flooding events, activates destabilizing sediment waves and finally, results in an unstable transitional state. The annual bank-line migration and lateral accretion of the river approach up to 227.50 m/year and 331.50 m/year, respectively (Sarma and Phukan, 2004) and the sand-bar disorderness is also a significant concern for regulating the in-channel flooding space. The bars are very dynamic in terms of size, which varies from 600 m^2 to as large as 100 km^2. Such extensive variability along with the lateral and longitudinal propagations resulted in complicated in-channel morphological processes. The braided belt width fluctuates from 1.2 km to 18 km (Karmaker et al., 2017; Chembolu and Dutta, 2018; Nandi et al., 2022) which facilitates an extensive mobility and flooding spaces to the river corridor. Furthermore, the effective water width at a highly braided section is considerably less (close to 2-3 km), which further highlights to the significance of hierarchical or overlapped freedom space concept and resilience-based management approach in the Brahmaputra River.

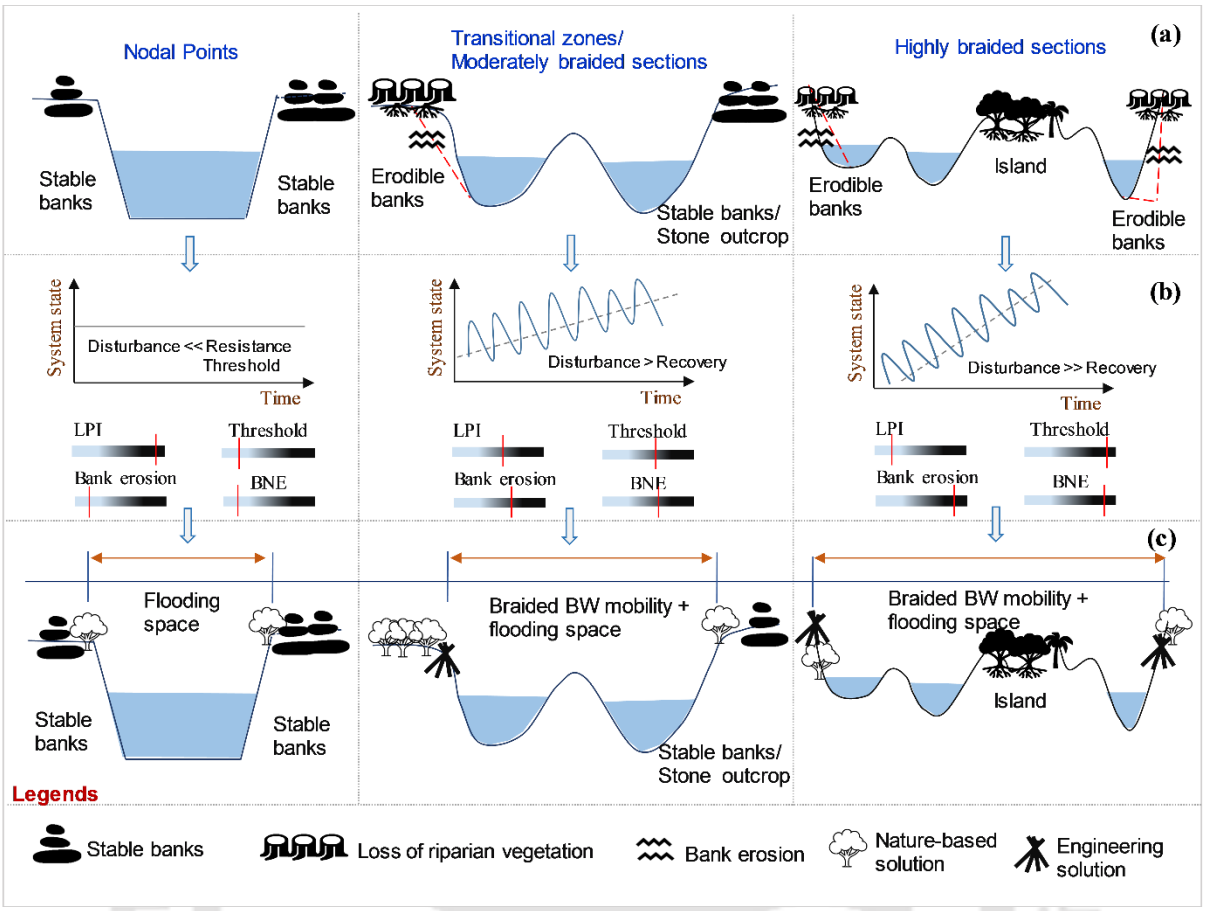

Figure 5.8 Conceptual diagram showing three dominant at-a-station hydraulic geometries and bank properties in the Brahmaputra River. (b) Relation between disturbance, resistance threshold and recovery, and temporal variation of system states. The variabilities of LPI, threshold, bank erosion potential and balance between nature-to-engineered solutions are also shown. (c) River freedom space concept and resilience-based management approach for a highly braided river system.

The Brahmaputra River exhibits stable banks and high LPI (more than 90%) at the nodal sections. Such reaches are absent from the braided signature and operate without the dominant thresholds. The pulse disturbances induced by periodic floods and high flows fall well below the resistance threshold offered by the physiographic settings. In addition, the channel constrictions may act as a conduit for high flow-sediment transport and require minimum BNE (balance between nature-to-engineered solutions) and freedom space. In the moderately braided sections, the erodible banks and probable absence of riparian vegetation may require immediate attention of fluvial engineers and experts. The periodic disturbances offered by extreme events and high flows perpetually keep the channel form in transition. Therefore, a high BNE combined with in-situ bank erosion tests and stochastic

bank erosion models (Karmaker and Dutta, 2013) may aid in regulating the vulnerable reaches. The intermediate probabilities of low-flow channels also indicate the prevalence of braided signature and oscillation of channel state between the two dominant thresholds. The locational probability images of the channel will also provide a view of the most likely natural or partly natural configuration for comparison with new engineered configurations. Further, such information will be helpful for nature-based solutions and engineering designs seeking to mimic regime conditions or to avoid inherently unstable areas. The highly braided sections are enriched with complex process-form interactions and display the overall identity of the dynamic Brahmaputra River. The disturbance frequency is smaller than the relaxation time and recovery adaption period. Therefore, the vulnerable reaches demand immediate consideration and a thorough understanding of channel thresholds and system state trajectory. The LPI map will be helpful in the restoration efforts and identifying the places where planting and nurturing of riparian vegetation and engineered solutions are most likely to proceed with the least likelihood of damage from braided belt width mobility and floods. The flooding space estimation with hydrodynamic modelling should be carried out at a seasonal scale, and societal feedbacks and field investigations should be implemented to assess the ground reality. Further, identification of riverine wetlands and preservation of their bio-geomorphological functionality is crucial to absorb the peak flood waves and reduce the damage. Such protection strategies combined with minimal intervention of in-channel and riparian vegetation cover can contribute to the gradual reduction of sand bar disorderness and enhanced bank stability.

The effective restoration strategies (nature-based or engineered) must be accompanied by a thorough understanding of the process-form relationships. A multifaceted, interdisciplinary approach should be formulated based on system state trajectory, LPI variability, proximity to thresholds, and in-channel fluvial landscape management for gradual dissipation of energy gradient. On the other hand, societal feedback, and field investigations should be promoted to enhance the resilience and recovery potential of the vulnerable reaches. To conclude, a hierarchical or overlapped freedom space concept and resilience-based approach are necessary to tame the Brahmaputra river.

5.7 CHAPTER SUMMARY

The present study has quantified the complex process-form relationships of the highly braided Brahmaputra River. In addition, locational probability theory, geomorphic

stationarity concept and hierarchical thresholds are developed to design a resilience-based freedom space management approach. The major conclusions of this chapter are as follows:

1. The geomorphic stationarity concept reveals that two additional local hydrologic nodes (LPI exceeding 80%) are observed in the high probability strip. These two nodes are spaced at a distance of 35 km and thereby producing a reach-averaged node spacing and scale of the planform evolution of 35-40 km.
2. Normalised process gradient is better related to sand bar adjustments than the normalised threshold exceedance. This suggests in a highly braided river system, the sand bar adjustments prevail over other forms of morphological adjustments at the initial stage of flood hydrograph and are closely dependent on the process gradient between the hierarchical thresholds.
3. The LPI map will be helpful in the restoration efforts and identifying the places where planting and nurturing of riparian vegetation and engineered solutions are most likely to proceed with the least likelihood of damage from braided belt width mobility and floods. Therefore, a multifaceted, interdisciplinary approach should be formulated based on system state trajectory, LPI variability, proximity to thresholds, and in-channel fluvial landscape management for gradual dissipation of energy gradient.

The study presented a new approach to understand the process-form relationships of a highly braided river system with the integration of GEE and hydro-geomorphological dataset. This study presented a new process-based approach to comprehend the system state and further design a resilience-based management practice. This work can be further extended to other large braided river systems with different morphological settings to better understand the channel dynamics.

6

SUMMARY AND FUTURE SCOPE

6.1 SUMMARY

The present research aims to understand the process-form relationships along the continuum of braided channel patterns. The study reaches included a weakly braided regulated river (the Brahmani), a paired anthropogenically disturbed catchment of two weakly braided rivers (the Ong and the Tel) and finally, the highly braided Brahmaputra River. This study attempted to investigate the river process-form relationships and underlying mechanics by analyzing the channel forming discharges, hierarchical energy dissipation process, morphological continuum, recovery trajectory, channel thresholds and geomorphic stationarity. The following sub-sections summarize the work completed and observations made in the present research.

6.1.1 Process-form relationships in a weakly braided river system

The objective has estimated the effective discharge for suspended sediment transport and its geomorphic implications as the channel-forming discharge in the regulated Brahmani River. The major conclusions of this chapter are as follows:

1. An overall reduction of transport effectiveness is observed in the Brahmani River after dam closure. The effective discharge converges to a moderate flood and can transport a maximum portion of suspended sediment load.

2. The seasonal stream power follows the trend of morphological adjustments better than peak stream power. Moreover, similar morphological characteristics indicate channel slope has a dominating role in defining stream power limited spatial variability.
3. The effective discharge integrated stream power curve accurately predicts the channel transition (from sinuous to weakly braided) in the Brahmani macrochannel. Most geomorphic adjustments occur below the macrochannel bankfull level and the river goes through a transition to accommodate the effective discharge in the inset channel.
4. The proposed probability of braiding captures the chute formation accurately, which signifies excess energy above the effective sediment transport and re-organizes chutes and diagonal bars close to the inset channel. The present study further highlights a hierarchy of energy dissipation and morphological continuum in the macrochannel of the Brahmani River.

6.1.2 Formulation of process-based recovery indicator for weakly braided river system

This objective has developed an entropy-based system state and river recovery indicators for anthropogenically disturbed macrochannel river systems. The major conclusions of this study are as follows:

1. The disorderness in bed-elevation at sub-bankfull stages is effectively captured by a system state indicator-CIE. The temporal variation of CIE has further addressed the existence of both thresholds modulated and filter dominated systems in macrochannel settings.
2. Vegetation density and CIE integrated recovery indicator (NRRI) symbolizes river health for channel-in-channel fluvial systems. The present study suggests that CIE and NRRI have followed fixed linear sequences of developmental stages, unless extreme events are absent as disturbing agents.
3. A gradual decline in CIE and subsequent stabilization of vegetated landforms can develop an ‘event-driven’ state, where floods exceeding the low-flow channel (LFE) directly impact on the river recovery trajectory.
4. Finally, the dominance between self-organization of vegetated landforms and fluvial disturbances develops an additional degree of freedom and further decides

the recovery state of macrochannel and planform fluctuations between the end-points of the morphological continuum (sinuous and weakly braided states).

6.1.3 Understanding the process-form relationships and development of resilience-based management approach for highly braided river system

This objective has quantified the complex process-form relationships of the highly braided Brahmaputra River. In addition, locational probability theory, geomorphic stationarity concept and hierarchical thresholds are developed to design a resilience-based freedom space management approach. The major conclusions of this study are as follows:

1. The geomorphic stationarity concept reveals that two additional local hydrologic nodes (LPI exceeding 80%) are observed in the high probability strip. These two nodes are spaced at a distance of 35 km and thereby producing a reach-averaged node spacing and scale of the planform evolution of 35-40 km.
2. Normalised process gradient is better related to sand bar adjustments than the normalised threshold exceedance. This suggests in a highly braided river system, the sand bar adjustments prevail over other forms of morphological adjustments at the initial stage of flood hydrograph and are closely dependent on the process gradient between the hierarchical thresholds.
3. The LPI map will be helpful in the restoration efforts and identifying the places where planting and nurturing of riparian vegetation and engineered solutions are most likely to proceed with the least likelihood of damage from braided belt width mobility and floods. Therefore, a multifaceted, interdisciplinary approach should be formulated based on system state trajectory, LPI variability, proximity to thresholds, and in-channel fluvial landscape management for gradual dissipation of energy gradient.

6.2 FUTURE SCOPE

The present research has provided better insights into understanding the process-form relationships and management approaches along the continuum of braided channels. The current work can be extended further with a prime focus on the following aspects:

- Effective discharge integrated stream power curve presented a new approach to predict the transitional channel pattern in a regulated weakly braided river. This

work can be further extended to regulated rivers with different morphological settings to better understand the channel dynamics.

- The fluvial systems in developing countries are poorly gauged, and assessing CIE and system disorderness with the continuous hydraulic and hydrological dataset is challenging. Therefore, the delicate balance between big data and remote sensing-based tools with archival benchmark information, 'place-based understanding' and 'reading the landscape' frameworks will be essential to capture and inform process-form relationships of fine-scale geomorphic units.
- The process-based understanding of highly braided river can be further applied to other large dynamic river systems to better understand the system state and recovery trajectory.

PUBLICATIONS

JOURNALS

1. C. Pradhan, V. Chembolu, S. Dutta, & R. Bharti (2021). Role of effective discharge on morphological changes for a regulated macrochannel river system. Geomorphology, 385, 107718. https://doi.org/10.1016/j.geomorph.2021.107718

2. C. Pradhan, S.K. Padhee, S. Dutta & R. Bharti (2022). A process-based recovery indicator for anthropogenically disturbed river system, Nature Scientific Reports, 12(1), 1-14. https://doi.org/10.1038/s41598-022-14542-x

3. C. Pradhan, V. Chembolu, R. Bharti & S. Dutta (2021). Regulated rivers in India: research progress and future directions. ISH Journal of Hydraulic Engineering, https://doi.org/10.1080/09715010.2021.1975319

4. C. Pradhan, K.K. Nandi, S. Dutta, & Rishikesh Bharti (2021). Does the river freedom space dynamics control large scale bank erosion in the Brahmaputra River? Journal of Transactions, SITA, NESAC-Govt. of Assam. (General Article).

5. C. Pradhan, V. Chembolu & S. Dutta (2019). Impact of river interventions on alluvial channel morphology. ISH Journal of Hydraulic Engineering, 25:1, 87-93. https://doi.org/10.1080/09715010.2018.1453878

6. C. Pradhan, K.K. Nandi, R. Bharti & S. Dutta (2022). Understanding the process-form relationships and development of resilience-based management approach for a highly braided river system (In Catena) **(Under review)**

7. C. Pradhan, S. Dutta & R. Bharti. Flow and colonizing vegetation interactions in a braided river: Exploring the spatio-temporal dynamics of vegetated landforms using Google earth engine (Invited for submission in the Journal of Hydrobiologia) **(To be submitted)**

8. C. Pradhan, C. Ganapathi, R. Bharti & S. Dutta. Geomorphological evolution and sediment regime study in a transboundary Himalayan river system. (In River Research and Application). **(To be submitted)**

BOOK CHAPTERS

1. C. Pradhan, S.K. Padhee, S. Dutta, & R. Bharti (2022). Assessment of Fluvial Controls and Cross-Sectional Recovery Indicators in a Large Regulated River. Recent Trends in River Corridor Management. Lecture Notes in Civil Engineering, vol 229. Springer, Singapore. https://doi.org/10.1007/978-981-16-9933-7_3

2. C. Pradhan, Suresh Modalavalasa, S. Dutta & Rishikesh Bharti (2020). A geomorphic approach to evaluate river recovery potential for regulated river basin. In Riverflow 2020, 7th-10th July, 2020, Delft, Netherland DOI: 10.1201/b22619-253

CONFERENCES

1. C. Pradhan, S. Dutta & R. Bharti (2021). Understanding River Freedom Space and Seasonal Variation of Surface Water Dynamics in Large Fluvial Landscapes: Implications for Floods and Anthropogenic Stress; Abstract submitted to AGU Fall Meeting 2021.

2. C. Pradhan, S. Dutta & R. Bharti (2021). Assessing The River Freedom Space along the continuum of braided channel patterns using advanced geo-spatial analysis, 4th International Conference on the status and future of the World's Large Rivers, Moscow 2021.

3. C. Pradhan, S.K. Padhee, S. Dutta & R. Bharti (2021). An entropy-based investigation on the river recovery potential in a regulated river basin, EGU General Assembly 2021, online, 19–30 Apr 2021, EGU21-9362, https://doi.org/10.5194/egusphere-egu21-9362, 2021.

4. C. Pradhan, S.K. Padhee, S. Dutta & R. Bharti (2021). Assessment of transport effectiveness and recovery trajectory in regulated Mahanadi river, International Conference on River Corridor Research and Management (RCRM 2021), IIT Jammu, 2021/2/27.

5. C. Pradhan, S. Pani, S. Dutta & R. Bharti (2019). Temporal Changes in Geomorphic Effectiveness of Floods in Regulated River Basins, 2019/7/29, 16th Annual Meeting, AOGS 2019, Singapore.

6. C. Pradhan, S. Dutta & R. Bharti (2017). A spatio- Temporal Analysis of Channel Migration using Remote sensing, field investigation and GIS techniques: The Kameng River (Lower Reach), India; 9th International conference of Geomorphology, 6-11th November,2017, New Delhi, India.

7. C. Pradhan, R. Bharti and S. Dutta (2017). Assessment of post-impoundment geomorphic variations along Brahmani River using remote sensing, IEEE International Geoscience and Remote Sensing Symposium (IGARSS), Fort Worth, TX, 2017, pp. 5598-5601, DOI: 10.1109/IGARSS.2017.8128274.

8. C. Pradhan, V. Chembolu and S. Dutta (2016). Impacts of River Interventions on Alluvial Channel Morphology- Hydro International, Organized by Indian Society of Hydraulics, 8-10th December, 2016, CWPRS, Pune.

SYMPOSIUM/MASTERCLASS

1. Participated in the Master Class "*River functions under pressure*", by Hervé Piégay, Jorge Abad and Virginia Ruiz-Villanueva, Delft, 10th July 2020, 10th International Conference on Fluvial Hydraulics River Flow 2020, Delft, Netherland.

APPENDIX A

ONE DIMENSIONAL MODELING

A.1 HEC-RIVER ANALYSIS SYSTEM

HEC-RAS is a one dimensional hydrodynamic and morphological model allows user to perform one dimensional steady, unsteady flow analysis, movable sediment transport and water quality analysis. This section discusses the mathematical equations used in performing steady and unsteady flow calculations in HEC-RAS.

A.1.1 Steady Flow Analysis

Energy equation is used in HEC-RAS for computing the water surface profiles from one cross section to another. The equation is

$$Z_2+Y_2+{\alpha V_2^2}/{2g}=Z_1+Y_1+{\alpha V_1^2}/{2g}+h_L$$

Z_1, Z_2 = elevation of main channel inverts

Y_1, Y_2 = depth of water at cross sections

V_1, V_2 = average velocities

h_L= energy head loss and α_1 α_2 = weighted velocity coefficients

A.1.2 Unsteady Flow Analysis

In HEC-RAS, unsteady flow equations are expressed in terms of set of partial differential equations to solve the water flow in the open channel govern by gravity. The governing equations i.e. continuity equation and momentum equations are listed below.

$$\frac{\partial A}{\partial t}+\frac{\partial Q}{\partial x}+q_l = 0$$

$$\frac{\partial Q}{\partial t}+\frac{\partial QV}{\partial x}+gA\left(\frac{\partial Z}{\partial x}+S_f\right)=0$$

Where,

A is total flow area

q_l is lateral flow per unit length

S_f is friction slope

These equations are approximated using implicit finite difference scheme and are solved with necessary boundary conditions. Flow hydrograph is provided as upstream boundary condition and stage hydrograph, normal depth or rating curve can be provided as downstream boundary conditions.

The details on working with HEC-RAS is discussed in detail on http://www.hec.usace.army.mil/software/hec-ras.

APPENDIX B

FIELD INVESTIGATIONS TO FLUVIAL SYSTEMS IN INDIA

Brahmani, 2014

Brahmani, 2014

Manas, 2016

Kameng, 2017

Kameng, 2017

Brahmaputra, 2018

Mahanadi, 2020

Mahanadi, 2020

REFERENCES

Abe, G., & Erinjery Joseph, J. (2015). Changes in streamflow regime due to anthropogenic regulations in the humid tropical Western Ghats, Kerala State, India. Journal of Mountain Science, 12(2), 456-470. https://doi.org/10.2307/1467936

Agoramoorthy, G. (2015). The future of India's obsolete dams: Time to review their safety and structural integrity. Futures, 67, 22-25. https://doi.org/10.1016/j.futures.2015.02.001

Akhtar, M. P., Sharma, N. A. Y. A. N., & Ojha, C. S. P. (2011). Braiding process and bank erosion in the Brahmaputra River. International Journal of Sediment Research, 26(4), 431-444. https://doi.org/10.1016/S1001-6279(12)60003-1

Alabyan, A. M., & Chalov, R. S. (1998). Types of river channel patterns and their natural controls. Earth Surface Processes and Landforms: The Journal of the British Geomorphological Group, 23(5), 467-474. https://doi.org/10.1002/(SICI)1096-9837(199805)23:5<467::AID-ESP861>3.0.CO;2-T.

Amsler, M. L., Ramonell, C. G., & Toniolo, H. A. (2005). Morphologic changes in the Paraná River channel (Argentina) in the light of the climate variability during the 20th century. Geomorphology, 70(3-4), 257-278. https://doi.org/10.1016/j.geomorph.2005.02.008

Andrews, E. D. (1980). Effective and bankfull discharges of streams in the Yampa River basin, Colorado and Wyoming. Journal of Hydrology, 46(3-4), 311-330. https://doi.org/10.1016/0022-1694(80)90084-0

Annual report of Brahmaputra board for the year 2018-19, http://brahmaputraboard.gov.in/wp-content/uploads/2020/06/annual_report_2018-19_English.pdf

Ardiclioglu, M., Bilgin, H., Genc, O., & Agiralioglu, N. (2010). Determination of discharge by entropy concept in natural river. In Fourth International Conference on Water Observation and Information System for Decision Support.

Arunbabu, E., Ravichandran, S., & Sreeja, P. (2014). Sedimentation and internal phosphorus loads in Krishnagiri Reservoir, India. Lakes & Reservoirs: Research & Management, 19(3), 161-173. https://doi.org/10.1111/lre.12069

Ashmore, P. (2013). Morphology and dynamics of braided rivers, J.F. Shroder (Ed.), Treatise on Geomorphology, Academic Press, San Diego (2013), pp. 289-312. 10.1016/B978-0-12-374739-6.00242-6.

Ashmore, P. E., & Day, T. J. (1988). Effective discharge for suspended sediment transport in streams of the Saskatchewan River basin. Water Resources Research, 24(6), 864-870. https://doi.org/10.1029/WR024i006p00864

Ashworth, P. J. (1996). Mid-channel bar growth and its relationship to local flow strength and direction. Earth surface processes and landforms, 21(2), 103-123. https://doi.org/10.1002/(SICI)1096-9837(199602)21:2<103::AID-ESP569>3.0.CO;2-O

Bahuguna, B. K., Nautiyal, R., Nautiyal, P., & Singh, H. R. (2004). Stream regulation: Variations in the density, composition and diversity of benthic macroinvertebrates occurring in the up and downstream sections of the impounded zone of the river. Tropical Ecology, 45(2), 251-262.

Bakalial, B., Biswas, S. P., Borah, S., & Baruah, D. (2014). Checklist of fishes of Lower Subansiri River drainage, northeast India. Annals of Biological Research, 5(2), 55-67.

Baker, W. L. (1989). Macro-and micro–scale influences on riparian vegetation in western Colorado. Annals of the Association of American Geographers, 79(1), 65-78.
Bandyopadhyay, S., Sinha, S., Jana, N. C., & Ghosh, D. (2014). Entropy application to evaluate the stability of landscape in Kunur River Basin, West Bengal, India. Current Science, 1842-1853.
Banerjee, M. (1999). A report on the impact of Farakka Barrage on the human fabric. New Delhi: South Asian Network on Dams, Rivers and People.
Bankhead, N. L., Thomas, R. E., & Simon, A. (2017). A combined field, laboratory and numerical study of the forces applied to, and the potential for removal of, bar top vegetation in a braided river. Earth Surface Processes and Landforms, 42(3), 439-459. https://doi.org/10.1002/esp.3997
Baptist, M. J., Penning, W. E., Duel, H., Smits, A. J., Geerling, G. W., Van der Lee, G. E., & Van Alphen, J. S. (2004). Assessment of the effects of cyclic floodplain rejuvenation on flood levels and biodiversity along the Rhine River. River Research and Applications, 20(3), 285-297. https://doi.org/10.1002/rra.778
Barik, S. K., Adhikari, D., Pandey, H. N., Mishra, S. K., Tiwary, R., Singh, P. P., ... and Chakraborty, P. (2014). "Perspective plan for development of Tawang river basin. Cumulative Impact Assessment of Proposed Hydel Power Projects, Determination of Basin Carrying Capacity and Landscape Level Biodiversity Management Plan".
Barman, B. C., Sahu, R. B., and Bhandari, G. (2014). "Backwater profile during barrage gate operation for variable pond levels." ISH J. Hydraul. Eng., 20(3), 239-249.
Barman, B., Kumar, B., & Sarma, A. K. (2018). Turbulent flow structures and geomorphic characteristics of a mining affected alluvial channel. Earth Surface Processes and Landforms, 43(9), 1811-1824. https://doi.org/10.1002/esp.4355
Bassi, N., Kumar, M. D., Sharma, A., & Pardha-Saradhi, P. (2014). Status of wetlands in India: A review of extent, ecosystem benefits, threats and management strategies. Journal of Hydrology: Regional Studies, 2, 1-19. https://doi.org/10.1016/j.ejrh.2014.07.001
Bastia, F., & Equeenuddin, S. M. (2016). Spatio-temporal variation of water flow and sediment discharge in the Mahanadi River, India. Global and Planetary Change, 144, 51-66. https://doi.org/10.1016/j.gloplacha.2016.07.004
Bawa, N., Jain, V., Shekhar, S., Kumar, N., & Jyani, V. (2014). Controls on morphological variability and role of stream power distribution pattern, Yamuna River, western India. Geomorphology, 227, 60-72. https://doi.org/10.1016/j.geomorph.2014.05.016
Beaumont, P. (1978). Man's impact on river systems: a world-wide view. Area, 38-41.
Beisner, B. E., Haydon, D. T., & Cuddington, K. (2003). Alternative stable states in ecology. Frontiers in Ecology and the Environment, 1(7), 376-382.
Benson, M. A., & Thomas, D. M. (1966). A definition of dominant discharge. Hydrological Sciences Journal, 11(2), 76-80. https://doi.org/10.1080/02626666609493460
Bertoldi, W., Gurnell, A. M., & Welber, M. (2013). Wood recruitment and retention: The fate of eroded trees on a braided river explored using a combination of field and remotely-sensed data sources. Geomorphology, 180, 146-155. https://doi.org/10.1016/j.geomorph.2012.10.003
Bertoldi, W., Zanoni, L., & Tubino, M. (2010). Assessment of morphological changes induced by flow and flood pulses in a gravel bed braided river: The Tagliamento River (Italy). Geomorphology, 114(3), 348-360. https://doi.org/10.1016/j.geomorph.2009.07.017
Bhuiyan, M. A., Kumamoto, T., & Suzuki, S. (2015). Application of remote sensing and GIS for evaluation of the recent morphological characteristics of the lower Brahmaputra-Jamuna River, Bangladesh. Earth Science Informatics, 8(3), 551-568. https://doi.org/10.1007/s12145-014-0180-4
Biron, P. M., Buffin-Bélanger, T., Larocque, M., Choné, G., Cloutier, C. A., Ouellet, M. A., ... & Eyquem, J. (2014). Freedom space for rivers: a sustainable management approach to enhance river resilience. Environmental management, 54(5), 1056-1073. https://doi.org/10.1007/s00267-014-0366-z
Boothroyd, R. J., Williams, R. D., Hoey, T. B., Tolentino, P. L., & Yang, X. (2021). National-scale assessment of decadal river migration at critical bridge infrastructure in the Philippines. Science of the Total Environment, 768, 144460. https://doi.org/10.1016/j.scitotenv.2020.144460
Borgohain, P. L. (2019). Downstream impacts of the Ranganadi hydel project in Brahmaputra Basin, India: Implications for design of future projects. Environmental Development, 30, 114-128. https://doi.org/10.1016/j.envdev.2019.04.005
Borgohain, P. L., Phukan, S., & Ahuja, D. R. (2019). Downstream channel changes and the likely impacts of flow augmentation by a hydropower project in River Dikrong, India. International Journal of River Basin Management, 17(1), 25-35. https://doi.org/10.1080/15715124.2018.1439497
Boruah, S., Gilvear, D., Hunter, P., & Sharma, N. (2008). Quantifying channel planform and physical habitat dynamics on a large braided river using satellite data—The Brahmaputra, India. River Research and Applications, 24(5), 650-660. https://doi.org/10.1002/rra.1132

Boyd, J., & Banzhaf, S. (2007). What are ecosystem services? The need for standardized environmental accounting units. Ecological economics, 63(2-3), 616-626. https://doi.org/10.1016/j.ecolecon.2007.01.002
Bridge, J. S. (1985). Paleochannel patterns inferred from alluvial deposits; a critical evaluation. Journal of Sedimentary Research, 55(4), 579-589. https://doi.org/10.1306/212F8738-2B24-11D7-8648000102C1865D
Bridge, J. S. (1993). The interaction between channel geometry, water flow, sediment transport and deposition in braided rivers. Geological Society, London, Special Publications, 75(1), 13-71. https://doi.org/10.1144/GSL.SP.1993.075.01.02
Brierley, G. J. (1996). Channel morphology and element assemblages: a constructivist approach to facies modelling. Advances in fluvial dynamics and stratigraphy, 263-298.
Brierley, G. J., & Fryirs, K. A. (2013). Geomorphology and river management: applications of the river styles framework. John Wiley & Sons.
Brierley, G., & Fryirs, K. (2000). River styles in Bega Catchment, NSW, Australia: implications for river rehabilitation. Environmental Management, 25(6), 661-679.
Brierley, G., Fryirs, K., Cullum, C., Tadaki, M., Huang, H. Q., & Blue, B. (2013). Reading the landscape: Integrating the theory and practice of geomorphology to develop place-based understandings of river systems. Progress in Physical Geography, 37(5), 601-621.
Bristow, C.S. (1987). Brahmaputra River: channel migration and deposition. in Ethridge, F.G., Flores, R.M., and Harvey, M.D., eds., Recent Developments in Fluvial Sedimentology: SEPM, Special Publication 39, p. 63–74
Bristow, C. S., & Best, J. L. (1993). Braided rivers: perspectives and problems. Geological society, London, special publications, 75(1), 1-11. https://doi.org/10.1144/GSL.SP.1993.075.01.01
Brookes, A., Gregory, K. J., & Dawson, F. H. (1983). An assessment of river channelization in England and Wales. Science of the Total Environment, 27(2-3), 97-111.
Brotherton, D. I. (1979). On the origin and characteristics of river channel patterns. Journal of Hydrology, 44(3-4), 211-230. https://doi.org/10.1016/0022-1694(79)90132-X
Brunner, G. W. (1995). HEC-RAS river analysis system. Hydraulic reference manual. Version 1.0. Hydrologic Engineering Center Davis CA.
Buffin-Bélanger, T., Biron, P. M., Larocque, M., Demers, S., Olsen, T., Choné, G., ... & Eyquem, J. (2015). Freedom space for rivers: An economically viable river management concept in a changing climate. Geomorphology, 251, 137-148.
Chadha, R. K., Gupta, H. K., Kumpel, H. J., Mandal, P., Rao, A. N., Kumar, N., ... & Satyanarayana, H. V. S. (1997). Delineation of active faults, nucleation process and pore pressure measurements at Koyna (India). In Seismicity Associated with Mines, Reservoirs and Fluid Injections (pp. 551-562). Birkhäuser, Basel.
Chander, R. (1997). On categorising induced and natural tectonic earthquakes near new reservoirs. Engineering Geology, 46(2), 81-92. https://doi.org/10.1016/S0013-7952(96)00099-3
Charlton, R. (2007). Fundamentals of fluvial geomorphology. Routledge.
Chaturvedi, A. K. (2015). Scope for small hydro projects in India. In Energy Sustainability Through Green Energy (pp. 427-452). Springer, New Delhi.
Chaudhuri, D. (2006). Life of maithon reservoir on ground of sedimentation: Case study in India. Journal of Hydraulic Engineering, 132(9), 875-880. https://doi.org/10.1061/(ASCE)0733-9429(2006)132:9(875)
Chembolu, V., & Dutta, S. (2018). An entropy based morphological variability assessment of a large braided river. Earth Surface Processes and Landforms, 43(14), 2889-2896.
Chembolu, V., Kakati, R., & Dutta, S. (2019). A laboratory study of flow characteristics in natural heterogeneous vegetation patches under submerged conditions. Advances in Water Resources, 133, 103418.
Coe, M. T., Latrubesse, E. M., Ferreira, M. E., & Amsler, M. L. (2011). The effects of deforestation and climate variability on the streamflow of the Araguaia River, Brazil. Biogeochemistry, 105(1), 119-131.
Coleman, J. M. (1969). Brahmaputra River: channel processes and sedimentation. Sedimentary geology, 3(2-3), 129-239. https://doi.org/10.1016/0037-0738(69)90010-4
Collins, B. D., Montgomery, D. R., Fetherston, K. L., & Abbe, T. B. (2012). The floodplain large-wood cycle hypothesis: A mechanism for the physical and biotic structuring of temperate forested alluvial valleys in the North Pacific coastal ecoregion. Geomorphology, 139, 460-470.
CR, Amarnath., & Thatikonda, S. (2020). Study on backwater effect due to Polavaram Dam Project under different return periods. Water, 12(2), 576. https://doi.org/10.3390/w12020576

Croke, J., Fryirs, K., & Thompson, C. (2013). Channel–floodplain connectivity during an extreme flood event: implications for sediment erosion, deposition, and delivery. Earth Surface Processes and Landforms, 38(12), 1444-1456.

Croke, J., Reinfelds, I., Thompson, C., & Roper, E. (2014). Macrochannels and their significance for flood-risk minimisation: examples from southeast Queensland and New South Wales, Australia. Stochastic environmental research and risk assessment, 28(1), 99-112. https://doi.org/10.1007/s00477-013-0722-1

Croke, J., Thompson, C., & Fryirs, K. (2017). Prioritising the placement of riparian vegetation to reduce flood risk and end-of-catchment sediment yields: Important considerations in hydrologically-variable regions. Journal of Environmental Management, 190, 9-19. https://doi.org/10.1016/j.jenvman.2016.12.046

Crowder, D. W., & Knapp, H. V. (2005). Effective discharge recurrence intervals of Illinois streams. Geomorphology, 64(3-4), 167-184. https://doi.org/10.1016/j.geomorph.2004.06.006

CWC (Central Water Commission) (2007). "Report of Working Group to advise WQAA on the minimum flows in the rivers." New Delhi: CWC, Ministry of Water Resources, Government of India

CWC, N. (2019). National register of large dams. Central Water Commission, Ministry of water resources, Government of India.

Daley, J. S., & Cohen, T. J. (2018). Climatically-controlled river terraces in eastern Australia. Quaternary, 1(3), 23.

Das Sarkar, S., Sahoo, A. K., Gogoi, P., Raman, R. K., Hoshalli Munivenkatappa, M., Kumari, K., ... & Das, B. K. (2019). Phytoplankton biomass in relation to flow dynamics: the case of a tropical river Mahanadi, India. Tropical Ecology, 60(4), 485-494.

Das, B. C., Ghosh, S., Islam, A., & Roy, S. (Eds.). (2020). Anthropogeomorphology of Bhagirathi-Hooghly River System in India. CRC Press.

Das, D., & Mallik, J. (2020). Koyna earthquakes: a review of the mechanisms of reservoir-triggered seismicity and slip tendency analysis of subsurface faults. Acta Geophysica, 68(4), 1097-1112.

Defra, A. (2005). Making Space for Water: Taking Forward a New Government Strategy for Flood and Coastal Erosion Risk Management. Delivery Plan. Defra, London. http://coastaladaptationresources.org/PDF-files/1329-Making-space-for-water.pdf. Accessed 12 Mar 2014

Deng, S., Xia, J., Zhou, M., & Lin, F. (2019). Coupled modeling of bed deformation and bank erosion in the Jingjiang Reach of the middle Yangtze River. Journal of Hydrology, 568, 221-233. https://doi.org/10.1016/j.jhydrol.2018.10.065

Deng, X., Xu, Y., Han, L., Yu, Z., Yang, M., & Pan, G. (2015). Assessment of river health based on an improved entropy-based fuzzy matter-element model in the Taihu Plain, China. Ecological Indicators, 57, 85-95.

DeRose, R. C., Gomez, B., Marden, M., & Trustrum, N. A. (1998). Gully erosion in Mangatu Forest, New Zealand, estimated from digital elevation models. Earth Surface Processes and Landforms: The Journal of the British Geomorphological Group, 23(11), 1045-1053. https://doi.org/10.1002/(SICI)1096-9837(1998110)23:11%3C1045::AID-ESP920%3E3.0.CO;2-T

DHI, (2006). Managed river flows for RHEP. New Delhi: DHI Water and Environment

Doyle, M. W., Shields, D., Boyd, K. F., Skidmore, P. B., & Dominick, D. (2007). Channel-forming discharge selection in river restoration design. Journal of Hydraulic Engineering, 133(7), 831-837. https://doi.org/10.1061/(ASCE)0733-9429(2007)133:7(831)

Doyle, M. W., Stanley, E. H., Strayer, D. L., Jacobson, R. B., & Schmidt, J. C. (2005). Effective discharge analysis of ecological processes in streams. Water Resources Research, 41(11). https://doi.org/10.1029/2005WR004222

Dubey, A. K., Chembolu, V., & Dutta, S. (2020). Utilization of satellite altimetry retrieved river roughness properties in hydraulic flow modelling of braided river system. International Journal of River Basin Management, 1-14. https://doi.org/10.1080/15715124.2020.1830785

Dubey, A. K., Kumar, P., Chembolu, V., Dutta, S., Singh, R. P., & Rajawat, A. S. (2021). Flood modeling of a large transboundary river using WRF-Hydro and microwave remote sensing. Journal of Hydrology, 598, 126391. https://doi.org/10.1016/j.jhydrol.2021.126391

Dury, G. H. (1973). Magnitude-frequency analysis and channel morphology. Fluvial Geomorphology: New York, State University of New York, 91-121.

Economics Times. (2019). "Energy demand growth fastest in the world"< https://economictimes.indiatimes.com/industry/energy/power/energy-demand-growth-fastest-in-the-world/articleshow/70082035.cms?from=mdr>

Farina, G., Alvisi, S., Franchini, M., & Moramarco, T. (2014). Three methods for estimating the entropy parameter M based on a decreasing number of velocity measurements in a river cross-section. Entropy, 16(5), 2512-2529.
Ferguson, R. I. (1987). Hydraulic and sedimentary controls of channel pattern. River channels: Environments and processes, 129-158.
Ferguson, R. I. (1993). Understanding braiding processes in gravel-bed rivers: progress and unsolved problems. Geological Society, London, Special Publications, 75(1), 73-87.
Ferguson, R. J., & Brierley, G. J. (1999). Downstream changes in valley confinement as a control on floodplain morphology, lower Tuross River. New South Wales, Australia: a constructivist approach to floodplain analysis. In: Varieties of Fluvial Forms, 377-406.
Fiorentino, M., Claps, P., & Singh, V. P. (1993). An entropy-based morphological analysis of river basin networks. Water Resources Research, 29(4), 1215-1224.
Fisk, H. N. (1947). Geology of the Mississippi Valley Region.
Fisk, R. T., & Mordvin, O. E. (1944). Studies on Staphylo-cocci. III. Further Observations on Bacteriophage Typing of Staphylococcus aureus. American Journal of Hygiene, 40(3), 232-8.
Foote, A. L., Pandey, S., & Krogman, N. T. (1996). Processes of wetland loss in India. Environmental Conservation, 23(1), 45-54. https://www.jstor.org/stable/44519180
Friend, P. F., & Sinha, R. (1993). Braiding and meandering parameters. Geological Society, London, Special Publications, 75(1), 105-111. https://doi.org/10.1144/GSL.SP.1993.075.01.05
Fryirs, K. A., & Brierley, G. J. (2012). Geomorphic analysis of river systems: an approach to reading the landscape. John Wiley & Sons.
Fryirs, K. A., & Brierley, G. J. (2016). Assessing the geomorphic recovery potential of rivers: forecasting future trajectories of adjustment for use in management. Wiley Interdisciplinary Reviews: Water, 3(5), 727-748.
Fryirs, K. A., Brierley, G. J., Hancock, F., Cohen, T. J., Brooks, A. P., Reinfelds, I., ... & Raine, A. (2018). Tracking geomorphic recovery in process-based river management. Land Degradation & Development, 29(9), 3221-3244.
Fryirs, K., & Brierley, G. (2000). A geomorphic approach to the identification of river recovery potential. Physical Geography, 21(3), 244-277.
Fryirs, K., & Brierley, G. (2022). Assemblages of geomorphic units: A building block approach to analysis and interpretation of river character, behaviour, condition and recovery. Earth Surface Processes and Landforms, 47(1), 92-108.
Fryirs, K., & Brierley, G. J. (2001). Variability in sediment delivery and storage along river courses in Bega catchment, NSW, Australia: implications for geomorphic river recovery. Geomorphology, 38(3-4), 237-265.
Fryirs, K., Brierley, G. J., Hancock, F., Cohen, T. J., Brooks, A. P., Reinfelds, I., ... & Raine, A. (2018). It'sa good news story! Tracking geomorphic recovery of rivers in eastern New South Wales as part of process-based river management. In Australian Stream Management Conference (9th: 2018) (pp. 697-704). River Basin Management Society.
Fryirs, K., Lisenby, P., & Croke, J. (2015). Morphological and historical resilience to catastrophic flooding: the case of Lockyer Creek, SE Queensland, Australia. Geomorphology, 241, 55-71. https://doi.org/10.1016/j.geomorph.2015.04.008
Gao, P., Li, Z., You, Y., Zhou, Y., & Piégay, H. (2022). Assessing functional characteristics of a braided river in the Qinghai-Tibet Plateau, China. Geomorphology, 403, 108180. https://doi.org/10.1016/j.geomorph.2022.108180
Garg, V., & Jothiprakash, V. (2013). Evaluation of reservoir sedimentation using data driven techniques. Applied Soft Computing, 13(8), 3567-3581. https://doi.org/10.1016/j.asoc.2013.04.019
Gaurav, K., Métivier, F., Devauchelle, O., Sinha, R., Chauvet, H., Houssais, M., & Bouquerel, H. (2014). Morphology of the Kosi megafan channels. Earth Surf Dyn, 2, 1023-1046.
Gautama, K., Girib, S., Donchytsb, G., & Bhattacharyaa, B. (2021). Assessing morphological changes and impact on ecology in Koshi River using remote sensing and cloud computing. Rivers in an uncertain future, 36.
Geomorphic, P. (2004). Belt width delineation procedures. Submitted to the Toronto and Region Conservation Authority. http://sustainabletechnologies.ca/wp/wp-content/uploads/2013/01/Belt-Width-Delineation-Procedures.pdf.
Gholami, A., Bonakdari, H., Mohammadian, M., Zaji, A. H., & Gharabaghi, B. (2019). Assessment of geomorphological bank evolution of the alluvial threshold rivers based on entropy concept parameters. Hydrological Sciences Journal, 64(7), 856-872.
Ghosh, A. K., Pattnaik, A. K., & Ballatore, T. J. (2006). Chilika Lagoon: Restoring ecological balance and livelihoods through re-salinization. Lakes & Reservoirs: Research & Management, 11(4), 239-255.

Ghosh, S., & Guchhait, S. K. (2014). Hydrogeomorphic variability due to dam constructions and emerging problems: a case study of Damodar River, West Bengal, India. Environment, development and sustainability, 16(3), 769-796. https://doi.org/10.1007/s10668-013-9494-5
Ghosh, S., & Guchhait, S. K. (2016). Dam-induced changes in flood hydrology and flood frequency of tropical river: a study in Damodar River of West Bengal, India. Arabian Journal of Geosciences, 9(2), 1-26. https://doi.org/10.1007/s12517-015-2046-6
Gilvear, D. J. (1993). River management and conservation issues on formerly braided river systems; the case of the River Tay, Scotland. Geological Society, London, Special Publications, 75(1), 231-240.
Goel, M. K., Jain, S. K., & Agarwal, P. K. (2002). Assessment of sediment deposition rate in Bargi Reservoir using digital image processing. Hydrological sciences journal, 47(S1), S81-S92. https://doi.org/10.1080/02626660209493024
Gomez, B., Coleman, S. E., Sy, V. W. K., Peacock, D. H., & Kent, M. (2007). Channel change, bankfull and effective discharges on a vertically accreting, meandering, gravel-bed river. Earth Surface Processes and Landforms, 32(5), 770-785. https://doi.org/10.1002/esp.1424
Gopal, B., & Chauhan, M. (2006). Biodiversity and its conservation in the Sundarban mangrove ecosystem. Aquatic sciences, 68(3), 338-354. https://doi.org/10.1007/s00027-006-0868-8
Goswami, D. C. (1985). Brahmaputra River, Assam, India: Physiography, basin denudation, and channel aggradation. Water Resources Research, 21(7), 959-978. https://doi.org/10.1029/WR021i007p00959
Graf, W. L. (1977). The rate law in fluvial geomorphology. American Journal of Science, 277(2), 178.
Graf, W. L. (2000). Locational probability for a dammed, urbanizing stream: Salt River, Arizona, USA. Environmental Management, 25(3). DOI:10.1007/s002679910025
Greco, M., & Mirauda, D. (2015). An entropy based velocity profile for steady flows with large-scale roughness. In Engineering Geology for Society and Territory-Volume 3 (pp. 641-645). Springer, Cham.
Gregory, K. J. (2019). Human influence on the morphological adjustment of river channels: The evolution of pertinent concepts in river science. River Research and Applications, 35(8), 1097-1106.
Gregory, K.J. (1978) In: Embleton, C., Brunsden, D. & Jones, D.K.C. (Eds.) Fluvial processes in British basins: The impact of hydrology and the prospect for hydrogeomorphology In Geomorphology: Present problems and future prospects. Oxford: Oxford University Press, 40–72
Griffin, E. R., & Smith, J. D. (2004). Floodplain stabilization by woody riparian vegetation during an extreme flood. Riparian vegetation and fluvial geomorphology, 8, 221-236.
Gunjan, P., Mishra, S. K., Lohani, A. K., & Chandniha, S. K. (2020). The study of morphological characteristics for best management practices over the Rampur watershed of Mahanadi River Basin using prioritization. Journal of the Indian Society of Remote Sensing, 48(1), 35-45.
Gupta, A. (1995). Magnitude, frequency, and special factors affecting channel form and processes in the seasonal tropics. Washington DC American Geophysical Union Geophysical Monograph Series, 89, 125-136. DOI: 10.1029/GM089p0125
Gupta, A., Kale, V. S., & Rajaguru, S. N. (1999). The Narmada River, India, through space and time. Varieties of fluvial form, 114-143.
Gupta, H. K. (1992). Reservoir induced earthquakes. Elsevier.
Gupta, H., & Chakrapani, G. J. (2005). Temporal and spatial variations in water flow and sediment load in Narmada River Basin, India: natural and man-made factors. Environmental Geology, 48(4), 579-589. https://doi.org/10.1007/s00254-005-1314-2
Gupta, H., Kao, S. J., & Dai, M. (2012). The role of mega dams in reducing sediment fluxes: A case study of large Asian rivers. Journal of Hydrology, 464, 447-458. https://doi.org/10.1016/j.jhydrol.2012.07.038
Gupta, S., Collier, J. S., Palmer-Felgate, A., & Potter, G. (2007). Catastrophic flooding origin of shelf valley systems in the English Channel. Nature, 448(7151), 342-345. https://doi.org/10.1038/nature06018
Gurnell, A. (2014). Plants as river system engineers. Earth Surface Processes and Landforms, 39(1), 4-25.
Gurnell, A. M., Corenblit, D., García de Jalón, D., González del Tánago, M., Grabowski, R. C., O'hare, M. T., & Szewczyk, M. (2016). A conceptual model of vegetation–hydrogeomorphology interactions within river corridors. River research and applications, 32(2), 142-163.
Hardy, A., Oakes, G., & Ettritch, G. (2020). Tropical wetland (TropWet) mapping tool: the automatic detection of open and vegetated waterbodies in Google Earth engine for tropical wetlands. Remote Sensing, 12(7), 1182. https://doi.org/10.3390/rs12071182
Harman, W.A., Jennings, G.D., Patterson, J.M., Clinton, D.R., Slate, L.O., Jessup, A.G., Everhart, J.R., & Smith, R.E. (1999). Bankfull hydraulic geometry relationships for North Carolina streams. AWRA Wildland Hydrology Proceedings, pp.401-408.
Harmar, O. P., & Clifford, N. J. (2007). Geomorphological explanation of the long profile of the Lower Mississippi River. Geomorphology, 84(3-4), 222-240. https://doi.org/10.1002/esp.1294

Hazarika, L. P., Baruah, D., Borah, S., & Biswas, S. P. (2013). Diversity assessment of macroinvertebrates in the dam progressed Subansiri river in the North–Eastern India.
Heitmuller, F. T., Hudson, P. F., & Asquith, W. H. (2015). Lithologic and hydrologic controls of mixed alluvial–bedrock channels in flood-prone fluvial systems: Bankfull and macrochannels in the Llano River watershed, central Texas, USA. Geomorphology, 232, 1-19. https://doi.org/10.1016/j.geomorph.2014.12.033
Henck, A. C., Montgomery, D. R., Huntington, K. W., & Liang, C. (2010). Monsoon control of effective discharge, Yunnan and Tibet. Geology, 38(11), 975-978. https://doi.org/10.1130/G31444.1
Heritage, G. L., Charlton, M. E., & O'Regan, S. (2001). Morphological classification of fluvial environments: An investigation of the continuum of channel types. The Journal of Geology, 109(1), 21-33.
Heritage, G. L., Large, A. R. G., Moon, B. P., & Jewitt, G. (2004). Channel hydraulics and geomorphic effects of an extreme flood event on the Sabie River, South Africa. Catena, 58(2), 151-181.
Heritage, G. L., Van Niekerk, A. W., Moon, B. P., Broadhurst, L. J., Rogers, K. H., & James, C. S. (1997). The geomorphological response to changing flow regimes of the Sabie and Letaba river systems. Water Research Commission Report, 376(1), 97.
Heritage, G., Tooth, S., Entwistle, N., & Milan, D. (2015). Long-term flood controls on semi-arid river form: evidence from the Sabie and Olifants rivers, eastern South Africa. Proceedings of the International Association of Hydrological Sciences, 367, 141-146.
Hickin, E. J. (1968). Channel morphology, bankfull stage and bankfull discharge of streams near Sydney. Australian journal of Science, 30(7), 274-275.
Higgins, A., Restrepo, J. C., Ortiz, J. C., Pierini, J., & Otero, L. (2016). Suspended sediment transport in the Magdalena River (Colombia, South America): Hydrologic regime, rating parameters and effective discharge variability. International Journal of Sediment Research, 31(1), 25-35. https://doi.org/10.1016/j.ijsrc.2015.04.003
Huang, Q., Long, D., Du, M., Zeng, C., Qiao, G., Li, X., ... & Hong, Y. (2018). Discharge estimation in high-mountain regions with improved methods using multisource remote sensing: A case study of the Upper Brahmaputra River. Remote Sensing of Environment, 219, 115-134. https://doi.org/10.1016/j.rse.2018.10.008
Hundey, E. J., & Ashmore, P. E. (2009). Length scale of braided river morphology. Water Resources Research, 45(8). https://doi.org/10.1029/2008WR007521
Integrated hydrological data year book (2012), CWC, New Delhi.
Integrated hydrological data year book, CWC. (2012), Hydrological Data Directorate Information Systems Organisation Water Planning & Projects Wing Central Water Commission, New Delhi.
Islam, A., & Guchhait, S. K. (2017). Analysing the influence of Farakka Barrage Project on channel dynamics and meander geometry of Bhagirathi river of West Bengal, India. Arabian Journal of Geosciences, 10(11), 1-18. https://doi.org/10.1007/s12517-017-3004-2
Islam, A., & Guchhait, S. K. (2020). Characterizing cross-sectional morphology and channel inefficiency of lower Bhagirathi River, India, in post-Farakka barrage condition. Natural Hazards, 103(3), 3803-3836. https://doi.org/10.1007/s11069-020-04156-9
Jain, S. K., & Kumar, P. (2014). Environmental flows in India: towards sustainable water management. Hydrological Sciences Journal, 59(3-4), 751-769. https://doi.org/10.1080/02626667.2014.896996
Jain, S. K., Singh, P., & Seth, S. M. (2002). Assessment of sedimentation in Bhakra Reservoir in the western Himalayan region using remotely sensed data. Hydrological Sciences Journal, 47(2), 203-212. https://doi.org/10.1080/02626660209492924
Jain, V. (2018). Geomorphic effectiveness of a long profile shape and the role of inherent geological controls in the Himalayan hinterland area of the Ganga River basin, India. Geomorphology, 304, 15-29. https://doi.org/10.1016/j.geomorph.2017.12.022
Jain, V., Sinha, R., Singh, L. P., & Tandon, S. K. (2016). River systems in India: The anthropocene context. In Proc. Indian Nat. Sci. Acad (Vol. 82, pp. 747-761).
Javernick, L., Redolfi, M., & Bertoldi, W. (2018). Evaluation of a numerical model's ability to predict bed load transport observed in braided river experiments. Advances in Water Resources, 115, 207-218. https://doi.org/10.1016/j.advwatres.2018.03.012
Jin, L., Whitehead, P. G., Rodda, H., Macadam, I., & Sarkar, S. (2018). Simulating climate change and socio-economic change impacts on flows and water quality in the Mahanadi River system, India. Science of the Total Environment, 637, 907-917.
Jothiprakash, V., & Garg, V. (2009). Reservoir sedimentation estimation using artificial neural network. Journal of Hydrologic Engineering, 14(9), 1035-1040. https://doi.org/10.1061/(ASCE)HE.1943-5584.0000075
Kakati, R., Chembolu, V., & Dutta, S. (2022). 3D Modelling of Hybrid River Training Works. In River Hydraulics (pp. 371-377). Springer, Cham.

Kale, V. S. (2002). Fluvial geomorphology of Indian rivers: an overview. Progress in physical geography, 26(3), 400-433. https://doi.org/10.1191/0309133302pp343ra
Kale, V. S. (2003). Geomorphic effects of monsoon floods on Indian rivers. In Flood problem and management in South Asia (pp. 65-84). Springer, Dordrecht. https://doi.org/10.1007/978-94-017-0137-2_3
Kale, V. S., Karlekar, S. N., & Deodhar, L. A. (1986). Channel morphology and hydraulic characteristics of Vashishthi River, Maharashtra (India). Transactions Institute of Indian Geographers, 8, 113-126.
Kale, V.S. (2008). A half-a-century record of annual energy expenditure and geomorphic effectiveness of the monsoon-fed Narmada River, central India. Catena. 75(2), 154-163. https://doi.org/10.1016/j.catena.2008.05.004
Kang, T., Kimura, I., & Shimizu, Y. (2020). Numerical simulation of large wood deposition patterns and responses of bed morphology in a braided river using large wood dynamics model. Earth Surface Processes and Landforms, 45(4), 962-977. https://doi.org/10.1002/esp.4789
Karmaker, T., & Dutta, S. (2013). Modeling seepage erosion and bank retreat in a composite river bank. Journal of hydrology, 476, 178-187. https://doi.org/10.1016/j.jhydrol.2012.10.032
Karmaker, T., & Dutta, S. (2016). Prediction of short-term morphological change in large braided river using 2D numerical model. Journal of Hydraulic Engineering, 142(10), 04016039. https://doi.org/10.1061/(ASCE)HY.1943-7900.0001167
Karmaker, T., Medhi, H., & Dutta, S. (2017). Study of channel instability in the braided Brahmaputra river using satellite imagery. Current Science, 1533-1543.
Kasprak, A., Wheaton, J. M., Ashmore, P. E., Hensleigh, J. W., & Peirce, S. (2015). The relationship between particle travel distance and channel morphology: Results from physical models of braided rivers. Journal of Geophysical Research: Earth Surface, 120(1), 55-74. https://doi.org/10.1002/2014JF003310
Kaushal, R.K., Sarkar, A., Mishra, K., Sinha, R., Nepal, S., & Jain, V. (2020). Spatio-temporal variability in stream power distribution in the Upper Kosi River basin, Central Himalaya: Controls and geomorphic implications. Geomorphology 350, 106888. https://doi.org/10.1016/j.geomorph.2019.106888
Kelly, S. E. A. N. (2006). Scaling and hierarchy in braided rivers and their deposits: examples and implications for reservoir modelling. Braided rivers: Process, deposits, ecology and management, 36, 75-106.
Khan, M. Y. A., Daityari, S., & Chakrapani, G. J. (2016). Factors responsible for temporal and spatial variations in water and sediment discharge in Ramganga River, Ganga Basin, India. Environmental Earth Sciences, 75(4), 1-18. https://doi.org/10.1007/s12665-015-5148-2
Khan, S., & Fryirs, K. (2020). An approach for assessing geomorphic river sensitivity across a catchment based on analysis of historical capacity for adjustment. Geomorphology, 359, 107135.
Khan, S., Sinha, R., Whitehead, P., Sarkar, S., Jin, L., & Futter, M. N. (2018). Flows and sediment dynamics in the Ganga River under present and future climate scenarios. Hydrological Sciences Journal, 63(5), 763-782. https://doi.org/10.1080/02626667.2018.1447113
Khedkar, G. D., Lutzky, S., Rathod, S., Kalyankar, A., & David, L. (2014). A dual role of dams in fragmentation and support of fish diversity across the Godavari River basin in India. Ecohydrology, 7(6), 1560-1573. https://doi.org/10.1002/eco.1470
Kleinhans, M.G. & van den Berg, J.H. (2011). River channel and bar patterns explained and predicted by an empirical and a physics-based method. Earth Surface Processes and Landforms, 36(6), pp.721-738.
Kline, M., & Cahoon, B. (2010). Protecting river corridors in Vermont 1. JAWRA Journal of the American Water Resources Association, 46(2), 227-236. https://doi.org/10.1111/j.1752-1688.2010.00417.x
Knighton, D. (2014). Fluvial forms and processes: a new perspective. Routledge.
Knighton, D., (1998). Fluvial Forms and Processes: A New Perspective. Taylor & Francis
Knighton, D., A. & Nanson, G.C., (1993). Anastomosis and the continuum of channel pattern. Earth. Surf. Proc. Land. 18(7), 613-625. https://doi.org/10.1002/esp.3290180705
Kong, Q., Xin, Z., Zhao, Y., Ran, L., & Xia, X. (2022). Health Assessment for Mountainous Rivers Based on Dominant Functions in the Huaijiu River, Beijing, China. Environmental Management, 1-14.
Kudnar, N. S. (2020). GIS-based assessment of morphological and hydrological parameters of Wainganga River Basin, Central India. Modeling Earth Systems and Environment, 6(3), 1933-1950. https://doi.org/10.1007/s40808-020-00804-y
Kumar, P., Chaube, U. C., & Mishra, S. K. (2007, October). Environmental flows for hydropower projects–a case study. In International conference on small hydropower-hydro Sri Lanka (Vol. 22, p. 24).
Lakra, W. S., Sarkar, U. K., Kumar, R. S., Pandey, A., Dubey, V. K., & Gusain, O. P. (2010). Fish diversity, habitat ecology and their conservation and management issues of a tropical River in Ganga basin, India. The Environmentalist, 30(4), 306-319. https://doi.org/10.1007/s10669-010-9277-6
Lane, E. W. (1957). A study of the shape of channels formed by natural streams flowing in erodible material.

Lane, S. N., Westaway, R. M., & Murray Hicks, D. (2003). Estimation of erosion and deposition volumes in a large, gravel-bed, braided river using synoptic remote sensing. Earth Surface Processes and Landforms: The Journal of the British Geomorphological Research Group, 28(3), 249-271. https://doi.org/10.1002/esp.483
Langat, P. K., Kumar, L., & Koech, R. (2019). Monitoring river channel dynamics using remote sensing and GIS techniques. Geomorphology, 325, 92-102. https://doi.org/10.1016/j.geomorph.2018.10.007
Langbein, W.B., & Leopold, L.B., (1964). Quasi-equilibrium states in channel morphology. Am. J. Sci. 262(6), 782-794. https://doi.org/10.2475/ajs.262.6.782
Larsen, A., May, J. H., & Carah, X. (2019). Late Quaternary biotic and abiotic controls on long-term sediment flux in a northern Australian tropical river system. Earth Surface Processes and Landforms, 44(12), 2494-2509.
Larsen, E. W., Premier, A. K., & Greco, S. E. (2006). Cumulative effective stream power and bank erosion on the Sacramento river, California, USA 1. JAWRA Journal of the American Water Resources Association, 42(4), 1077-1097. https://doi.org/10.1111/j.1752-1688.2006.tb04515.x
Lecce, S. A. (1997). Spatial patterns of historical overbank sedimentation and floodplain evolution, Blue River, Wisconsin. Geomorphology, 18(3-4), 265-277.
Leddy, J. O., Ashworth, P. J., & Best, J. L. (1993). Mechanisms of anabranch avulsion within gravel-bed braided rivers: observations from a scaled physical model. Geological Society, London, Special Publications, 75(1), 119-127.
Leduc, P., Peirce, S., & Ashmore, P. (2019). Challenges and applications of structure-from-motion photogrammetry in a physical model of a braided river. Earth Surface Dynamics, 7(1), 97-106. https://doi.org/10.5194/esurf-7-97-2019
Lenzi, M.A., Mao, L., & Comiti, F. (2006). Effective discharge for sediment transport in a mountain river: Computational approaches and geomorphic effectiveness. J. Hydrol. 326(1-4), 257-276. https://doi.org/10.1016/j.jhydrol.2005.10.031
Leopold, L. B., & Langbein, W. B. (1962). The concept of entropy in landscape evolution (Vol. 500). US Government Printing Office.
Leopold, L. B., & Wolman, M. G. (1957). River channel patterns: braided, meandering, and straight. US Government Printing Office.
Leopold, L.B. (1994). A View of the River. Harvard University Press.
Leopold, L.B., Wolman, M.G., & Miller, J.P. (1964). Fluvial Processes in Geomorphology. W.H. Freeman, San Francisco. pp 522.
Lewin, J., & Brewer, P. A. (2001). Predicting channel patterns. Geomorphology, 40(3-4), 329-339. https://doi.org/10.1016/S0169-555X(01)00061-7
Liro, M. (2014). Conceptual model for assessing the channel changes upstream from dam reservoir. Quaestiones Geographicae, 33(1).
Liro, M. (2016). Development of sediment slug upstream from the Czorsztyn Reservoir (southern Poland) and its interaction with river morphology. Geomorphology, 253, 225-238. https://doi.org/10.1016/j.geomorph.2015.09.018
Liro, M. (2019). Dam reservoir backwater as a field-scale laboratory of human-induced changes in river biogeomorphology: A review focused on gravel-bed rivers. Science of the Total Environment, 651, 2899-2912. https://doi.org/10.1016/j.scitotenv.2018.10.138
Lisenby, P.E., Croke, J., & Fryirs, K.A. (2018). Geomorphic effectiveness: a linear concept in a non-linear world. Earth. Surf. Proc. Land. 43(1), 4-20. https://doi.org/10.1002/esp.4096
Lokhtin, V. M. (1897). About a mechanism of river channel. Voprosy gidrotekhniki svobodnykh rek, 23-59.
Lotsari, E., Wainwright, D., Corner, G. D., Alho, P., & Käyhkö, J. (2014). Surveyed and modelled one-year morphodynamics in the braided lower Tana River. Hydrological processes, 28(4), 2685-2716. https://doi.org/10.1002/hyp.9750
Luo, X. X., Yang, S. L., Wang, R. S., Zhang, C. Y., & Li, P. (2017). New evidence of Yangtze delta recession after closing of the Three Gorges Dam. Scientific Reports, 7(1), 1-10.
Ma, Y., Huang, H.Q., Xu, J., Brierley, G.J., &Yao, Z. (2010). Variability of effective discharge for suspended sediment transport in a large semi-arid river basin. Journal of Hydrology, 388(3-4), 357-369. https://doi.org/10.1016/j.jhydrol.2010.05.014
Majumder, A., Ghosh, S., Dasgupta, A., & Seth, D. (2012). Analyzing reservoir sedimentation of Panchet Dam, India using remote sensing and GIS. Panchakotessays, 2(3), 82-95.
Malavoi, J.R., Bravard, J.P., Pie´gay, H., He´rouin, E., & Ramez, P. (1998). De´termination de l'espace de liberte´ des cours d'eau. Guide technique no. 2, SDAGE RMC. http://sierm.eaurmc.fr/sdage/documents/guide-tech-2.pdf
Malini, B. H., & Rao, K. N. (2004). Coastal erosion and habitat loss along the Godavari delta front- a fallout of dam construction (?). Current Science, 87(9), 1232-1236.

Marston, R. A., Girel, J., Pautou, G., Piegay, H., Bravard, J. P., & Arneson, C. (1995). Channel metamorphosis, floodplain disturbance, and vegetation development: Ain River, France. Geomorphology, 13(1-4), 121-131. https://doi.org/10.1016/0169-555X(95)00066-E
Miall, A. D. (1977). A review of the braided-river depositional environment. Earth-Science Reviews, 13(1), 1-62.
Milan, D. J., Tooth, S., & Heritage, G. L. (2020). Topographic, hydraulic, and vegetative controls on bar and island development in mixed bedrock-alluvial, multichanneled, dryland rivers. Water Resources Research, 56(5), e2019WR026101.
Mirza, M. (2004). The Ganges water diversion: environmental effects and implications—an introduction. In The Ganges water diversion: environmental effects and implications (pp. 1-12). Springer, Dordrecht. https://doi.org/10.1007/978-1-4020-2792-5_1
Montgomery, D. R. (2008). Dreams of natural streams. Science, 319(5861), 291-292.
Montgomery, D. R., & Buffington, J. M. (1998). Channel processes, classification, and response. River Ecology and Management: Lessons from the Pacific Coastal Ecoregion, RJ Naiman and RE Bilby (Editors). Springer-Verlag, New York, New York, 13-42.
Moon, B. P., Van Niekerk, A. W., Heritage, G. L., Rogers, K. H., & James, C. S. (1997). A geomorphological approach to the ecological management of rivers in the Kruger National Park: the case of the Sabie River. Transactions of the institute of British Geographers, 31-48.
Moramarco, T., Ammari, A., Burnelli, A., Mirauda, D., & Pascale, V. (2008). Entropy theory application for flow monitoring in natural channels.
Mosselman, E. (2006). Bank protection and river training along the braided Brahmaputra-Jamuna River, Bangladesh. Braided rivers: Process, deposits, ecology and management, 36, 279-287.
Mou, N., Wang, C., Yang, T., & Zhang, L. (2020). Evaluation of development potential of ports in the Yangtze river delta using FAHP-entropy model. Sustainability, 12(2), 493.
Mount, N. J., Tate, N. J., Sarker, M. H., & Thorne, C. R. (2013). Evolutionary, multi-scale analysis of river bank line retreat using continuous wavelet transforms: Jamuna River, Bangladesh. Geomorphology, 183, 82-95. https://doi.org/10.1016/j.geomorph.2012.07.017
MoWR (Ministry of Water Resources), (2002). National Water Policy. Ministry of Water Resources. New Delhi: Government of India.
Muralidharan, D., Andrade, R., & Rangarajan, R. (2007). Evaluation of check-dam recharge through water-table response in ponding area. Current science, 92(10), 1350-1352.
Murray, A. B., & Paola, C. (1994). A cellular model of braided rivers. Nature, 371(6492), 54-57.
Myburgh, W. J., & Bredenkamp, G. J. (2005). The distribution and extent of declared weeds and invader plants in the macro channel of the Olifants River System, Mpumalanga. Koedoe, 48(1), 67-75.
Naganna, S. R., & Deka, P. C. (2018). Variability of streambed hydraulic conductivity in an intermittent stream reach regulated by vented dams: A case study. Journal of hydrology, 562, 477-491. https://doi.org/10.1016/j.jhydrol.2018.05.006
Naha, S., Rico-Ramirez, M. A., & Rosolem, R. (2021). Quantifying the impacts of land cover change on hydrological responses in the Mahanadi river basin in India. Hydrology and Earth System Sciences, 25(12), 6339-6357.
Naiman, R. J., Bechtold, J. S., Drake, D. C., Latterell, J. J., O'Keefe, T. C., & Balian, E. V. (2005). Origins, patterns, and importance of heterogeneity in riparian systems. In Ecosystem function in heterogeneous landscapes (pp. 279-309). Springer, New York, NY.
Nandi, K. K., Pradhan, C., Dutta, S., & Khatua, K. K. (2022). How dynamic is the Brahmaputra? Understanding the process-form-vegetation interactions for hierarchies of energy dissipation. Ecohydrology. https://doi.org/10.1002/eco.2416
Narasayya, K. (2013). Assessment of reservoir sedimentation using remote sensing satellite imageries. Asian Journal of Geoinformatics, 12(4).
Nash, D.B. (1994). Effective sediment-transporting discharge from magnitude-frequency analysis. J. Geol. 102(1), 79-95. https://doi.org/10.1086/629649
National Register of Large Dams Organisation (2019), NRLD, New Delhi.
National Register of Large Dams. (2019), Government of India, Central Water Commission Dam Safety Organisation, New Delhi.
Ncube, S., Beevers, L., Adeloye, A. J., & Visser, A. (2018). Assessment of freshwater ecosystem services in the Beas River Basin, Himalayas region, India. Proceedings of the International Association of Hydrological Sciences, 379, 67-72. https://doi.org/10.5194/piahs-379-67-2018
Newson, M. D. (2002). Geomorphological concepts and tools for sustainable river ecosystem management. Aquatic Conservation: Marine and Freshwater Ecosystems, 12, 365–379. https://doi.org/10.1002/aqc.532

Nilsson, C., & Berggren, K. (2000). Alterations of riparian ecosystems caused by river regulation: Dam operations have caused global-scale ecological changes in riparian ecosystems. How to protect river environments and human needs of rivers remains one of the most important questions of our time. BioScience, 50(9), 783-792. https://doi.org/10.1641/0006-3568(2000)050[0783:AORECB]2.0.CO;2

Niranjan, V., & Srinivasu, V. K. (2012). Small water harvesting and artificial recharge interventions in Singoda river basin, coastal Saurashtra. Hydrological and socio-economic impact occasional paper, (6-0512).

Nolan, K.M., Lisle, T.E., Kelsey, & H.M. (1987). Bankfull discharge and sediment transport in northwestern California. Erosion and sedimentation in the Pacific Rim. IAHS Publ. 165, 439–449.

O'Donnell, C. F., Sanders, M. D., Woolmore, C. B., & Maloney, R. (2016). Management and research priorities for conserving biodiversity on New Zealand's braided rivers. Wellington, New Zealand: Department of Conservation.

O'Donnell, J., Fryirs, K. A., & Leishman, M. R. (2016). Seed banks as a source of vegetation regeneration to support the recovery of degraded rivers: a comparison of river reaches of varying condition. Science of the Total Environment, 542, 591-602.

Ollero, A. (2010). Channel changes and floodplain management in the meandering middle Ebro River, Spain. Geomorphology, 117(3-4), 247-260. https://doi.org/10.1016/j.geomorph.2009.01.015

Outlook. (2017). "Mega Dams Are A Trend That The World Stopped Following Long Ago, But Why Hasn't India Yet?" <https://www.outlookindia.com/website/story/mega-dams-are-a-trend-that-the-world-stopped-following-long-ago-but-why-is-india/301976>

Pal, S. (2016). Impact of Massanjore dam on hydro-geomorphological modification of Mayurakshi river, Eastern India. Environment, development and sustainability, 18(3), 921-944. https://doi.org/10.1007/s10668-015-9679-1

Pal, S. (2017). Impact of Tilpara barrage on backwater reach of Kushkarni River: a tributary of Mayurakshi River. Environment, Development and Sustainability, 19(5), 2115-2142. https://doi.org/10.1007/s10668-016-9833-4

Panda, D. K., Kumar, A., & Mohanty, S. (2011). Recent trends in sediment load of the tropical (Peninsular) river basins of India. Global and Planetary Change, 75(3-4), 108-118. https://doi.org/10.1016/j.gloplacha.2010.10.012

Pandey, A., Chaube, U. C., Mishra, S. K., & Kumar, D. (2016). Assessment of reservoir sedimentation using remote sensing and recommendations for desilting Patratu Reservoir, India. Hydrological Sciences Journal, 61(4), 711-718. https://doi.org/10.1080/02626667.2014.993988

Pandey, S. (1993). Changes in waterbird diversity due to the construction of Pong Dam Reservoir, Himachal Pradesh, India. Biological conservation, 66(2), 125-130. https://doi.org/10.1016/0006-3207(93)90143-O

Panwar, S., Yang, S., Srivastava, P., Khan, M. Y. A., Sangode, S. J., & Chakrapani, G. J. (2020). Environmental magnetic characterization of the Alaknanda and Ramganga river sediments, Ganga basin, India. Catena, 190, 104529. https://doi.org/10.1016/j.catena.2020.104529

Parua, P. K. (2010). The Ganga: water use in the Indian subcontinent (Vol. 64). Springer Science & Business Media.

Peiry, J., Salvador, P. G., & Nouguier, F. (1994). L'incision des rivières dans les Alpes du nord: état de la question/River incision in the Northern French Alps. Géocarrefour, 69(1), 47-56.

Petts, G. E. Impounded rivers: perspectives for ecological management. Wiley (1984). Petts, G. E. (1984). Impounded rivers: perspectives for ecological management. Wiley.

Petts, G. E., & Gurnell, A. M. (2005). Dams and geomorphology: research progress and future directions. Geomorphology, 71(1-2), 27-47. https://doi.org/10.1016/j.geomorph.2004.02.015

Phillips, J. D., & Van Dyke, C. (2016). Principles of geomorphic disturbance and recovery in response to storms. Earth Surface Processes and Landforms, 41(7), 971-979.

Phillips, J.D. (2002). Geomorphic impacts of flash flooding in a forested headwater basin. J. Hydrol. 269(3-4), 236-250. https://doi.org/10.1016/S0022-1694(02)00280-9

Picco, L., Mao, L., Cavalli, M., Buzzi, E., Rainato, R., & Lenzi, M. A. (2013). Evaluating short-term morphological changes in a gravel-bed braided river using terrestrial laser scanner. Geomorphology, 201, 323-334. https://doi.org/10.1016/j.geomorph.2013.07.007

Pickup, G., & Warner, R. F. (1976). Effects of hydrologic regime on magnitude and frequency of dominant discharge. Journal of Hydrology, 29(1-2), 51-75.

Piégay, H., Darby, S. E., Mosselman, E., & Surian, N. (2005). A review of techniques available for delimiting the erodible river corridor: a sustainable approach to managing bank erosion. River research and applications, 21(7), 773-789. https://doi.org/10.1002/rra.881

Piégay, H., Grant, G., Nakamura, F., & Trustrum, N. (2006). Braided river management: from assessment of river behaviour to improved sustainable development. Braided rivers: process, deposits, ecology and management, 36, 257-275.
Pitlick, J., & Cress, R. (2002). Downstream changes in the channel geometry of a large gravel bed river. Water Resour. Res. 38 (10), 34-1–34-11. https://doi.org/10.1029/2001WR000898
Pradhan, C., Bharti, R., & Dutta, S. (2017, July). Assessment of post-impoundment geomorphic variations along Brahmani River using remote sensing. In 2017 IEEE International Geoscience and Remote Sensing Symposium (IGARSS) (pp. 5598-5601). IEEE. DOI: 10.1109/IGARSS.2017.8128274
Pradhan, C., Chembolu, V., & Dutta, S. (2019). Impact of river interventions on alluvial channel morphology. ISH Journal of Hydraulic Engineering, 25(1), 87-93. https://doi.org/10.1080/09715010.2018.1453878
Pradhan, C., Chembolu, V., Dutta, S., and Bharti, R. (2021a). "Role of effective discharge on morphological changes for a regulated macrochannel river system." Geomorphology, 385, 107718, ISSN 0169-555X, https://doi.org/10.1016/j.geomorph.2021.107718.
Pradhan, C., Chembolu, V., Bharti, R., & Dutta, S. (2021b). Regulated rivers in India: research progress and future directions. ISH Journal of Hydraulic Engineering, 1-13. https://doi.org/10.1080/09715010.2021.1975319
Pradhan, C., Padhee, S., Dutta, S., & Bharti, R. (2021c, April). An entropy-based investigation on the river recovery potential in a regulated river basin. In EGU General Assembly Conference Abstracts (pp. EGU21-9362). DOI: 10.5194/egusphere-egu21-9362
Pradhan, C., Dutta, S., & Bharti, R. (2021d, December). Understanding River Freedom Space and Seasonal Variation of Surface Water Dynamics in Large Fluvial Landscapes: Implications for Floods and Anthropogenic Stress. In AGU Fall Meeting 2021. AGU.
Pradhan, C., Modalavalasa S., Dutta S., and Bharti, R. (2020). "A geomorphic approach to evaluate river recovery potential for regulated river basin." In River Flow 2020 (1805-1809). CRC Press. DOI: 10.1201/b22619-253
Prasad, N. R., Garg, V., and Thakur, P. K. (2018). "Role of SAR data in water body mapping and reservoir sedimentation assessment." ISPRS Annals of the Photogrammetry, Remote Sensing and Spatial Information Sciences, 4, 151-158.
Prasujya, G., & Nayan, S. (2021). Spatio-temporal study of morpho-dynamics of the Brahmaputra River along its Majuli Island reach. Environmental Challenges, 5, 100217. https://doi.org/10.1016/j.envc.2021.100217
Rajawat, A. S., Chauhan, H. B., Ratheesh, R., Rode, S., Bhanderi, R. J., Mahapatra, M., ... & Ajai. (2015). Assessment of coastal erosion along the Indian coast on 1: 25,000 scale using satellite data of 1989–1991 and 2004–2006 time frames. Current Science, 347-353.
Ramesh, R., & Subramanian, V. (1988). Temporal, spatial and size variation in the sediment transport in the Krishna River basin, India. Journal of hydrology, 98(1-2), 53-65. https://doi.org/10.1016/0022-1694(88)90205-3
Rao, K. N., Subraelu, P., Kumar, K. C. V. N., Demudu, G., Malini, B. H., & Rajawat, A. S. (2010). Impacts of sediment retention by dams on delta shoreline recession: evidences from the Krishna and Godavari deltas, India. Earth Surface Processes and Landforms: The Journal of the British Geomorphological Research Group, 35(7), 817-827. https://doi.org/10.1002/esp.1977
Ray, M. R., & Sarma, A. K. (2011). Minimizing diurnal variation of downstream flow in hydroelectric projects to reduce environmental impact. Journal of Hydro-Environment Research, 5(3), 177-185. https://doi.org/10.1016/j.jher.2010.12.001
Reinfelds, I., & Nanson, G. (1993). Formation of braided river floodplains, Waimakariri River, New Zealand. Sedimentology, 40(6), 1113-1127.
Renganayaki, S. P., & Elango, L. (2013). A review on managed aquifer recharge by check dams: a case study near Chennai, India. International Journal of Research in Engineering and Technology, 2(4), 416-423.
Rinaldo, A., Banavar, J. R., & Maritan, A. (2006). Trees, networks, and hydrology. Water Resources Research, 42(6). https://doi.org/10.1029/2005WR004108
Rosatti, G. (2002). Validation of the physical modeling approach for braided rivers. Water Resources Research, 38(12), 31-1. https://doi.org/10.1029/2001WR000433
Rountree, M. W., Heritage, G. L., Rogers, K. H., & Acreman, M. C. (2001). In-channel metamorphosis in a semiarid, mixed bedrock/alluvial river system: Implications for instream flow requirements. IAHS Publications-Series of Proceedings and Reports-Intern Assoc Hydrological Sciences, 266, 113-124.
Rountree, M. W., Rogers, K. H., & Heritage, G. L. (2000). Landscape state change in the semi-arid Sabie River, Kruger National Park, in response to flood and drought. South African Geographical Journal, 82(3), 173-181.

Roy, N.G., & Sinha, R. (2014). Effective discharge for suspended sediment transport of the Ganga River and its geomorphic implication. Geomorphology 227, 18-30. https://doi.org/10.1016/j.geomorph.2014.04.029
Rudra, K. (2006). Shifting of the Ganga and land erosion in West Bengal. Centre for development and environmental policy, Occasional paper 8: 1-20, Indian Institute of Management, Kolkata.
Rumana, H. S., Jeeva, V., & Kumar, S. (2015). Impact of the low head dam/barrage on fisheries-a case study of Giri river of Yamuna basin (India)/Impact des barrages de seuil sur les pêcheries-Etude de cas sur la rivière Giri du bassin de Yamuna, en Inde. Transylvanian Review of Systematical and Ecological Research, 17(2), 119. DOI: 10.1515/trser-2015-0070
Saalim, S. M., Saraswat, R., & Nigam, R. (2022) Ecological preferences of living benthic foraminifera from the Mahanadi river-dominated north-western Bay of Bengal: A potential environmental impact assessment tool. Mar. Pollut. Bull. 175, 113-158.
Sambrook Smith, G. H., Ashworth, P. J., Best, J. L., Woodward, J., & Simpson, C. J. (2006). The sedimentology and alluvial architecture of the sandy braided South Saskatchewan River, Canada. Sedimentology, 53(2), 413-434.
Sanyal, J. (2017). Predicting possible effects of dams on downstream river bed changes of a Himalayan river with morphodynamic modelling. Quaternary International, 453, 48-62. https://doi.org/10.1016/j.quaint.2017.03.063
Sarker, M. H., & Thorne, C. R. (2006). Morphological response of the Brahmaputra–Padma–Lower Meghna river system to the Assam earthquake of 1950. Braided Rivers: process, deposits, ecology and management, 21, 289-310.
Sarma, J. N., & Acharjee, S. (2018). A study on variation in channel width and braiding intensity of the Brahmaputra River in Assam, India. Geosciences, 8(9), 343. https://doi.org/10.3390/geosciences8090343
Sarma, J. N., & Phukan, M. K. (2004). Origin and some geomorphological changes of Majuli Island of the Brahmaputra River in Assam, India. Geomorphology, 60(1-2), 1-19. https://doi.org/10.1016/j.geomorph.2003.07.013
Satyakumar, A. V., Pandey, A. K., Singh, A. P., & Tiwari, V. M. (2022). Delineation of structural and tectonic features in the Mahanadi basin, Eastern India: Inferences from Remote sensing and Land Gravity data. Journal of Asian Earth Sciences, 105116.
Saucier, R. T. (1994). Geomorphology and Quaternary geologic history of the Lower Mississippi Valley (Vol. 1). US Army Engineer Waterways Experiment Station.
Scheffer, M. (2020). Critical transitions in nature and society. In Critical Transitions in Nature and Society. Princeton University Press.
Schumm, S. A. (1969). River metamorphosis. Journal of the Hydraulics division, 95(1), 255-274. https://doi.org/10.1061/JYCEAJ.0001938
Schumm, S. A. (1977). The fluvial system John Wiley and Sons, 338 pp., New York. Schumm, S.A., 1981.
Schumm, S. A. (1979). Geomorphic thresholds: the concept and its applications. Transactions of the Institute of British Geographers, 4 (4), pp. 485-515, 10.2307/622211
Schumm, S. A., & Lichty, R. W. (1965). Time, space, and causality in geomorphology. American journal of science, 263(2), 110-119.
Sehgal, K. L. (1990). Report on impact of construction and completion of Beas Project (Stage I-Beas-Sutlej Link, and Stage II-Pong Dam) on limnology and fisheries of R. Beas. CIFRI/NRCCWF. 45pp. and.
Sehgal, K. L. (1999). “Coldwater fish and fisheries in the Indian Himalayas: rivers and streams.” Fish and fisheries at higher altitudes: Asia. Food and Agriculture Organization of the United Nations Technical Paper, 385, 41-63.
Shafroth, P. B., Stromberg, J. C., & Patten, D. T. (2002). Riparian vegetation response to altered disturbance and stress regimes. Ecological applications, 12(1), 107-123.
Shannon, C. E. (1948). A mathematical theory of communication. The Bell system technical journal, 27(3), 379-423.
Sharma, N., & Akhtar, M. P. (2017). Prospects of modeling and morpho-dynamic study for Brahmaputra river. In River System Analysis and Management (pp. 189-209). Springer, Singapore. https://doi.org/10.1007/978-981-10-1472-7_10
Sharma, P. J., Patel, P. L., & Jothiprakash, V. (2021). Impact assessment of Hathnur reservoir on hydrological regimes of Tapi River, India. ISH Journal of Hydraulic Engineering, 27(sup1), 433-445. https://doi.org/10.1080/09715010.2019.1574616
Sholtes, J. S., & Bledsoe, B. P. (2016). Half-yield discharge: Process-based predictor of bankfull discharge. Journal of Hydraulic Engineering, 142(8), 04016017. https://doi.org/10.1061/(ASCE)HY.1943-7900.0001137

Shukla, S., Jain, S. K., Kansal, M. L., & Chandniha, S. K. (2017). Assessment of sedimentation in Pong and Bhakra reservoirs in Himachal Pradesh, India, using geospatial technique. Remote Sensing Applications: Society and Environment, 8, 148-156. https://doi.org/10.1016/j.rsase.2017.08.008

Sichingabula, H.M. (1999). Magnitude-frequency characteristics of effective discharge for suspended sediment transport, Fraser River, British Columbia, Canada. Hydrol. Process 13(9), 1361-1380. https://doi.org/10.1002/(SICI)1099-1085(19990630)13:9<1361::AID-HYP808>3.0.CO;2-H

Silow, E. A., & Mokry, A. V. (2010). Exergy as a tool for ecosystem health assessment. Entropy, 12(4), 902-925.

Simon, A., & Rinaldi, M. (2006). Disturbance, stream incision, and channel evolution: The roles of excess transport capacity and boundary materials in controlling channel response. Geomorphology, 79(3-4), 361-383.

Simon, A., Dickerson, W., & Heins, A. (2004). Suspended-sediment transport rates at the 1.5-year recurrence interval for ecoregions of the United States: transport conditions at the bankfull and effective discharge?. Geomorphology 58(1-4), 243-262. https://doi.org/10.1016/j.geomorph.2003.07.003

Singh, K. P. (1968). Hydrologic design of Ramganga dam project. Journal of the Hydraulics Division, 94(1), 71-94. https://doi.org/10.1061/JYCEAJ.0001770

Singh, V. P. (1997). The use of entropy in hydrology and water resources. Hydrological processes, 11(6), 587-626.

Singh, P., Sharma, K., Swami, N., Rana, J. S., Gusain, M. P., & Gusain, O. P. (2019). Assemblages of benthic macroinvertebrate communities downstream of a dam on River Alaknanda in Garhwal Himalaya, Uttarakhand, India. International Journal of Ecology and Environmental Sciences, 45(4), 403-412.

Singh, V., Sharma, N., & Ojha, C. S. P. (Eds.). (2004). The Brahmaputra basin water resources (Vol. 47). Springer Science & Business Media.

Sinha, R., Jain, V., & Gaurav, K. (2019). Geomorphic changes and sediment dynamics in rivers: causes and consequences.

Sinha, R., Jain, V., Babu, G. P., & Ghosh, S. (2005). Geomorphic characterization and diversity of the fluvial systems of the Gangetic Plains. Geomorphology, 70(3-4), 207-225. https://doi.org/10.1016/j.geomorph.2005.02.006

Skelly, R. L., Bristow, C. S., & Ethridge, F. G. (2003). Architecture of channel-belt deposits in an aggrading shallow sandbed braided river: the lower Niobrara River, northeast Nebraska. Sedimentary Geology, 158(3-4), 249-270. https://doi.org/10.1016/S0037-0738(02)00313-5

Smakhtin, V. Y. (2006). An assessment of environmental flow requirements of Indian river basins (Vol. 107). IWMI.

Steiger, J., Tabacchi, E., Dufour, S., Corenblit, D., & Peiry, J. L. (2005). Hydrogeomorphic processes affecting riparian habitat within alluvial channel–floodplain river systems: a review for the temperate zone. River Research and Applications, 21(7), 719-737.

Subrahmanyam, V., Subrahmanyam, A. S., Murty, G. P. S., & Murthy, K. S. R. (2008). Morphology and tectonics of Mahanadi Basin, northeastern continental margin of India from geophysical studies. Marine Geology, 253(1-2), 63-72.

Sun, J., Lin, B., & Yang, H. (2015). Development and application of a braided river model with non-uniform sediment transport. Advances in Water Resources, 81, 62-74. https://doi.org/10.1016/j.advwatres.2014.12.012

Surian, N. (1999). Channel changes due to river regulation: the case of the Piave River, Italy. Earth Surface Processes and Landforms: The Journal of the British Geomorphological Research Group, 24(12), 1135-1151. https://doi.org/10.1002/(SICI)1096-9837(199911)24:12<1135::AID-ESP40>3.0.CO;2-F

Surian, N., Barban, M., Ziliani, L., Monegato, G., Bertoldi, W., & Comiti, F. (2015). Vegetation turnover in a braided river: frequency and effectiveness of floods of different magnitude. Earth Surface Processes and Landforms, 40(4), 542-558.

Surian, N., Ziliani, L., Comiti, F., Lenzi, M. A., & Mao, L. (2009). Channel adjustments and alteration of sediment fluxes in gravel-bed rivers of North-Eastern Italy: potentials and limitations for channel recovery. River research and applications, 25(5), 551-567. https://doi.org/10.1002/rra.1231

Syvitski, J. P., Cohen, S., Kettner, A. J., & Brakenridge, G. R. (2014). How important and different are tropical rivers?—An overview. Geomorphology, 227, 5-17. https://doi.org/10.1016/j.geomorph.2014.02.029

Syvitski, J. P., Vorosmarty, C. J., Kettner, A. J., & Green, P. (2005). Impact of humans on the flux of terrestrial sediment to the global coastal ocean. science, 308(5720), 376-380.

Szupiany, R. N., Amsler, M. L., Hernandez, J., Parsons, D. R., Best, J. L., Fornari, E., & Trento, A. (2012). Flow fields, bed shear stresses, and suspended bed sediment dynamics in bifurcations of a large river. Water resources research, 48(11). https://doi.org/10.1029/2011WR011677

Takagi, T., Oguchi, T., Matsumoto, J., Grossman, M. J., Sarker, M. H., & Matin, M. A. (2007). Channel braiding and stability of the Brahmaputra River, Bangladesh, since 1967: GIS and remote sensing analyses. Geomorphology, 85(3-4), 294-305. https://doi.org/10.1016/j.geomorph.2006.03.028

Talukdar, S., & Pal, S. (2017). Impact of dam on inundation regime of flood plain wetland of Punarbhaba river basin of barind tract of Indo-Bangladesh. International Soil and Water Conservation Research, 5(2), 109-121. https://doi.org/10.1016/j.iswcr.2017.05.003

Tejedor, A., Longjas, A., Edmonds, D. A., Zaliapin, I., Georgiou, T. T., Rinaldo, A., & Foufoula-Georgiou, E. (2017). Entropy and optimality in river deltas. Proceedings of the National Academy of Sciences, 114(44), 11651-11656.

Thiyagarajan, G., Valliammai, A., Raviraj, A., & Panneerselvam, S. (2020). Effect of artificial recharge structures in improving groundwater level. Int. J. Curr. Microbiol. App. Sci, 9(2), 923-928. https://doi.org/10.20546/ijcmas.2020.902.109

Thompson, C. J., Croke, J., Fryirs, K., & Grove, J. R. (2016). A channel evolution model for subtropical macrochannel systems. Catena, 139, 199-213.

Thorne, C. R., Russell, A. P., & Alam, M. K. (1993). Planform pattern and channel evolution of the Brahmaputra River, Bangladesh. Geological Society, London, Special Publications, 75(1), 257-276. https://doi.org/10.1144/GSL.SP.1993.075.01.16

Thorp, J. H., Thoms, M. C., & Delong, M. D. (2006). The riverine ecosystem synthesis: biocomplexity in river networks across space and time. River Research and Applications, 22(2), 123-147.

Tian, H., Banger, K., Bo, T., & Dadhwal, V. K. (2014). History of land use in India during 1880–2010: Large-scale land transformations reconstructed from satellite data and historical archives. Global and Planetary Change, 121, 78-88.

Tiwari, S., Verma, S., & Ghosh, S. (2016). Estimation of sedimentation rate of a reservoir using remote sensing data: a case study of tehri reservoir. International Journal of Latest Trends in Engineering and Technology, 7(3), 245-53. http://dx.doi.org/10.21172/1.73.034

Tobón-Marín, A., & Cañón Barriga, J. (2020). Analysis of changes in rivers planforms using google earth engine. International Journal of Remote Sensing, 41(22), 8654-8681. https://doi.org/10.1080/01431161.2020.1792575

Uday Kumar, A., & Jayakumar, K. V. (2018). Assessment of hydrological alteration and environmental flow requirements for Srisailam dam on Krishna River, India. Water Policy, 20(6), 1176-1190.

van Coller, A. L., Rogers, K. H., & Heritage, G. L. (2000). Riparian vegetation-environment relationships: complimentarity of gradients versus patch hierarchy approaches. Journal of Vegetation Science, 11(3), 337-350.

Van den Berg, J. H. (1995). Prediction of alluvial channel pattern of perennial rivers. Geomorphology, 12(4), 259-279. https://doi.org/10.1016/0169-555X(95)00014-V

Wakelin-King, G. A. (2022). Landscapes of the Lake Eyre Basin: the catchment-scale context that creates fluvial diversity. Transactions of the Royal Society of South Australia, 146(1), 109-167.

Wheaton, J. M., Brasington, J., Darby, S. E., Kasprak, A., Sear, D., & Vericat, D. (2013). Morphodynamic signatures of braiding mechanisms as expressed through change in sediment storage in a gravel-bed river. Journal of Geophysical Research: Earth Surface, 118(2), 759-779. https://doi.org/10.1002/jgrf.20060

Wheaton, J. M., Fryirs, K. A., Brierley, G., Bangen, S. G., Bouwes, N., & O'Brien, G. (2015). Geomorphic mapping and taxonomy of fluvial landforms. Geomorphology, 248, 273-295. https://doi.org/10.1016/j.geomorph.2015.07.010

Williams, G. P. (1978). Bank-full discharge of rivers. Water resources research, 14(6), 1141-1154.

Williams, P. F., & Rust, B. R. (1969). The sedimentology of a braided river. Journal of Sedimentary Research, 39(2).

Williams, R. D., Brasington, J., & Hicks, D. M. (2016). Numerical modelling of braided river morphodynamics: Review and future challenges. Geography Compass, 10(3), 102-127. https://doi.org/10.1111/gec3.12260

Williams, R. D., Brasington, J., Hicks, M., Measures, R., Rennie, C. D., & Vericat, D. (2013). Hydraulic validation of two-dimensional simulations of braided river flow with spatially continuous aDcp data. Water Resources Research, 49(9), 5183-5205. https://doi.org/10.1002/wrcr.20391

Williams, R. D., Measures, R., Hicks, D. M., & Brasington, J. (2016). Assessment of a numerical model to reproduce event-scale erosion and deposition distributions in a braided river. Water resources research, 52(8), 6621-6642. https://doi.org/10.1002/2015WR018491

Wolman, M. G., & Gerson, R. (1978). Relative scales of time and effectiveness of climate in watershed geomorphology. Earth surface processes, 3(2), 189-208. https://doi.org/10.1002/esp.3290030207

Wolman, M. G., & Miller, J. P. (1960). Magnitude and frequency of forces in geomorphic processes. The Journal of Geology, 68(1), 54-74. https://doi.org/10.1086/626637

WWF (Worldwide Fund for Nature), (2012). "Summary report. Assessment of environment flows for Upper Ganga basin." New Delhi: WWF-India.

Xue, C., Shao, C., & Chen, S. (2020). SDGs-based river health assessment for small-and medium-sized watersheds. Sustainability, 12(5), 1846.

Yang, Q., Lin, A., Zhao, Z., Zou, L., & Sun, C. (2016). Assessment of urban ecosystem health based on entropy weight extension decision model in urban agglomeration. Sustainability, 8(9), 869.

Yevjevich, V. (1972). Probability and statistics in hydrology. In Probability and statistics in hydrology. Water resources publications.

Zhang, Y., Yang, Z., & Li, W. (2006). Analyses of urban ecosystem based on information entropy. Ecological Modelling, 197(1-2), 1-12.

Zhao, S., Peng, C., Jiang, H., Tian, D., Lei, X., & Zhou, X. (2006). Land use change in Asia and the ecological consequences. Ecological Research, 21(6), 890-896. https://doi.org/10.1007/s11284-006-0048-2

Zheng, S., Xu, Y. J., Cheng, H., Wang, B., Xu, W., & Wu, S. (2018). Riverbed erosion of the final 565 kilometers of the Yangtze River (Changjiang) following construction of the Three Gorges Dam. Scientific reports, 8(1), 1-11.

Zhou, Z., Tuo, Y., Li, J., Chen, M., Wang, H., Zhu, L., & Deng, Y. (2022). Effects of hydrology and river characteristics on riverine wetland morphology variation in the middle reaches of the Yarlung Zangbo–Brahmaputra River based on remote sensing. Journal of Hydrology, 127497. https://doi.org/10.1016/j.jhydrol.2022.127497

Zuo, Q., Hao, M., Zhang, Z., & Jiang, L. (2020). Assessment of the happy river index as an integrated index of river health and human well-being: a case study of the Yellow River, China. Water, 12(11), 3064.